UNIVERSIDAD NACIONAL DE COLOMBIA

Supervised group connectivity analysis for enhancing the interpretability of brain activity

Jorge Iván Padilla-Buriticá

Universidad Nacional de Colombia
Facultad de Ingeniería y Arquitectura, Departamento de Ingeniería Eléctrica,
Electrónica y Computación
Ciudad, Colombia
2021

UNIVERSIDAD NACIONAL DE COLOMBIA

Análisis de conectividad supervisado y de grupo para mejorar la interpretación de actividad cerebral.

Jorge Iván Padilla-Buriticá

Thesis presented as partial requirement for the degree of:
Doctor of Engineering

Supervisor:
(Ph.D.) César Germán Castellanos Domínguez
Co-supervisor:
(Ph.D.) José Manuel Ferrández Vicente

Signal Processing and Recognition Research Group

Universidad Nacional de Colombia
Facultad de Ingeniería y Arquitectura, Departamento de Ingeniería Eléctrica, Electrónica y Computación
Ciudad, Colombia
2021

Contents

List of Figures

List of Tables

Notation

Variables and Functions

$\boldsymbol{Y}$	EEG data
$\boldsymbol{y}_t$	EEG data at time instant t
$\boldsymbol{\Xi}$	EEG measurement noise
$\boldsymbol{\epsilon}_t$	EEG measurement noise at time instant t
$\boldsymbol{Q}$	A priori covariance matrix of brain activity

Mathematical Operators

$\text{diag}(\cdot)$	Diagonal matrix constructed with the argument vector
$\text{trace}(\cdot)$	Trace of the argument
$\text{vec}(\cdot)$	Column major vectorization of the argument matrix
$\|\| \cdot \|\|_F$	Frobenius norm
$\|\| \cdot \|\|_p$	ℓ_p norm
$\Theta(\cdot)$	Energy function of the prior distribution of brain activity $\boldsymbol{J}$
$\exp\{\cdot\}$	Gaussian function

Abbreviations

EEG	Electroencephalography
MEG	Magnetoencephalography
RS	Resting state
SNR	Signal to noise ratio
fMRI	functional Magnetic Resonance Imaging
PET	Position Emission Tomography
ERP	Evoked Potential Responses
MNE	Minimum Norm Estimates
FC	Functional Connectivity
ICA	Independent Aomponent Analysis
SVD	Singular Value Decomposition
HMM	Hidden Markov Moldel
IRA	Iterative Regularization Algorithm
MAP	Maximum A Posteriori
ROI	Region of interest
ST	Short time
TVAR	Time varying autoregressive model
TA	Time adaptive
swADTF	spectrum-weighted adaptive directed transfer function
SOZ	Seizure onset zone

Acknowledgments

I want to thank Professor Germán Castellanos for being my tutor, despite having different perspectives on life, we have been able to advance my academic work. I also want to thank my co-tutor, José Manuel Ferrández, for his contributions to this work. I express my special thanks to the people who work in the Signal Processing and Recognition Group. Thank you for helping me in many tests, for providing possible solutions to academic problems. Still, most importantly, for accompanying me to enjoy life, smile, and have soccer hours every week, without you, it would have been impossible to advance.
Mainly I want to thank Juana Valeria Hurtado because it was she who achieved the first valuable results of this research and Frank Yesid Zapata, for completing the tests and achieving advanced development in connectivity analysis. To Juan David Martínez, Leonardo Duque, Ernesto Cuartas, Luisa Velásquez for being my friends and colleagues.. To Valentina and Elena because they have changed my life and filled me with love, finally, my family for accompanying me, having patience, and supporting me. Everyone thanks.
The projects support this research:

- *Programa de Doctorados Nacionales convocatoria 647 de 2014 funded by Colciencias-Colfuturo (Minciencias).*

Resumen

En este documento se presenta una metodología de análisis de conectividad cerebral, en la cual deben abordarse tres problemas principales, el primer problema para superar es el comportamiento no estacionario de la actividad cerebral, el segundo problema es la alta dimensión de las matrices de conectividad y finalmente el agrupamiento para seleccionar los sujetos de cada conjunto de analisis. Para llevar a cabo esta metodología, fueron empleadas 3 bases de datos, la primera relacionada con estimulos auditovs y visuales bajo el paradigma oddball, la segunda y la tercera una base de datos son motor imagery con diferente numero de sujetos. Los resultados obtenidos demuestran que la segmentación de los registros en el tiempo, favorece la estimación de conectividad, además, la propuesta de una regla supervisada para reducir dimension, garantiza la interpretabilidad fisiológica de los resultados que se obtienen. Finalmente se verificó que la actividad cerebral obtenida depende de los grupos de sujetos que se conformen. Se verificó la metodología teniendo en cuenta criteros de costo computacional, estabilidad numérica, probabilidad de error, así como interpretabilidad de los resultados obtenidos.

Palabras clave

No-estacionariedad, Detección de puntos de cambio, conectividad funcional, modelo supervisado, reducción de dimensión, clustering.

Abstract

This document presents a supervised group connectivity analysis methodology, in which three main problems must be addressed, the first problem to overcome is the non-stationary behavior of brain activity, the second problem is the high dimension of the connectivity matrices, and finally, the grouping to select the subjects of each set of analyzes. To carry out this methodology, three databases were used, the first related to auditory and visual stimuli under the oddball paradigm, the second and the third a database with motor imagery with a different number of subjects. The results obtained show that the segmentation of the recordings in time favors the estimation of connectivity, in addition, the proposal of a supervised rule to reduce dimension, guarantees the physiological interpretability of the results obtained. Finally, it was verified that the brain activity obtained depends on the groups of subjects that conform. The methodology was verified taking into account criteria of computational cost, numerical stability, probability of error, as well as the interpretability of the results obtained.

Keywords

Non-stationary, Change point detection, Functional connectivity, Supervised model, Dimensionality reduction, clustering

Chapter 1

Preliminaries

1.1 Introduction

Sophisticated methods have been developed to analyze brain behavior in recent years; most methodologies seek to extract information related to the underlying neural dynamics to construct biomarkers of brain states and identify pathologies and cognitive problems [Hari and Puce, 2017] [Ilmoniemi and Sarvas, 2017] [Astolfi et al., 2007].
With these methodologies, it is possible to construct representations in different domains such as space, time, and frequency, from the pre-processed brain recordings, giving rise to features that allow efficient discrimination between various tasks and brain states, achieving excellent results in classification tasks. Unfortunately, many of those results do not provide enough physiological interpretability to understand the functional interaction or connection between different brain regions [Drysdale et al., 2017] [Crouch et al., 2018, Omidvarnia et al., 2013] [Li et al., 2016b]. The last topics revealed the interest in developing methodologies that represent the statistical relationship between different brain areas, leading to the study known as brain connectivity analysiss [Friston et al., 2003] [Zerouali et al., 2014].
Connectivity analysis describes the electrophysiological behavior of the brain, through relationships in time and frequency domains that quantify synchronized activity, spatially distributed among regions that are functionally connected, preserving the principles of integration and segregation [Lang et al., 2012][Hutchison et al., 2013][Wendling et al., 2009] [Babiloni et al., 2016] [Thilaga et al., 2018].

To this end, the analysis has three different perspectives, which are:

1-Anatomical connectivity: usually called structural connectivity, being one that directly describes the human connectome, it is built from the neighborhoods of groups of neurons and neuronal fibers in the brain. Different tissues and physiological structures are taken into account in this type of connectivity [Sporns, 2007]. This type of connectivity remains stable in short intervals of time and is usually reviewed by health professionals to find any abnormal connection at the brain level. Anatomical connections may be determined by a variety of invasive and non-invasive tract-tracing methods, being Diffusion-Weighted Imaging (DWI) the most used method [Blinowska, 2011] [Venkataraman et al., 2011]. DWI measures the mobility of the water molecules in the soft tissues, and It can generate data with the direction of the nerve fibers in the brain that allow estimating structural connectivity [Van Essen et al., 2012] [Chilla et al., 2015].

2-Functional connectivity: is the statistical relationship between two-time series; at the physiological level. It provides information on the temporal and spatial dependencies of the brain's activation patterns[Bastos and Schoffelen, 2016]. For this type of connectivity, different measures have been developed based on correlation [Bakhshayesh et al., 2019], spectral coherence [Bowyer, 2016], phase locking [Vinck et al., 2011], among others, aiming to quantify relationships between different areas of the brain [Greenblatt et al., 2012]. These connectivity methods are commonly used in electroencephalography (EEG), and they have an interpretation similar to the statistical correlation. Therefore, they generate symmetric matrices, which are analyzed using networks and graph theory; through the construction of undirected adjacency matrices, later they are thresholded to choose connections, being possible the indirect quantification of brain changes [Friston, 2011].

3-Effective connectivity: It is defined as the influence of a neuronal population on another [Toppi et al., 2014] [Brázdil et al., 2007], allowing the construction of asymmetric matrices, which are studied as weighted graphs, to deduce the direction of the flow of information between different brain areas [Buijink et al., 2015]. This type of connectivity analysis requires a temporal model to estimate the statistical influence one time series has on another. The most used models are autoregressive, from which it is possible to get the Granger causality (GC), the best-known measure of effective

connectivity, allowing us to understand the organization of the brain [Nili et al., 2020]. The last two types of connectivity are applied for different neuroimaging analyzes, and both are used in multichannel EEG signals [Bijsterbosch et al., 2018]. However, in this thesis, the purpose is to consider only functional connectivity to indirectly approach the real anatomical connections, providing a non-invasive description to analyze the brain's function. This analysis is essential because it is an alternative to estimating a complete map of neural connections in the brain, known as a human connectome.

This document will present some strategies to deal with the main problems of functional connectivity analysis, which are:

First: a growing need for high-resolution connectivity measures that allow quantifying the relationship between local specialization and the global integration of brain processes [Aviyente et al., 2017].

Second: the non-stationary dynamics of EEG recordings are generated because the relationships between different areas of the brain inherently change over time. Therefore, the evaluation of pairwise interactions is affected, causing results that do not encode brain function appropriately [Bastos and Schoffelen, 2016].

Third: reduced confidence in connectivity analysis due to noisy links (to not mention the computational burden), which can be generated by high-dimensional connectivity matrices, including redundant or worthless features drawn from specific tasks from the extraction of all possible interactions between channels. [Van Wijk et al., 2010].

Regarding the first problem, there are many functional connectivity measures; some are based on information theory, others on spectral estimation, and others on directly establishing statistical relationships over time [Sakkalis, 2011]. However, in this work, I have opted for measures based on phase synchronization since they are less susceptible to volume conduction effect when performing connectivity analysis between EEG channels and are also appropriate for tasks in which there are multiple repetitions [Betzel et al., 2012].
To overcome the second problem about the non-stationary nature of EEG signals, many proposed approaches are based on the quasi-stationary activity of large neural populations, extracting measures of connectivity in a set of previously segmented time

intervals, which are statistically tested [Pereda et al., 2018], this type of approach is known as piecewise analysis [Kaplan et al., 2005]. However, in state of the art, there is no established criterion for EEG piecewise analysis, therefore in this work, a change point detection algorithm is proposed allowing to obtain time windows of different sizes, which is tested according to the changes in the first and second statistical moments.

Regarding the third problem related to dimensionality reduction of connectivity matrices, thresholding methods are employed, generally retaining the most potent connections (pairwise interaction), either by holding the values surpassing a given total weight or constraining the edge density in the graph [Váša et al., 2018]. Nonetheless, each particular thresholding rule influences the number of weak connections, which, in turn, yields a distinct effect on the structure and global properties of sparsified networks [Garrison et al., 2015]. Therefore, in this work, for this problem, a supervised statistical rule is proposed, selecting connections according to a hypothesis test, guaranteeing reliability, and preserving brain function's interpretability.

Moreover, to improve the impact of the proposed strategies, group analysis is included. That is a different stage to determine the generalized behavior and familiar patterns of a group of people from the studies done individually on subjects [Huster et al., 2015] [Huster and Raud, 2018]. To this end, the concatenation of single-subject connectivities into a group array is carried out. A hypothesis test is made, and the meaningful connections are selected, which are representative of the whole set or group-level [Morup et al., 2007].

This document presents a connectivity analysis to estimate the meaningful connectivity that considers the temporal characteristics of the underlying neural responses, evaluating the contribution of a set of connections to improve brain activity interpretability based on statistical significance. To this end, the piecewise functional connectivity analysis at the group level is done to address the non-stationarity of EEG data that causes brain networks to change over time. Furthermore, taking advantage of the labels available for EEG responses, a supervised statistical threshold algorithm reduces the worthless features while maintaining the most significant brain activity connections. The methodology can be used as an alternative to improve the performance and interpretability of other works, in order to contribute to the development of effective studies and treatments for neurological diseases such as schizophrenia [Shim et al., 2014], pathological tremors [Buijink et al., 2015],

epilepsy [Van Mierlo et al., 2014], Alzheimer's disease [Schumacher et al., 2019] [Güntekin et al., 2008], and Parkinson's disease [Allen et al., 2014], the better understanding of cognitive processes as emotions [Lithari et al., 2010, Liu et al., 2019] [Chen et al., 2015] and attention [Kiiski et al., 2020], and the improvement of Brain-Computer Interface (BCI) systems [Hamedi et al., 2016], among other applications.

1.2 Objectives

1.2.1 General Objective

To develop a brain connectivity analysis framework that improves the interpretation of brain activity, taking into account the non-stationarity behavior of the EEG and generalization at the group level.

1.2.2 Specific Objectives

- To develop a method that allows the estimation of brain connectivity, taking into account the non-stationarity behavior of the EEG.
- To introduce a methodology that allows selecting significant connections using the EEG recordings' information, taking into account their class labels.
- To develop a methodology to apply generalization at a group level, allowing a better interpretation of the brain function.

1.3 Outline

This work presents a methodology that allows us to approach the analysis of brain connectivity in the following parts:
In the first part, I conducted a conventional connectivity study, in which I measured connectivity by subjects. I also showed the brain connections' behavior that has more relevance in developing the task through thresholding. The second part presents a supervised methodology that includes tags' information to improve brain activity interpretation through connectivity. Then I did a topology analysis using different graph measurements(networks). The third part includes a segmentation methodology in time, which increases the previous methods' statistical performance, overcoming the non-stationary dynamics of the EEG; the analysis is also carried out at the group level. Finally, in the last part, different applications are presented on databases of emotions and motor imagery in a state of rest to separate the background activity from the relevant activity, taking advantage of our methodology.
Besides, a discussion of this work's critical aspects is included: The importance of correctly selecting the time window for estimating connectivity. On the other hand, it is necessary to make a fine selection of the relevant connectivities to obtain an accurate brain activity description. Also, the labels' information increases analytical performance, leading to better topology results and better physiological interpretation. Our methodology allows us to estimate brain connectivity to perform an adequate group analysis.

1.3.1 Publications of research results

This thesis is supported by the publications presented in international peer-reviewed journals mentioned below:

- Emotion discrimination using spatially compact regions of interest extracted from imaging EEG activity. Jorge I Padilla-Buritica, Juan D Martinez-Vargas, German Castellanos-Dominguez. Frontiers in computational neuroscience, 2016 [Padilla-Buritica et al., 2016].

- Supervised piecewise network connectivity analysis for enhanced confidence of auditory oddball tasks. Jorge I Padilla-Buritica, Juana V Hurtado, Germán Castellanos-Dominguez. Biomedical Signal Processing and Control, 2019 [Padilla-Buritica et al., 2019].

- Non-stationary group-level connectivity analysis for enhanced interpretability of oddball tasks. Jorge I Padilla-Buritica, Jose M Ferrandez-Vicente, German A Castaño, Carlos D Acosta-Medina, Frontiers in Neuroscience, 2020 [Padilla-Buritica et al., 2020].

In addition to the previous publications, other research results related to this thesis were presented; the following stand out:

- Spatial Resolution of EEG Source Reconstruction in Assessing Brain Connectivity Analysis. Jorge Ivan Padilla-Buriticá, Juan David Martínez-Vargas, A. Suárez-Ruiz, José Manuel Ferrández, Germán Castellanos-Dominguez. International Work-Conference on the Interplay Between Natural and Artificial Computation, 2017 [Padilla-Buriticá et al., 2017].

- Functional connectivity analysis using the oddball auditory paradigm for attention tasks. Juana Valeria Hurtado-Rincón, Francia Restrepo, Jorge Ivan Padilla, Hector Fabio Torres, German Castellanos-Dominguez. International Conference on Brain Informatics, 2018 [Hurtado-Rincón et al., 2018a].

- Influence of Time-Series Extraction on Binge Drinking Interpretability Using Functional Connectivity Analysis. Jorge Ivan Padilla-Buriticá, H. Torres, E. Pereda, A. Correa, G. Castellanos-Domínguez. International Conference on Brain Informatics, 2018 [Padilla-Buriticá et al., 2018].

- Group differences in time-frequency relevant patterns for user-independent BCI applications. Luisa F Velásquez-Martínez, F.Y. Zapata-Castaño, Jorge I Padilla-Buritica, José Manuel Ferrández Vicente, Germán Castellanos-Dominguez. International Work-Conference on the Interplay Between Natural and Artificial Computation, 2019 [Velásquez-Martínez et al., 2019].

Chapter 2

Human Connectome and brain connectivity

In neuroscience, connectivity analysis works on modeling the brain and its activity as a connected network based on the central concept of this area: *the connectome*.
The human connectome is a map that draws all the brain connections[Fornito et al., 2016]. According to the availability of brain information acquisition device, it allows to visualize and understand the following:

- The connections between each neuron and the synapses individually.
- Connections between axons (cell populations)
- The activity between different brain regions.

In this document, we will focus on a description of the connectome, and of different electrophysiological aspects of the brain. Besides, a description of the representation with graphs will be made, giving rise to a topological architecture of the brain.

2.1 The human brain

The nervous system is divided into two parts: the central system and the peripheral system. The first is made up of the brain and spinal cord, and the second is composed of the motor and sensory nerves that start from the central nervous system. The human brain is the main organ of the central nervous system and is located within the skull [Mai and Paxinos, 2011]; its main component is the cerebral cortex, a layer of folded

neuronal tissue, which covers the surface of the hemispheres. This organ is responsible for regulating and maintaining the vital functions of the body [Carter, 2019]. The adult human brain has an approximate volume of $1100cm^3$, and about 80 billion neurons [Herculano, 2009]. Likewise, the most relevant thing for the transformation of brain functioning is the complexity given by the connections that are established between the different neurons [Bassett and Gazzaniga, 2011].

On the other hand, this organ is divided into three main parts: the brainstem, cerebellum, and cerebrum. Of these, the cerebrum (telencephalon) is the one with the most significant weight, and volume [Vanderah and Gould, 2020]. The human brain is protected by the skull's bones, suspended in cerebrospinal fluid, and isolated from the blood by the blood-brain barrier. Still, its delicate nature makes it susceptible to many types of damage and disease [Penfield, 2015]. The most common physical injury forms are internal injuries from head trauma, stroke, or poisoning [Finger, 2013]. The human brain is also susceptible to degenerative diseases, such as epilepsy [Englot et al., 2016], Parkinson's disease [Ding et al., 2015], multiple sclerosis [Dobson and Giovannoni, 2019], and Alzheimer's disease [Kumar et al., 2015]. Some psychiatric disorders, such as schizophrenia [Mouchlianitis et al., 2016], depression [Acharya et al., 2015], are partially caused by brain dysfunctions, although the nature of such brain abnormalities is currently not well-known [Dinh et al., 2019].

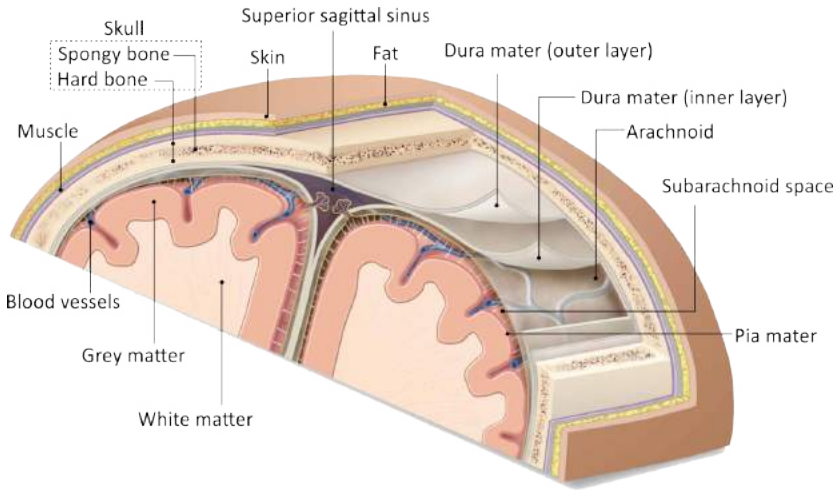

Figure 2.1: Distribution of layered-tissues conforming the human head.

Figure 2.1 shows the different layers conforming to the human head, where the brain's outmost layer is the cerebral cortex (grey matter). Mainly, this tissue has a folded

structure increasing the surface area and allowing complex connections. Likewise, the white matter that is contained and surrounded by gray matter mainly consists of tract fibers allowing the information transfer between separated areas in the brain [Hawrylycz et al., 2012].
The adult brain is composed of 78% water, 10% fat, and 8% protein. It accounts for only 2% of body weight and uses 20% of the energy we produce [Lui et al., 2011]. The parts into which it is divided are the following:

Brainstem : is located at the base of the brain. It controls vital functions such as heart rate, digestion, respiration, and blood pressure. Also, it connects the brain with the rest of the body through the spinal cord. The Brainstem is divided into the medulla oblongata, pons, and midbrain [Lynn and Bassett, 2019].

Cerebellum: is responsible for maintaining balance, posture and is involved in the movement of the entire body. It ensures that the actions are carried out in a coordinated and precise manner [Carter, 2019].

Cerebrum (Telencephalon): is the largest part of the brain containing the cerebral, this part is related to the senses, emotions, memories, and reactions [Blumenfeld, 2010]. In short, it is the head of our body. It is responsible for receiving, processing, and responding to different stimuli. For example: by resting the hand on a hot surface, the brain gets a signal that the temperature is very high, then it responds by sending an order to the muscles of the hand to withdraw it immediately [Waxman, 2016].

The cerebral cortex is a thin, folded layer. First, the brain is divided into two cerebral hemispheres, the left and the right. The right hemisphere is related to non-verbal expression, intuition, or recognition of faces, voices, melodies, etc. In this hemisphere, thoughts and memories are manifested through images [Hendelman, 2015]. The left hemisphere is related to the functions of speaking and writing, also, expression and understanding of language. It also has to do with functions such as analyzing, logical reasoning, solving numerical problems, among others. Both hemispheres are connected through a structure called the corpus callosum. The right hemisphere is in charge of controlling the left side of the body, while the left hemisphere controls the right part of the body. Each hemisphere is divided into four lobes [Baillet et al., 2001]:

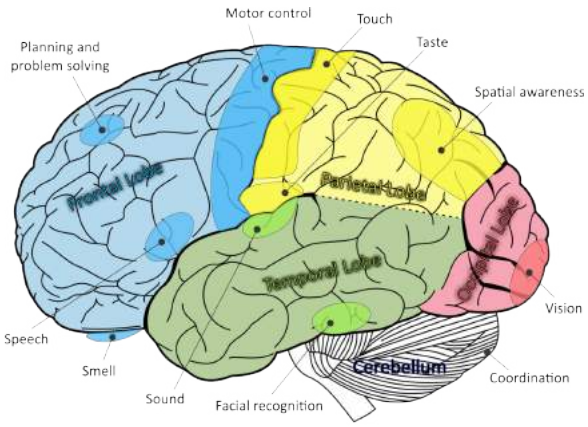

Figure 2.2: Brain structures and function areas. Figure adapted from [Gray and Goss, 1974] public licensee.

- Frontal, made up of areas that process conscious thought and problem-solving.
- Parietal is responsible for the perception of stimuli related to touch, pressure, temperature, and pain.
- Temporal, it processes the perception and recognition of auditory and memory-related stimuli.
- Occipital is made up of structures that are responsible for processing visual stimuli.

Figure 2.2 shows different areas of the brain, in which specialized processes related to the senses are carried out, as well as motor processing, memory, and information analysis[Stevenson et al., 2014].

2.1.1 Neural Activity and Action Potentials

EEG Generation

The EEG is the measurement of the currents that flow during synaptic excitations of many pyramidal neurons in the cerebral cortex [Olejniczak, 2006]. When neurons are activated, they generate synaptic currents in dendrites; These currents generate electric fields measured on the scalp by systems such as the electroencephalograph (EEG system). Electric fields result from different sums of postsynaptic potentials generated

from the dipoles existing between the body of pyramidal neurons (soma) and apical dendrites (which branch off neurons) [Schmidt et al., 2012]. On the other hand, The current in the brain is generated mostly by pumping the positive ions of sodium, Na+, potassium, K+, calcium, Ca++, and the negative ion of chlorine, Cl−, through the neuron membranes in the direction governed by the membrane potential[Carter, 2019].

Layer	**Resistivity**
Scalp	2.22 Ωm
Skull	177 Ωm
Brain	2.22 Ωm

Table 2.1: The three main layers of the brain including their approximate resistivities (Ω = ohm)

.

As shown in Table 2.1, the skull attenuates the signals approximately one hundred times more than the other layers. On the other hand, most of the internal noise is generated within the brain [Sanei and Chambers, 2013]. In contrast, the external noise is generated on the scalp so that only significant populations of active neurons can generate enough potential to be recorded using the electrodes of the scalp.

Electroencephalography (EEG)

In 1985 the first findings of electrical phenomena at the brain level in rabbits and monkeys occurred; later, in 1875, and Hans Berger obtained the first human EEG recording in 1924 [Malmivuo et al., 1995, Berger, 1934]. From these advances, the most used registry at a clinical and investigative level is the EEG. A typical EEG setup is shown in Figure 2.3a using the so-called $10-20$ system; however, currently, mounts are containing about 250 electrodes distributed in an adjustable silicone cap (Figure 2.3b) that can be adapted to most human heads[Liu et al., 2017, Marino et al., 2016].

Different methods currently developed in state of the art to process EEG, allow to remove interferences, select frequency bands, refer channels, even overcome the non-stationary dynamics of the record, allowing a better interpretation of brain activity.

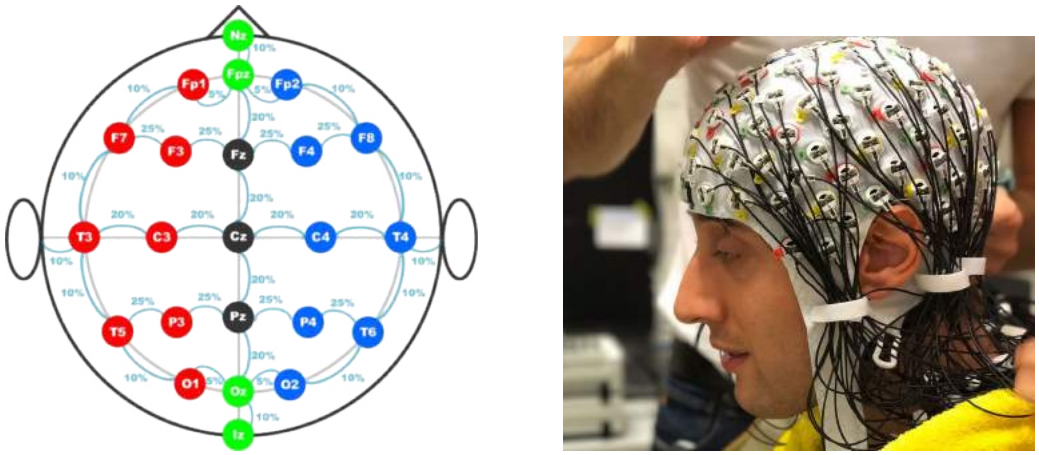

(a) Typical $10-20$ EEG system electrode distribution.

(b) hdEEG helmet with 128 electrodes.

Figure 2.3: EEG arrays. Fig.(a) was adapted from [Trans Cranial Technologies Ltd., 2012] with public license. Fig.(b) was adquired in the Laboratory of Movement Control and Neuroplasticity, Department of Movement Sciences, KU Leuven, Belgium.

2.1.2 Brain rhythms

The brain produces different electrical impulses that travel through neurons and later reach the scalp; the electrical dynamics of these impulses give rise to EEG signals, which are made up of different brain waves or rhythms [Sanei and Chambers, 2013]. Brain waves are significant because they are associated with different states of consciousness, such as intense concentration, alertness, deep sleep, drowsiness, relaxation, hypnosis, altered states of consciousness [Hu and Zhang, 2019]. These waves have different frequency of oscillation and location in time, giving rise to the following definitions:

Delta Waves ($< 4Hz$): are generally above 1hz, as below it could mean brain death, besides, these types of waves are generated in a state of deep sleep [Olejniczak, 2006].

Theta waves (4 - 8Hz): are waves of greater amplitude and lower frequency, they appear during states of inspiration and generation of ideas and creative solutions. It is a state in which the tasks performed have been automated, and it is no longer necessary to have an attentional and conscious control of their execution, the subject being able to distance themselves from them mentally [Zhang et al., 2018].

Alpha waves (8 - 12*Hz*): represents a state of low brain activity and relaxation. These waves are slower and older; a person who has finished a task and sits down to rest is often in an alpha state, as well as the person who is taking a walk, enjoying the scenery [Ergenoglu et al., 2004].

Beta waves (12-30*Hz*): are produced when the brain is awake and involved in mental activities. They are vast waves, and those with the highest speed of propagation denote intense mental training. Generally, when a person is concentrating, studying, doing a math problem, etc., his brain is emitting these types of waves [Gola et al., 2013].

2.2 Brain as network

At the systems level, the brain distributes computing across multiple different computers. A good analogy is a P2P network that spreads task processing across multiple computers, where each computer is specialized to perform some specific aspect of computing [Ebrahim et al., 2014]. Taking this as a reference, if we call computers *nodes* (which can represent anything, for example, brain regions) and connections *edges*, we can say that the brain is an interconnected network [Sporns, 2018]. Allowing us to have a quantitative and visual approach to understand the networks work as a whole [Sakkalis, 2011]. We should take advantage of modern network approaches to study the brain because these approaches can provide fundamental insights into how simple elements organize into dynamic patterns, thus significantly adding to the insights that can gain by considering the individual components in isolation. Therefore, it is necessary to understand and quantify the principles of brain integration and segregation [Greenblatt et al., 2012].

2.2.1 Integration and segregation

One of the most important and surprising features of the brain is its ability to reconfigure connections to process and respond appropriately to stimuli [Sporns, 2007]. Dynamic reconfiguration is understood as the increase or decrease in connections with increased neuronal activity. In the brain, an increase in the cohesion of neural circuits is known as integration, and a decrease is known as segregation [Greenblatt et al., 2012]. Integration is linked to the rapid exchange of information between different and distant

areas, while segregation is associated with information processing in localized areas. The brain changes from a segregated to an integrated state depending on the nature and strength of the stimuli it receives [Hurtado-Rincon et al., 2014].

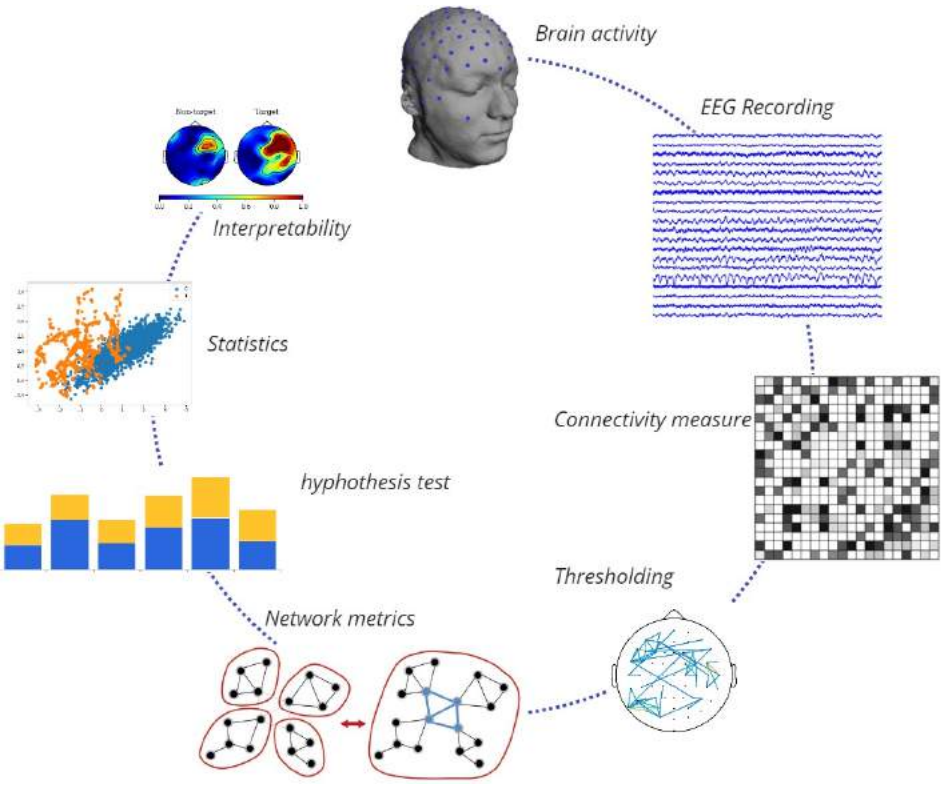

Figure 2.4: The general scheme of brain connectivity analysis includes thresholding to carry out network analysis using graphs.

Therefore, the stimuli that arrive through the senses are processed in a segregated way in the cerebral cortex to be partially or totally integrated according to the needs. While watching a video, we incorporate images and sounds, ignoring smells and other stimuli [De Vico Fallani et al., 2014]. However, when we notice an odor, the brain goes into a warning state to integrate and analyze all the available information to make quick decisions. Despite the importance of integration and segregation, the physiological mechanisms linked to brain dynamics are still not well understood and are being studied. Besides, another unknown element is the sensitivity of the integration-segregation capacity with respect to the number of physical connections existing between the brain regions [Sakkalis, 2011].

A general summary of this thesis can be seen in figure 2.4, where brain activity is estimated at the scalp level to quantify the principles of integration and segregation based on the level of connectivity between different areas.

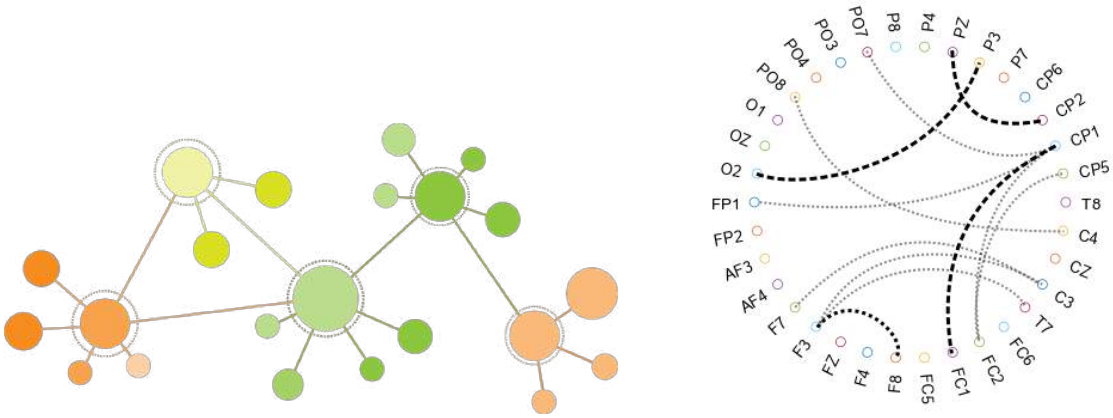

(a) General representation of a network.

(b) Circular connectivity diagram2.

Figure 2.5: EEG arrays. Fig.(a) was adapted from [Trans Cranial Technologies Ltd., 2012] with public license. Fig.(b) was adquired in the Laboratory of Movement Control and Neuroplasticity, Department of Movement Sciences, KU Leuven, Belgium.

On the other hand, Figure 2.5a shows a general representation of a network, made up of nodes and edges, whose relationship can be quantified using graph theory. In Figure 2.5b, An example of a circular connectivity diagram between different EEG channels is presented.It is essential to mention that the work related to integration and segregation is done both at the cortical and scalp levels; in both cases, it must take restrictions into account.

2.2.2 Human connectome

According to the way neurons are linked to each other, a complex network is built that describes the brain's functioning [Dimitriadis et al., 2017]. When it is possible to know how the elements of the network are connected and also understand the dynamics of the connections [De Vico Fallani et al., 2014], it can be said that there is a complete description of the complex network [Preti et al., 2017].
The human connectome describes the complete set of all the neural connections of

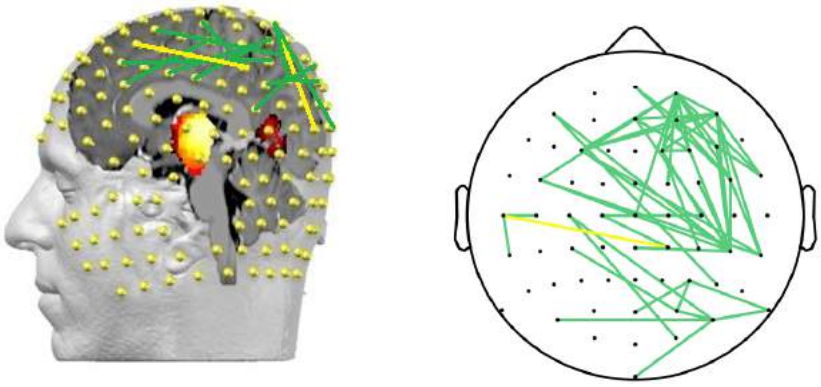

(a) 3D head side view with connectivity links.

(b) Top view of the head with connections between channels.

Figure 2.6: EEG arrays. Fig.(a) was adapted from [Trans Cranial Technologies Ltd., 2012] with public license. Fig.(b) was adquired in the Laboratory of Movement Control and Neuroplasticity, Department of Movement Sciences, KU Leuven, Belgium.

the human brain as a complex network [Fox, 2018]. The principles of integration and segregation between the elements of the network can be quantified, allowing the construction of a network map [Sporns, 2018]. This map is critical to analyze the function and dynamics of brain activity; usually, the map is constructed at the cortical level [Betzel and Bassett, 2017]. However, this work will build the map at the scalp level, which allows an analysis that provides arguments that can be used as an alternative for other neuroscience studies (See Figure 2.6, where a map of the most relevant connectivities is presented when carrying out a cognitive task.).

However, one of the most significant challenges will be to discover how these networks shape the integrated activity and dynamics of the brain regions to relate it to our health, behavior, and cognitive states [Sporns, 2007]. Therefore, the closest solution is the connectome, the fundamental piece of brain connectivity analysis [Bowyer, 2016], which provides a complete description of how the brain regions are interconnected when any activity is carried out [Thee et al., 2018].

2.3 Summary

In this chapter, the generation of electrical activity at the brain level and its respective acquisition through EEG recording has been reviewed. The definition of brain rhythms and their electrophysiological significance are also included. On the other hand, this chapter highlights the description of the brain as an interconnected network, where the principles of integration and segregation are fulfilled, which can be quantified and analyzed using graph theory, giving rise to the concept of the connectome. The entire set of interactions between brain regions that occur when a task is carried out is fully described. As mentioned so far, we only describe the connectome as a map of the brain connectivity network; however, it has not yet been delved into how it will address other problems related to obtaining it. These aspects that will be treated in the following chapters provide alternative solutions for issues such as non-stationarity, the thresholding of connections, and later the assembly of the estimated connectivities to give a correct physiological interpretation.

Chapter 3

Piecewise functional connectivity analysis with fixed window

We present a network connectivity analysis to assess a relevant vector, valuing the contribution of connection node sets in distinguishing between labeled response stimuli. To this end, the piecewise computation of Phase Locking Index is performed, suggesting a combination procedure to reflect the whole recording span with a single relevance value. Further, we use a supervised, statistical thresholding algorithm to reduce the connectivity matrix dimension, holding the links that mostly differentiate the brain responses to each evoked stimulus. Obtained results in an auditory oddball task show that the developed analysis yields a relevant node set for δ and θ waves that becomes more coherent, connected with improved consistency of performed group-level connectivity graphs.

3.1 Introduction

In the development of physiologically relevant studies, oddball tasks are used very often to identify perceptual differences, facilitate a deeper interpretation of attention and memory tasks. In this way, to supply significant evidence about cognition tasks and brain function, relationships between neuroimaging measures and behavior are increasingly investigated, often using electroencephalography (EEG) due to qualities like his high temporal resolution, affordability, and portability. Mainly, event-related potential (ERP) components are employed to reflect canonical neural operations, which are brain activities predictably modulated

within Spatio-temporal windows [Bridwell et al., 2018]. This allows neuroimaging measures to advantage from tracking the evoked time-variant responses in different brain structures. In this aspect,graph-based methods are employed to characterize EEG functional connectivity, intending to provide a more nuanced view of the neural dynamics during target detection/novelty processing in normative and pathological populations [Blinowska, 2011].

During the study of brain networks, they are faced with several limitations: One need is to provide a delicate balance between local specialization and global integration of brain processes through high-resolution connectivity measures [Aviyente et al., 2017]; Brain networks change intrinsically and dramatically over time due to non-stationary EEG, degrading the assessment of pairwise interactions, which are operationalized through the partial or complete correlation/information between all pairs of regional time series [Bastos and Schoffelen, 2016]; A high-dimensional connectivity matrix can result from the extraction of all possible inter-channel interactions, including redundant features from specific tasks and making the connectivity analysis confidence be diminished because of noisy links without taking into account computational cost issues [Van Wijk et al., 2010]

Many of the approaches are based on quasi-stationary activity in large neuronal populations due to EEG signals' non-stationary nature. They are extracted from a set of previously segmented time intervals synchronization measurements, which are modeled or even statistically tested [Pereda et al., 2018], as stationary [Kaplan et al., 2005]. It is worth mentioning that various neural dynamics can be ignored when removing segments in multiple trial tasks as a cause of the Spatio-temporal activity of ERP. For the dimensionality reduction of connectivity matrices, the thresholding methods have proven to be of great help, preserving the most decisive edges, that is, the interaction by pairs, either by holding the edges surpassing a given absolute weight by constraining the edge density [Váša et al., 2018]. However, the number of weak connections is influenced by each specific threshold rule. which produces a different effect on the global properties of sparsified networks and their structure [Garrison et al., 2015]

However, one of the significant problems is from the data sets of a single-subject to determine the latent structure that should directly generalize across subjects. For this reason, two main approaches of group-level analysis are widely considered [Huster and Raud, 2018]: Concatenation of single-subject data into a group array from which a latent structure of sources is calculated, being representative of the sample as a whole [Morup et al., 2007] and clustering of components estimated from

EEG data [Huster et al., 2015]. Indistinctly of the group-level strategy, nevertheless, the activity patterns are far from being time-locked across trials perfectly. Also, there is significant variability across subject samples. Hense, standard approaches for group-level performance degrade sharply.
we present a graph network analysis that takes into account the temporal characteristics of the neural responses for the estimation of a relevant connectivity vector, determining the contribution of a link node-set in differentiating between labeled ERP stimuli, with the primary purpose of reducing the variability of a neural process in the entire sample. This chapter employs a supervised, statistical thresholding algorithm to reduce the worthless features due to the network's brain change over time (non-stationarity of EEG). We have the labels for the EEG responses, holding the connections that differentiate the brain's responses to each evoked stimulus.

3.2 Materials and Methods

EEG Database description and preprocessing

Six females and eleven males ($M = 17$ subjects, with a mean age among the participants 27.7 years).Subjects participated in three runs following the oddball auditory paradigm, having two labeled stimuli $\lambda = \{l, l'\}$. It is worth mentioning that the first two auditory stimuli of each run were non-target, that is, a 390 Hz pure tone selected within a trough of the scanner sound spectrum, while the target sound was a broadband *laser gun*. Concerning attentional tasks, subjects were asked to react to target stimuli, using a button press as described in [Muraskin et al., 2018]. Linked to the acquisition protocol of validated database, Figure 3.1 shows the trial timing of the attention task-oriented paradigm with a series of auditory stimuli, the frequently presented, designate as *Non-Target*, and comprising both rarely presented sounds, designate as *Target*. The implemented trial timing of each stimulus lasts 200 ms uniformly distributed variable inter-trial interval.
Scalp data were acquired at 1000 Hz sampling rate using an EEG data acquisition system with a custom cap configuration of $C = 34$ channels. The following preprocessing Butterworth filters were used: 1-Hz high pass to remove direct current drift; notched filter (centered at 60 and 120 Hz) to eliminate the electrical power line and its first harmonic, respectively; and a low pass filter with a cut frequency at 120-Hz to exclude high-frequency artifacts not having neurophysiological content.

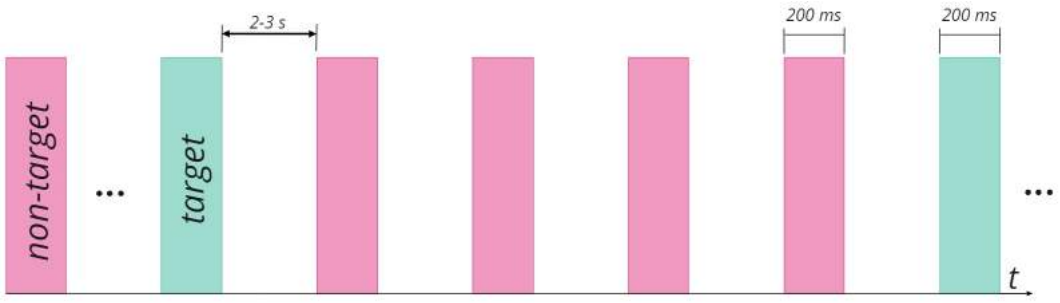

Figure 3.1: Trial timing of the attention task-oriented paradigm, displaying a series of auditory stimuli.

The whole pipeline encompasses a linear-phase finite-impulse-response filter to avoid distortions from phase delays [Walz et al., 2013]. As a result, the observation EEG dataset $\{\boldsymbol{X}^{\lambda}_{mn} \in \mathbb{R}^{C \times T \times N}\}$ is collected from each subject $m \in M$, holding $n \in N$ trials and recorded out from each c-th scalp electrode, $c \in C$, at time sample $t \in T$, being $N = 375, T = 1.5s$.

3.2.1 Subject-level inter-channel connectivity

To study the pairwise functional connectivity within the recording time span $T \in \mathbb{R}^{+}$, we use *Phase Locking Index* (*PLI*) that quantifies the asymmetry of phase difference distribution between two specific channels c, c', defined as:

$$y_{ft}(c, c') = \left| \boldsymbol{E}\{\text{sgn}\left(\sin(\Delta\Phi_{ft}(n; c, c'))\right) : \forall n \in N\} \right|, \forall c, c' \in C, c \neq c' \tag{3.1}$$

where notations sgn and $\boldsymbol{E}\{\cdot : \forall n\}$ stand for *sgn* function and averaging operator over n, respectively. $\Delta\Phi_{ft}(; c, c') \in \mathbb{R}[0, \pi]$ is the instantaneous phase difference $\Delta\Phi_{ft}(; c, c') \in \mathbb{R}[0, \pi]$ that is the angle computed through the continuous wavelet transform coefficients $W_{ft}(;) \in \mathbb{R}^{+}$ as follows:

$$\Delta\Phi_{ft}(n; c, c') = \frac{W_{ft}(n; c) W_{ft}(n; c')}{|W_{ft}(n; c)||W_{ft}(n; c')|}, \; t \in T \tag{3.2}$$

In the following, connectivity analysis is performed only for low-frequency bands $\Omega \in \{\delta, \theta\}$ *Hz* since previous studies on cognitive dynamics have shown that oscillatory ERP responses are mainly composed of both waves [Güntekin and Başar, 2010]. Hence, we obtain the inter-channel connectivity vector, noted as $\hat{\boldsymbol{y}}^{\Omega}_{t} \in \mathbb{R}^{V}$, holding elements

$\hat{y}_t^{\Omega}(v)\in\mathbb{R}$ computed by averaging each connectivity measure across the frequency domain within either wave $\Delta F_{\Omega}\in\{\Delta F_{\delta} = [2\text{-}5], \Delta F_{\theta} = [5\text{-}8]\}$ as follows:

$$\hat{y}_t^{\Omega}(v) = \boldsymbol{E}\{y_{ft}(v) : \forall f \in \Delta F_{\Omega}\} \tag{3.3}$$

where the pairwise variable is noted as $v\in\{c, c'\in V, c\neq c'\}$, being $V = C(C\text{-}1)/2$. Here, a sixth-order Daubechies wavelet function is used, for which coefficients $D5$ and $D6$ corresponding to 2-5 Hz and 5-8 Hz have been selected to extract ΔF_{δ} and ΔF_{θ}, respectively.

3.2.2 Piecewise construction of supervised group-level connectivity graphs

From the above subject-level phase, we obtain the time-course of inter-channel connectivity vector $\hat{\boldsymbol{y}}_{tm}^{\Omega}\in\mathbb{R}^V$ that is calculated for every subject $m\in M$. To get the connectivity values are frequently extracted from a set of quasi-stationary time segments (piecewise analysis),to cope with the EEG nonstationarity as shown in [Kaplan et al., 2005]. To this end, the recording time T is split into a set of non-overlapping intervals $\Delta\tau_i\subset T$, each one equally lasting $\Delta\tau_1$. Consequently, a node connectivity vector $\tilde{\boldsymbol{y}}_{\tau m}^{\Omega}\in\mathbb{R}^V$ is built within the interval set $\{\Delta\tau_i\}$ as below:

$$\tilde{\boldsymbol{y}}_{\tau m}^{\Omega} = \boldsymbol{E}\{\hat{\boldsymbol{y}}_{tm}^{\Omega} : \forall t \in \Delta\tau_i\},\ \tau \in [0, \Delta\tau_1]$$

Also,we present that the connections that reach Also, we formulate a supervised statistical threshold algorithm whereby the connections that reach a specific value are selected and thus eliminate false links and noise,(noted as STh:

$$\kappa_{\tau}^{\Omega\lambda}(v) = \begin{cases} 1, & \mathcal{M}_p\{\tilde{y}_{\tau m}^{\Omega}(v)|l, l' : \forall m\}<\bar{p} \wedge\ \lambda = \mathrm{sgn}(\zeta) \\ 0, & \text{Otherwise} \end{cases} \tag{3.4}$$

where $\mathcal{M}_p\{\tilde{y}_{\tau m}^{\Omega}(v)|\lambda{:}\forall m\}$ measures the statistical differences between the label groups across the subject set.We use the non-parametric Mann-Whitney test,Aiming at validating whether two labeled samples are likely to derive from the same population, the statistical measure is frequently performed on EEG connectivity tasks [Hussain et al., 2017], converting sum-of-ranks to a value $\zeta\in\mathbb{R}$ under a significance level $p\in\mathbb{R}[0, 1]$. Note that we assign the following label values: target – $l = 1$, non-target

– $l' = -1$. Also, to adjust for multiple comparisons at different frequency bands δ and θ a correction for multiple comparisons is performed by the false discovery rate, validating each one of the connections.

Nonetheless, the relevance value $\kappa_{\tau}^{\Omega\lambda}(v) \in \mathbb{R}^{+}$ is computed piecewise over each time interval $\Delta\tau_i$. Consequently, to reflect thoroughly the recording span T with a single relevance value, we assume that value $\kappa^{\Omega\lambda}(v)$ becomes significant if the rule yields 1 in 4.5,at least, one time across the interval set τ, computing each connectivity relevance by the following concatenation procedure:

$$\begin{aligned} \kappa^{\Omega\lambda}(v) &= \bigcup_{\forall\tau_i} \kappa_{\tau}^{\Omega\lambda}(v) \\ &= \kappa_{\tau_1}^{\Omega\lambda}(v) \parallel \kappa_{\tau_2}^{\Omega\lambda}(v) \parallel \ldots \parallel \kappa_{\tau_6}^{\Omega\lambda}(v) \end{aligned} \tag{3.5}$$

$$\begin{aligned} \kappa^{\Omega\lambda}(v) &= \bigcup_{\forall\tau_i} \kappa_{\tau}^{\Omega\lambda}(v) \\ &= [\kappa_{\tau_1}^{\Omega\lambda}(v) \vee \kappa_{\tau_2}^{\Omega\lambda}(v) \vee \ldots \vee \kappa_{\tau_6}^{\Omega\lambda}(v)] \wedge [\kappa_{1}^{\Omega\lambda}(v) \vee \kappa_{2}^{\Omega\lambda}(v) \vee \ldots \vee \kappa_{m}^{\Omega\lambda}(v)] \end{aligned} \tag{3.6}$$

where notation $\parallel$ stands for OR logical operator.

For each subject m, therefore, we obtain a resulting graph $\boldsymbol{g}_{tm}^{\Omega\lambda} = [\hat{\boldsymbol{y}}_{tm}^{\Omega\lambda}\boldsymbol{\kappa}^{\Omega\lambda}]$, $t \in T$, where $\boldsymbol{\kappa} \in \mathbb{N}^{V}$ is the relevant connectivity vector, extracted from the supervised group-level connectivity measurements which encodes the assessed contribution of the connection node set.

Finally, all significant links estimated by thresholding the pairwise functional connectivity constitute the brain graph with a topology quantified by the node strength as the sum of weighted links between a given node and all other graph vertices. That is, $\bar{g} = \boldsymbol{E}\{g(v) : \forall v \in V\}$.So, as a brain graph measure, the average node strength is frequently used in oddball auditory studies to reflect how strongly a node is connected to others.

3.3 Results

In the Figure 3.2, we propose the pipeline of the supervised piecewise network connectivity analysis for validation, evaluating two stages: Subject-level pairwise connectivity analysis and Piecewise computation of group-level connectivity graphs.

Nevertheless, aiming to enhance the interpretation of the first stage's results, an assessment of evoked strange auditory potentials is performed.

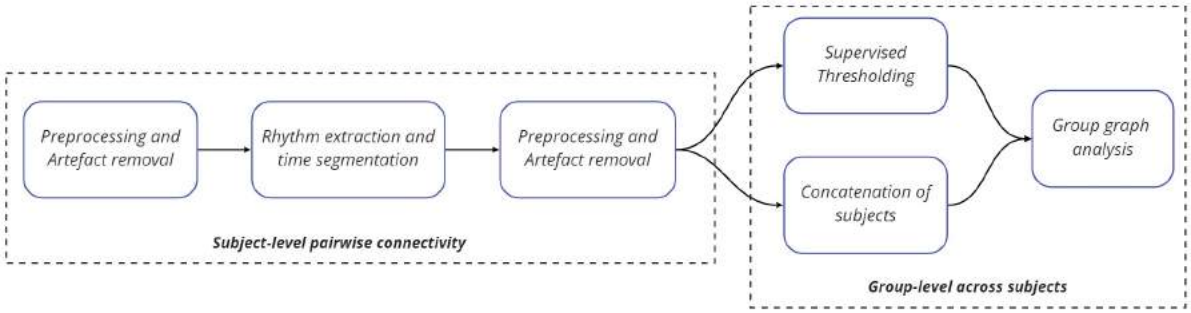

Figure 3.2: Pipeline of the supervised piecewise network connectivity analysis.

Estimation of evoked auditory oddball potentials A representative ERP waveform is extracted from each subject by averaging across his trial set acquired in either evoked condition separately (target and non-target). Figure 3.3a displays the grand average ERP waveform that is averaged across all subjects, holding positive and negative components that shows the difference in ERP amplitudes between stimuli. This measured dissimilarity highlights at electrodes related to the stimulus processing. As displayed in Figure 3.3b, between 300 and 450 ms after onset stimulus, the topography sequence of the target condition concentrates the energy in central, frontal and temporal locations, related to attention mechanisms in task processing [Polich, 2007].

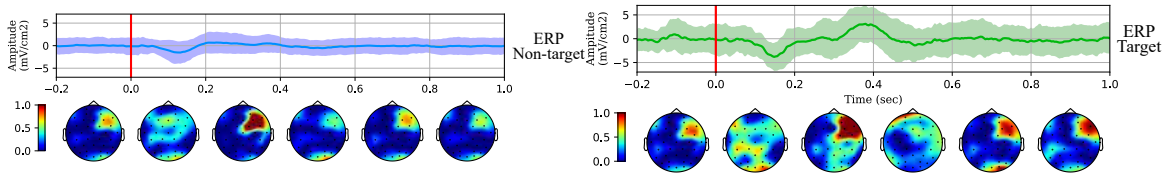

(a) Auditory ERP (b) Visual ERP

Figure 3.3: Different ERPs.

Subject-level pairwise connectivity estimation Visual inspection of functional connectivity dynamics (top and middle rows) in Fig. 3.4 evidences the relationship

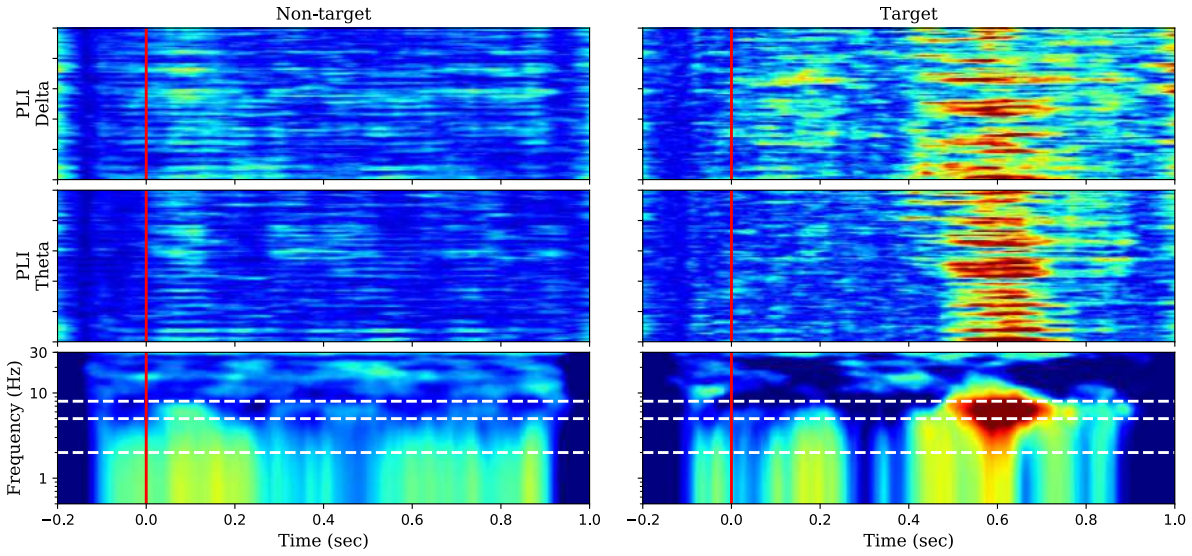

Figure 3.4: Functional connectivity estimation across the node and subject sets of either estimated for considered stimulus. Baseline interval of normalization is 200 *ms* (before red line).

between PLI and the grand-average ERP time-courses. Note that the PLI measure is normalized to highlight the connectivity patterns generated by each evoked stimulus, being each PLI mean-value averaged over the trial set $\{n \in N\}$ and on a given baseline interval [Aviyente et al., 2017]. Thus, the baseline interval before the elicited stimulus (marked with red line) does not hold any significant functional connectivity in either stimulus. On the contrary, the target connectivity grows significantly after the stimulus onset in comparison with non-target. Therefore, PLI holds discriminative information concentrated at particular time intervals and spectral rhythms.

The bottom row also shows the spectral representation of assessed functional connectivity that has been averaged across the node and subjects to consider the overall response, that is:

$$\boldsymbol{E}\{y_{f,t}(v) : \forall v \in V, m \in M\} \tag{3.7}$$

As seen, the connectivity spectrum of the target response is more powerful than non-target. Furthermore, there is a time-frequency peak within 400 and 650 *ms* after each response is evoked, located at the low-frequencies between 1 and 6 *Hz*, confirming the existence of functional ERP networks in δ and θ waves as widely suggested in literature [Cooper et al., 2016, Harper et al., 2017]. In fact, similar attention tasks

increase theta phase synchronization between frontal and temporal electrodes as reported in [Gruber et al., 2018, Lee et al., 2014].

Piecewise computation of group-level connectivity graphs To consider the group-level influence on the obtained functional connectivity graphs, the supervised thresholding algorithm in 4.5 is contrasted with the unsupervised amplitude rule (noted as UTh) defined, for a given cut-off value $q \in [0, 1]$, as follows [van den Heuvel et al., 2017]:

$$\kappa_{\tau}^{\Omega\lambda}(v) = \begin{cases} 1, & q \max(\boldsymbol{E}\{\tilde{y}_{\tau m}^{\Omega}(v) : \forall m \in M\}) \\ 0, & \text{Otherwise} \end{cases} \tag{3.8}$$

The choice of a cut-off value is performed heuristically within the range $q \in [0.4, 0.9]$. 3.1 shows that $q = 0.7$ is a suitable level, ruling a trade-off between computational cost (number of connections) and accuracy (confidence).

q	0.4		0.5		0.6		0.7		0.8		0.9	
$p = 0.01$	1	0	1	0	1	0	1	0	0	0	0	0
$p = 0.05$	1	1	1	1	1	1	1	0	1	0	0	0
$\#\ Cx$	459	347	198	156	98	68	36	33	15	13	4	3

Table 3.1: Tunning of cut-off value for the unsupervised thresholding rule at different p values. Notation # Cx stands for the assessed number of connections. Shaded columns are δ, while unshaded – θ waveforms.

To provide a spatio-temporal interpretation of selected links,3.5a compares stationary and piecewise thresholding. The former extracts a single connectivity value from the whole recording time T, while the latter combines the PLI from six non-overlapped intervals $(\Delta\tau_i \subset T, \Delta\tau = 200)\, ms$ using the rule in 4.7. Note that all significant links are plotted using the information held by κ about electrodes, that is, how many times each channel turns to be relevant. Despite stationary thresholding presents differences between stimuli, the piecewise thresholding highlights the discriminant brain connections.

In comparison to the UTh algorithm, the supervised thresholding highlights further the distinction between stimuli, making clear the more differentiating channels

and, therefore, improving their interpretation. Thus, *STh* shows an increased connectivity between the frontal and temporal/parietal electrodes of target detection as reported in [Han et al., 2017]. Also, *STh* reveals an enhanced connectivity of θ and δ waves between the medial frontal cortex and other cortical regions (including the parietal) during attention and surprise/novelty processing as described in [Gulbinaite et al., 2014]. Consequently, the use of piecewise connectivity extraction together with the supervised thresholding results in more reasonable, connected locations, enabling to construct a meaningful explanation of oddball paradigm stimuli.

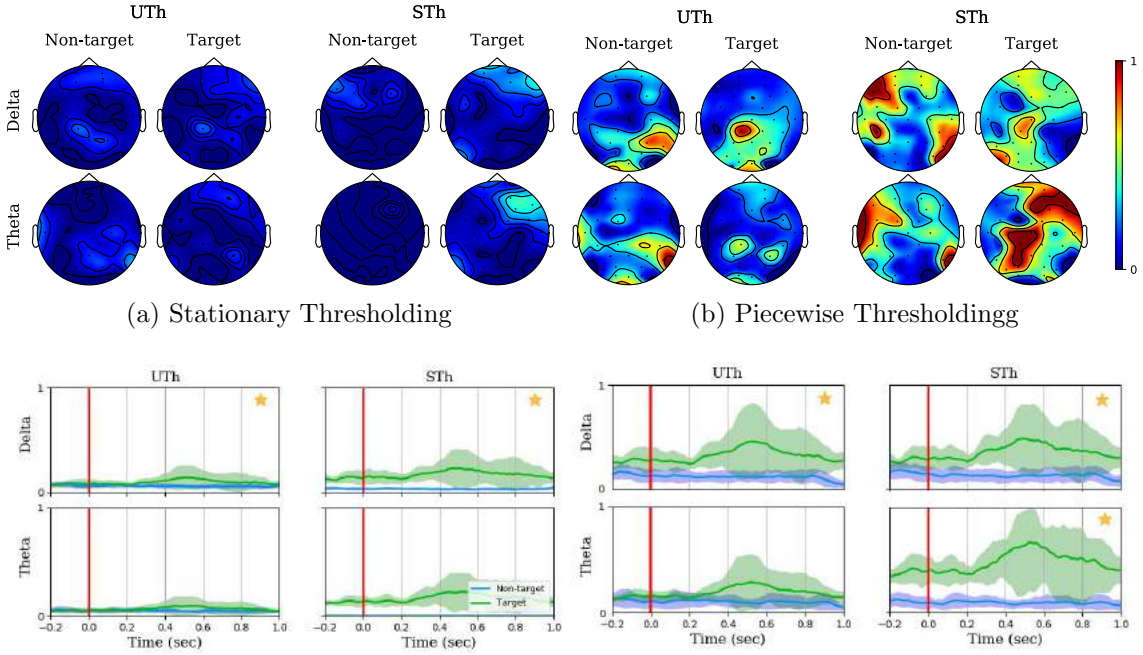

(a) Stationary Thresholding (b) Piecewise Thresholdingg

(c) Stationary Thresholding (d) Piecewise Thresholding

Figure 3.5: Estimated brain graphs from stationary and piecewise thresholding.Node strength, Blue line – Non target, Green line – Target

Figures 3.5c and 3.5d prove that the use of proposed group-level brain graphs enhances the connectivity estimation through the time domain, displaying the time-variant node strength values averaged across all subjects and node set. It is worth noting that the distinction between stimuli grows synchronously with evoked auditory potential, being most evident in the *STh* algorithm.

Besides, we investigate the consistency of performing group-level connectivity graphs by subtracting one (i.e., having 16 tested subjects) and two subjects (15) from the

training set (17). To this end, we determine whether each thresholding rule fulfills the confidence test levels that are adjusted to $p = 0.01$ and $p = 0.05$, testing several times each subject scenario. In the case of piecewise graph computation, 3.2 shows that, regardless of the validated waveform, *STh* meets either interval estimate, excluding one or two subjects from the training set. In turn, *UTh* demands the whole subject set for fitting the confidence value fixed at $p = 0.01$ and just for δ wave. In the remaining cases, subtraction of training subjects makes weak the piecewise group-level estimator consistency. In the case of performing stationary network graphs, the influence of *UTh* becomes worse, while the *STh* rule outperforms everywhere though just for the δ wave.

	Stationary $\Delta\tau_i = 200$						Piecewise $\Delta\tau_i = 200$						Piecewise $\Delta\tau_i = \text{var}$					
rule	15		16		17		15		16		**17**		180		220		240	
*STh***	0	0	0	0	1	0	0	0	1	0	**1**	**1**	1	1	1	0	0	0
*UTh***	0	0	0	0	1	0	0	0	0	0	**1**	**0**	1	0	0	0	0	0
*STh**	0	0	1	1	1	1	1	0	1	1	**1**	**1**	1	1	1	0	1	0
*UTh**	0	0	1	0	1	0	0	0	1	0	**1**	**0**	1	0	1	1	0	0

Table 3.2: Confidence test performed for the compared group-level connectivity graphs. Notations ** and * stand for confidence values fixed at $p = 0.01$ and $p = 0.05$, respectively. Shaded columns are δ, while unshaded – θ waveforms.

Lastly, we analyze the piecewise interval influence on the connectivity graph consistency. Having the whole subject set, 3.2 also presents the confidence assessed for $\Delta\tau_i = 180\,ms$, proving that the consistency equals to the case of $\Delta\tau_i = 200\,ms$ (see the bold columns), but at the higher computational burden. However, by increasing the piecewise window ($\Delta\tau_i = 220, 240$), either thresholding rule performance degrades.

3.4 Concluding remarks

To improve the confidence of auditory oddball paradigms, we present a graph network connectivity analysis that computes a relevant connectivity vector, including the contribution of each connection node in terms of distinguishing between labels. To this end, we perform piecewise computation of group-level connectivity graphs to deal with the non-stationarity of EEG data that makes the brain networks change over time. Also,

taking advantage of the labeled EEG responses, we introduce a supervised, statistical thresholding algorithm to reduce all redundant or worthless connectivities, holding the connections that differentiate the most the brain responses to each evoked stimulus. The proposed relevant graph network analysis relies on a couple of contributions: *i*) the piecewise connectivity computation that demands the interval tuning, which must be carried out carefully. *ii*) The concatenation procedure to reflect thoroughly the whole recording span with a single relevance value.

The validating results obtained on a concrete attention task show that the developed relevant analysis results in a node set, connected, with improved consistency of performing group-level connectivity graphs, improving the interpretation of functional connectivity dynamics of involved oddball paradigm stimuli in attention tasks. Although the proposed piecewise graph network connectivity analysis depends on the piecewise interval.

As future work, we intend to validate EEG data with more complicated dynamics. To overcome more effectively nonstationarities of neural responses and structural homogeneity of latent processes across the sample, we plan to introduce an elaborate group-level strategy, including more complex approaches for graph analysis as well as enhanced relevance metrics [Hurtado-Rincon et al., 2014].

Chapter 4

Time-varying functional connectivity networks

Neural responses of oddball tasks can be used as a physiological biomarker to evaluate the brain potential of information processing under the assumption that the differential contribution of deviant stimuli can be assessed accurately. Nevertheless, the non-stationarity of neural activity causes the brain networks to fluctuate hugely in time, deteriorating the estimation of pairwise synergies. To deal with the time variability of neural responses, we have developed a piecewise multi-subject analysis that is applied over a set of time intervals within the stationary assumption holds. To segment the whole stimulus-locked epoch into multiple temporal windows, we experimented with two approaches for piecewise segmentation of EEG recordings: a fixed time-window, at which the estimates of FC measures fulfill a given confidence level, and variable time-window, which is segmented at the change points of the time-varying classifier performance. Employing the weighted Phase Lock Index as a functional connectivity metric, we have presented the validation in a real-world EEG data, proving the effectiveness of variable time segmentation for connectivity extraction when combined with a supervised thresholding approach. Consequently, we performed a piecewise group-level analysis of electroencephalographic data that deals with non-stationary functional connectivity measures, evaluating more carefully the contribution of a link node-set in discriminating between the labeled oddball responses.

To evaluate the brain potential the neuronal responses obtained in the oddball task can be used as physiological biomarkers under the assumption that they can accurately assess the contribution of the stimuli. Unfortunately, the non-stationary dynamics of

brain activity cause brain networks to fluctuate quite a bit over time, making difficult the pairwise estimation of synergies. To cope with the temporal variability of neural responses, we have developed a multi-subject piecewise analysis that is applied over a set of time intervals within the stationary assumption. We have used two different approaches to segmentation over time; the first was to use a fixed window in which the estimates of the functional connectivity measures meet a given level of confidence. Second, a variable window is used for segmenting the window at the points of change of the time-varying classifier.

4.1 Introduction

Investigation in oddball tasks regards detection and analysis of neural responses, mostly relying on event-related potentials (ERP) like the well-known P300 that is associated with attentional orientation processes elicited by target stimulus identification [Harper et al., 2017]. P300 can be used as a physiological biomarker to evaluate the brain potential of information processing [Li et al., 2018]. Intending to perform analysis with enhanced physiological interpretation, auditory and visual oddball tasks are often employed to identify perceptual differences, providing a more profound understanding in applications like attention and memory tasks [Kiat et al., 2018], affective computing, motor imagery, as well as in media and information literacy [Schaadt et al., 2013], among others. However, because of data acquisition and analysis limitations, an open issue in interpreting ERP responses is to assess confidently the brain networks that may reflect the differential contribution of deviant stimuli, requiring more cognitive resources than the processing of standard stimuli [Hurtado-Rincón et al., 2018b, Schlüter and Bermeitinger, 2017].
In practice, the differences of functional brain networks are investigated for uncovering the corresponding effect of stimulus sequence, assuming that brain activities are predictably modulated within some spatio-temporal windows [Bridwell et al., 2018]. This fact allows the use of neuroimaging measures to benefit from tracking the evoked time-variant responses in diverse brain structures. To date, for investigating brain activity changes in ERP-related tasks, different methods have been proposed: Time-frequency signal processing for the study of ERP energy distribution across time and frequency [Aviyente et al., 2017], time-varying network analysis among brain regions to uncover the detailed and dynamic information processing in the corresponding cognition process [Li et al., 2016a],

and functional connectivity (FC) that provides a powerful way to investigate the neural dynamics of target detection/novelty processing emerged in normative and pathological populations, quantifying the working neural activity in terms of functional brain networks [Blinowska, 2011]. Besides the fact that FC can be implemented at a reasonable cost on high-density electroencephalographic (EEG) recordings [Toppi et al., 2012], its advantages lie in the ability to map statistical patterns of dynamic coupling between distributed brain regions, i.e., the connectivity of brain areas at the channel-level. Thus, a major driving force for the rapid expansion of functional brain networks is the availability of relational data recording couplings and interactions among elements of neural systems [Sporns, 2018].

Despite the evident impact of channel-level connectivity analysis, it lacks a standard analytic framework and supplies deficient spatial resolution [Bathelt et al., 2013], resulting in several limitations: *i*) A growing need for connectivity measures extracted from high-resolution EEG data to provide a trade-off between local specialization and global integration of brain tasks, assuring caution for the interpretation of connectivity estimates at the same time [Bastos and Schoffelen, 2016]; *ii*) Extraction/modeling of informative graph-based neuromarkers from all feasible inter-channel interactions, which may result in high dimensional connectivity matrices with redundant or worthless features, hindering a proper data analysis because of noisy links (not mentioning the computational cost issues) [Van Wijk et al., 2010, De Vico Fallani et al., 2014]. Lastly, *iii*) EEG non-stationarity that makes the brain networks intrinsically and dramatically change over time, degrading the assessment of pairwise interactions, which are typically operationalized through the full or partial correlation/information between all pairs of regional time series [Pereda et al., 2018].

To undertake the dimensionality reduction of connectivity matrices, thresholding methods are employed, typically, maintaining the most robust edges (i.e., pairwise interactions), either by holding the edges that surpass an a priori fixed weight or by constraining the edge density [Váša et al., 2018]. Each particular thresholding rule, however, determines diversely the number of strong connections, yielding a distinct effect on the structure and global properties of sparsified networks [Garrison et al., 2015]. For this reason, the choice of edge reduction methods can profoundly impact the results and interpretation of the performed FC analysis [Bielczyk et al., 2018]. As a baseline approach, statistical thresholding presents itself well to a principled choice of threshold, based on hypothesis tests of significance. Nevertheless, the amplitudes of spontaneous fluctuations in

brain activity may be an essential source of within-subject and between-subject variability that is likely to be carried through into connectivity estimates (directly or indirectly) [Bijsterbosch et al., 2018]. For enhancing the discriminant ability between bi-class stimuli, the inclusion of label sets in the hypothesis rule to estimate the statistical difference between the target and non-target data [**?**]. In the functional brain network research, however, an open challenge is the selection of appropriate edge reduction to detect the time-varying changes in brain activity, mostly addressing sources of inter-subject and inter-trial variance of EEG recordings [Thilaga et al., 2015].

On the other hand, many commonly used measures of synchronicity assume the FC is stationary in terms of the spatial and time domains [Hansen et al., 2015], which in reality are often strongly non-stationary [Terrien et al., 2013]. To overcome this issue, the quasi-stationary activity of large neuronal populations is considered by extracting synchronization estimates from a set of previously segmented time intervals, which are statistically verified [Pereda et al., 2018] or within the stationary assumption holds [Kaplan et al., 2005]. In the latter approach, non-overlapping segments are used with the purpose of dividing the grand-average ERP into time-windows to evaluate the functional network changes [Thee et al., 2018]. Thus, there are two main approaches for piecewise segmenting within the estimates of FC measures are extracted from EEG recordings: fixed time window and variable window along the ERP response. Nevertheless, the piecewise segmentation approach of time windowing demands a trade-off between the stationary assumption and the window length, which limits the accuracy of the temporal detection of abrupt changes that can reflect salient biological mechanisms in the underlying systems [Hassan et al.,]. Despite advances in the field of dynamic connectivity, fixed sliding window approaches for the detection of fluctuations in functional connectivity are still widely used [Liuzzi et al., 2019]. Therefore, the quasi-stationary window interval must be tuned carefully.

Aiming at enhancing the interpretation of oddball tasks, we develop a piecewise group-level analysis that improves the confidence of the estimated non-stationary functional connectivity measures, assessing more accurately the contribution of the link node-set in distinguishing between labeled ERP stimuli. For achieving the piecewise segmentation, we experiment with two approaches for piecewise segmentation of EEG recordings: Fixed time-window, at which the estimates of FC measures fulfill a given confidence level, and variable time-window segmented at the change points of the time-varying classifier performance. During validation, the classifier accuracy is calculated by a Linear Discriminant Analysis algorithm that is fed by a feature set

extracted through the widely used common spatial patterns, enabling observation of the temporal progression of task-relevant components and localization of the event-locked time with the maximal discrimination between conditions. For the sake of simplification, the FC analysis is carried out on a specific narrow segment of interest (near stimulus onset) [Wang et al., 2014], omitting other neural dynamics that may be spread the modulated ERP thoroughly. Performed brain graph analysis on real EEG data shows slow variations of relevant links, growing synchronously with the evoked potentials. As a result, the use of variable segmentation, together with the supervised thresholding, allows performing a reduced set of relevant brain areas, but with enough confidence to construct a meaningful explanation of oddball paradigm stimuli. Therefore, the presented group-level approach allows inferring the latent structure of multi-subject datasets, addressing the sources of non-stationarity usually observed in EEG recordings. The agenda in this chapter is as follows: In the beginning, the proposed methodology is presented that includes the data acquisition followed by a basic definition of used FC metrics, as well as the piecewise construction of group-level connectivity, and considered graph parameters. Then, all obtained results are evaluated and followed by their discussion and concluding remarks.

4.2 Materials and Methods

EEG Database Description and Preprocessing

Six females and eleven males (M=17 subjects, aging in average 27.7 years) participated in three runs following the visual and auditory oddball paradigms, each one having two labeled stimuli: target and non-target, i.e., $\lambda=\{l, l'\}$. In total, 375 (125 per run) stimuli per task were presented, each one lasting 200 ms within a 2-3 s uniformly-distributed inter-trial interval and generated at target probability 0.2. Always, the first two evoked responses of each run had been a non-target. To implement the visual task, the target and non-target stimuli were, respectively, a large red circle and a small green circle depicted on isoluminant gray backgrounds (3.45 and 1.15 degree visual angles). For the auditory task, the standard stimulus was a 390 Hz pure tone, which had been selected to lie within a trough of the scanner sound frequency spectrum, and the target sound was a broadband *laser gun* sound so that EEG discriminator performance matched the one of visual tasks. Because the study focused on task-related attentional states, subjects were asked to respond to target stimuli, using a button

press with the right index finger on an MR (*Magnetic Resonance*) compatible button response pad. Stimuli were presented to subjects using E-Prime software (Psychology Software Tools) and a VisuaStim Digital System (Resonance Technology), comprising headphones and 600×800 goggle display as detailed in [Muraskin et al., 2018]. Scalp data were acquired at 1000 Hz sampling rate (that is, t=0.001 s) using an EEG data acquisition system with a custom cap configuration of C=34 channels, for which the following preprocessing Butterworth filters were used: 1-Hz high pass to remove direct current drift; notched filter (centered at 60 and 120 Hz) to eliminate the electrical power line and its first harmonic, respectively; and a low pass filter with a cut frequency at 120-Hz, excluding high-frequency artifacts without neuro-physiological content. As a result, the observation EEG dataset $\{\boldsymbol{X}^{\lambda}_{tmn}\in\mathbb{R}^{C\times T\times N\times M}\}$ is collected from each subject $m\in M$, holding $n\in N$ trials (N=375) and recorded out from each c-th scalp electrode, $c\in C$, at time sample $t\in T$. All trial-level signals were baseline-corrected by subtracting the mean prestimulus interval activity from -200 to $+800$ ms, so that the recording time length is adjusted to T=1s, aiming to preserve representative connections of the frontal, parietal, and temporal regions.

Subject-level Inter-channel Connectivity

To investigate the pairwise functional connectivity of oddball tasks, we use *Phase Locking Index* (*PLI*) as a FC metric that quantifies the asymmetry of phase difference distribution between two specific channels c, c' (with $\forall c, c'\in C, c\neq c'$) and its weighted version (*wPLI*), being each one defined within the recording time span $T\in\mathbb{R}^{+}$ as follows:

$$PLI : y_{ft}(c,c') = \Big|\boldsymbol{E}\{\operatorname{sgn}\big(\Delta\Phi_{ft}(n;c,c')\big) : \forall n\in N\}\Big|, \tag{4.1a}$$

$$wPLI : y_{ft}(c,c'), = \frac{\Big|\boldsymbol{E}\{|(\Delta\Phi_{ft}(n;c,c'))|\operatorname{sgn}\big(\Delta\Phi_{ft}(n;c,c')\big) : \forall n\}\Big|}{\boldsymbol{E}\{|(\Delta\Phi_{ft}(n;c,c'))| : \forall n\}} \tag{4.1b}$$

where notations sgn and $\boldsymbol{E}\{\cdot : \forall n\}$ stand for sgn function and averaging operator over n, respectively. All FC metrics are normalized to highlight the connectivity patterns generated by each evoked stimulus, being each FC mean-value averaged over the trial set $\{n\in N\}$ and on a given baseline interval [Aviyente et al., 2017]. Instantaneous phase difference $\Delta\Phi_{ft}(;c,c')\in[0,\pi]$ is the angle of the continuous wavelet transform coefficients

$W_{ft}(;)\in\mathbb{R}^{+}$ computed through the band-pass filtered input matrix $\boldsymbol{X}_{tf}$ as follows:

$$\Delta\Phi_{ft}(n;c,c') = \frac{W_{ft}(n;c)W^{*}_{ft}(n;c')}{|W_{ft}(n;c)||W^{*}_{ft}(n;c')|},\ t\in T, f\in\Omega \tag{4.2}$$

where notation * stands for complex conjugate.
Since previous studies on cognitive dynamics have shown that oscillatory evoked responses are mainly composed of low-frequency bands $\Omega\in\{\delta,\theta,\alpha,\beta\}\ Hz$ [Güntekin and Başar, 2010], connectivity analysis is performed inside the following waves (rhythms) of interest: $\Omega\in\{\delta,\theta\}$ for auditory tasks, while $\Omega\in\{\alpha,\beta\}$ for visual tasks. Hence, we obtain the inter-channel connectivity vector, noted as $\hat{\boldsymbol{y}}^{\Omega}_{t}\in\mathbb{R}^{V}$, holding elements $\hat{y}^{\Omega}_{t}(v)\in\mathbb{R}$ that are computed by averaging each connectivity measure across the frequency domain within the corresponding waves of interest as follows:

$$\hat{y}^{\Omega}_{t}(v) = \boldsymbol{E}\{y_{ft}(v) : \forall f\in\Delta F_{\Omega}\} \tag{4.3}$$

where ΔF_{Ω} is the bandwidth of each one of the considered waves. Here, the pairwise variable is denoted as $v\in\{c,c'\in V, c\neq c'\}$, being $V=C(C\text{-}1)/2$ the amount of paired links.

4.2.1 Piecewise Construction of Group-level Connectivity

As a result of the above subject-level stage, we can estimate the inter-channel connectivity vector $\hat{\boldsymbol{y}}^{\Omega}_{m}=\{\hat{y}^{\Omega}_{tm}(v)\in\mathbb{R}[0,1]:\forall t\in T\}$ for each m-th subject. However, the estimates are still non-stationary in a way that some links may appear and disappear anywhere/anytime. To deal with this time-variant behavior, we extract the evolution connectivity vectors $\hat{\boldsymbol{y}}^{\Omega}_{tm}\in\mathbb{R}^{V}$ within quasi-stationary time segments using the piecewise strategy, as suggested for subject-level extraction in [Kaplan et al., 2005]. To that end, the whole recording time length T is split into N_{τ} non-overlapping segments (time-windows denoted by τ_i), so that, under the assumption that the brain networks remain stationary within τ_i, we assess a single connectivity value by concatenating the vector set across measures, $\forall t\in\tau_i\subset T$. Because of the invariability assumption, we suggest the expected value as a representative estimate to construct the node connectivity vector $\tilde{\boldsymbol{y}}^{\Omega}_{im}\in\mathbb{R}^{V}$ within i-th interval set $\{\tau_i:i\in N_{\tau}\}$ as below:

$$\tilde{\boldsymbol{y}}^{\Omega}_{im} = \boldsymbol{E}\{\hat{y}^{\Omega}_{tm}(v) : \forall t\in\tau_i\},\ \forall v\subset V$$

In practice, as the number of subjects increases, the amount of false links (erratically presented) rises also. Intending to remove these noisy links, the multi-subject analysis

provides a set of selected connections (that is, relevant connectivity set) that reaches a specified cutoff value. We propose the selected links to be computed piecewise by using the following unsupervised amplitude thresholding rule (noted as $pUTh$):

$$\kappa_i^{\Omega}(v) = \begin{cases} 1, & q \max(\boldsymbol{E}\{\tilde{\boldsymbol{y}}_{im}^{\Omega}(v) : \forall m \in M\}) \\ 0, & \text{Otherwise} \end{cases} \tag{4.4}$$

where $q \in \mathbb{R}^+$ is a given cut-off value that is fixed heuristically within the range $q \in [0.4, 0.9]$.

Nevertheless, the rule in 4.4 provides information about the brain networks that are relevant over the entire measured data, without accounting for any labels. Instead, one might be more interested in selecting the relevant connection set, reflecting the influence of label sets on discriminating between tasks. Therefore, we introduce the prior information about labels across the subject set through the following supervised, statistical thresholding algorithm:

$$\kappa_i^{\Omega}(v) = \begin{cases} 1, & \mathcal{M}\{\tilde{y}_{im}^{\Omega\lambda}(v)|\lambda : \forall m\} < p \\ 0, & \text{Otherwise} \end{cases} \tag{4.5}$$

where functional $\mathcal{M}\{\cdot|\lambda{:}\forall m\}$ assesses the statistical discrepancies, which appear when integrating information across all subjects, in the links between each labeled connectivity set, $\{\tilde{y}_{im}^{\Omega\lambda}(v)|\lambda\}$.

Nevertheless, the class of statistical measures is limited to implementing the algorithm in 4.5 due to the estimated relevance set fails for normality and homoscedasticity, applying Kolmogorov-Smirnov and Bartlett's tests, respectively. Instead, we validate whether two labeled samples are likely to derive from the same population, using the non-parametric Mann-Whitney test that is often conducted on EEG connectivity [Hussain et al., 2017]. However, we cannot expect the connectivity values to be uncorrelated between different piecewise intervals. Therefore, the statistical significance of connectivity is corrected using the False Discovery Rate as a robust statistical correction for multiple comparisons at different frequency bands. Namely, we test each one the node-links over δ and θ for auditory, while α and β for visual stimuli as performed in [Genovese et al., 2002]. Thus, the bi-valued relevance set $\{\kappa_i^{\Omega}(v){:}\forall \Delta\tau_i\}$ in 4.54.4 is calculated piecewise over all time windows, reflecting the variability of brain networks through the whole recording length T. Note that the relevance time-series may be employed to extract the time-evolving dynamics of multi-subject connectivity.

Likewise, relying on the evident premise that EEG data had been acquired following the same conditions on all piecewise intervals, we measure the statistical differences of the time window set, yielding the connectivity relevance values as follows:

$$\kappa_m^{\Omega}(v) = \begin{cases} 1, & \mathcal{M}\{\tilde{y}_{im}^{\Omega\lambda}(v)|\lambda : \forall\Delta\tau_i\}<p \\ 0, & \text{Otherwise} \end{cases} \tag{4.6}$$

Consequently, the supervised piecewise connectivity analysis, denoted as *pSTh*, is accomplished through the sequential combination of rules **??**.
Lastly, we assess the group-level analysis over the subset set, thoroughly within the recording length of T, with a single connectivity relevance by the following concatenation procedure:

$$\kappa^{\Omega}(v) = \left(\kappa_1^{\Omega}(v) \vee \ldots \vee \kappa_i^{\Omega}(v) \vee \ldots \vee \kappa_{N_\tau}^{\Omega}(v)\right) \wedge \left(\kappa_1^{\Omega}(v) \vee \ldots \vee \kappa_m^{\Omega}(v) \vee \ldots \vee \kappa_M^{\Omega}(v)\right) \tag{4.7}$$

where notations $\vee$ and $\wedge$ stand for OR and AND logical operators, respectively. The main rationale behind the use of logical conjunction is to gather all common multi-subject dynamics.

4.2.2 Graph Connectivity Analysis

From the piecewise FC analysis, we construct a resulting graph $\hat{\boldsymbol{y}}_{im}^{\Omega}\boldsymbol{\kappa}^{\Omega}{:}\forall i, m$, where $\boldsymbol{\kappa}{=}[\kappa^{\Omega}(v){:}\forall v]$ (with $\boldsymbol{\kappa}{\in}\mathbb{N}^V$) is the relevant connectivity vector that encodes the assessed contribution of the link node set, extracted from the group-level FC measurements.
All relevant links, which have been estimated by thresholding the pairwise FC measure, constitute the brain functional network with a topology that is quantified by the following graph parameters frequently used in the group-level analysis of oddball paradigms [Boccaletti et al., 2006]:

- *Network Density* is the ratio between the number of graph edges to the total amount of possible links, $D{=}C/V$, assessing the physical wiring cost of the network.

- *Node Strength*, $\gamma(v)$, that reflects how strongly a node is associated with others and is computed by the weighted sum of links connected to the node as follows:

$$\gamma_t^{\Omega}(v) = \kappa^{\Omega}(v) \sum\nolimits_{\forall m} \hat{y}_{tm}^{\Omega}(v),\ \forall t \in T \tag{4.8}$$

  Note that each $\gamma(v)$ value can be rewritten in terms of $\gamma(c)$ by unfolding the adjacent node vectors on the channel space.

4.3 Results

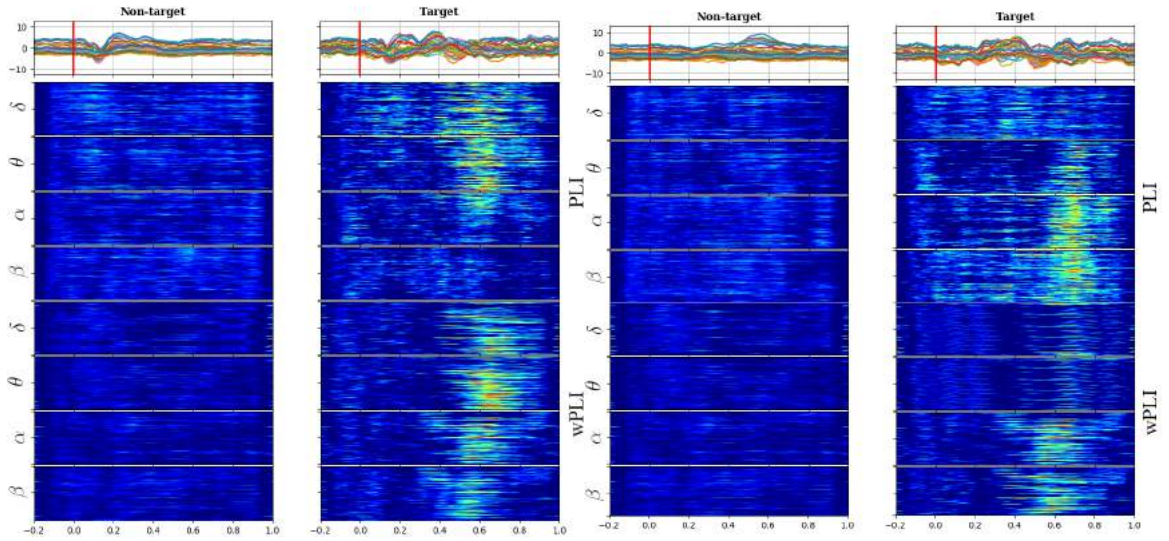

(a) Auditory ERP (b) Visual ERP

Figure 4.1: Estimation of functional connectivity measures in auditory (left column) and visual (right) tasks. Top row: Time-courses of evoked responses extracted from all channels, which are averaged across the whole subject set (a red line marks the stimulus onset). FC trajectories along the time length computed separately for each oscillation: *PLI* (middle row) and *wPLI* (bottom row).

4.3.1 Computation of Functional Connectivity Measures

Subject-level pairwise connectivity estimation: 4.1 displays the functional connectivity measures estimated from scalp EEG data for both analyzed tasks: auditory (left column) and visual (right column). With the purpose of following the relationship between the evoked responses and computed FC measures, the top row represents the ERP time-courses of each grand average that is calculated by averaging across all subject and trial sets, making clear the distinction in ERP amplitudes between either evoked condition (target and non-target) and becoming more evident within the range between 300 and 450 *ms* after the stimulus onset that is marked by a red line.
Further, the FC values are extracted separately for the oscillations of interest, having the following bandwidths: $\Delta F_\Omega \in \{\Delta F_\delta = [2\text{-}5],\ \Delta F_\theta = [5\text{-}8],\ \Delta F_\alpha = [8\text{-}14],\ \Delta F_\beta = [14\text{-}30]\}\ Hz$.

Visual inspection of connectivity dynamics evidences its relationship between the ERP time-courses and either functional connectivity measure (*PLI* (middle row) and *wPLI* (bottom row)), assessed for each pairwise link (vertical axis). Thus, the baseline time-window before the stimulus onset does not hold notable FC values extracted in both cases of stimulation. By contrast, the target functional connectivity grows meaningfully after the elicitation, presenting appreciable differentiation between the target and non-target conditions at different time instants. Moreover, the assessment of phase-synchronization performed by either index (*PLI* or *wPLI*) results in connectivity estimates very related to the ERP amplitude peaks, being most evident in the δ and θ waves of auditory tasks and α and β of visual tasks. Consequently, either FC estimation allows for improving in a different way the individualizing patterns of the extracted waves, depending on the contemplated oddball paradigm activity.

4.3.2 Piecewise Computation of Group-level Connectivity Graphs

During validation, two approaches for piecewise segmentation of EEG recordings are tested: *i*) Fixed window method that adjusts an equally lasting time window $\tau_i{=}\tau, \forall i$, at which the estimates of FC measures better fulfill an a priori fixed confidence level. *ii*) Wrapped method that adjusts each time window τ_i differently at the change points of the time-varying classifier performance.

Tuning of equally lasting time window: In this case, to capture the time-variant behavior of ERP responses, the non-overlapping segment of analysis is adjusted to obtain the FC estimates with high confidence (namely, $p{\leq}0.02$), providing an affordable computational burden. For the purpose of comparison, we introduce the stationary version of either rule (denoted as *UTh* nor *STh*, respectively), when adjusting the time window to the recording length, $\tau_i{=}T$, and therefore the piecewise analysis is not performed. Note that the amplitude algorithm in 4.4 demands tuning of the cut-off value, which is heuristically fixed to $q{=}0.7$, as an adequate level, ruling a trade-off between computational cost (number of connections) and accuracy (confidence of connectivity estimates) [Váša et al., 2018]. Thus, Figure 4.2 depicts the confidence achieved by each one of the tested thresholding rules, showing that neither stationary rule version (*UTh* nor *STh*) reaches the value of $p{\leq}0.05$. This conclusion holds, regardless of the analyzed wave or the considered task. On the other hand, the piecewise strategy allows achieving better confidence when extracting all FC values

from the time window τ. Moreover, the use of labels improves the FC estimation remarkably, even fulfilling a higher confidence level of $p \leq 0.02$ (red line). By applying the non-stationary FC estimation, however, the interval length τ affects the achieved performance. Although the highest regarded confidence $p \leq 0.02$ is fitted at different time windows, distinct values are minimizing p in each task.

It is worth noting that the *wPLI* measure produces better performance within a wider interval range, and therefore, it will be the only metric considered in the following. In particular, the level of $p \leq 0.05$ is reached within the examined τ=[40-250], for which 4.3 displays the topographic maps that reflect all significant nodes extracted by $\boldsymbol{\kappa}$ (see 4.5), that is, how many times each channel turns to be relevant. As seen for the target stimulation of both tasks, the topographic map changes as the non-overlapped interval τ varies, revealing that the EEG connectivity patterns move gradually from one to another. This situation holds for each wave and may result in different interpretations of influencing brain zones. To avoid this issue, the best τ is selected as the value that minimizes the highest considered confidence $p \leq 0.02$ for each task. Namely, τ=100 – for auditory and τ=50 – visual.

In general, oddball responses should be more located in frontal and parietal lobes. Moreover, auditory stimuli also generate salient activity in the temporal areas, whereas visual stimuli – in occipital regions [Volpe et al., 2007]. Nevertheless, 4.3 shows spurious activations in central regions, which may be produced by either the acquisition artifacts of EGG data at the scalp level or the volume conduction effect as explained in [Li et al., 2020].

Tuning of variable time window: For adjusting the segmentation interval, we utilize the temporal progression obtained for the accuracy performance in discriminating between oddball stimuli, employing an algorithm of Linear Discriminant Analysis and 10-fold leave-one-out validation (See details of implementation in [Velasquez-Martinez et al., 2018]). The estimated accuracy changes are displayed in 4.4, showing that either response (auditive marked in blue line and visual in red line) behaves differently, even that both discrimination tasks have similar peak group-mean accuracy (close to 0.84). The visual stimulus discrimination curve decays smoother and slower than the auditive does, as has been noted previously by [Walz et al., 2013].

The segmentation interval set, $\{\tau_i\}$, is obtained at the time points when the temporal progression changes its behavior. Thus, both derivatives of each temporal progression are presented, for which the dashed lines mark the identified change points within each non-overlapping time-window is delimited. Specifically, the following sets are attained:

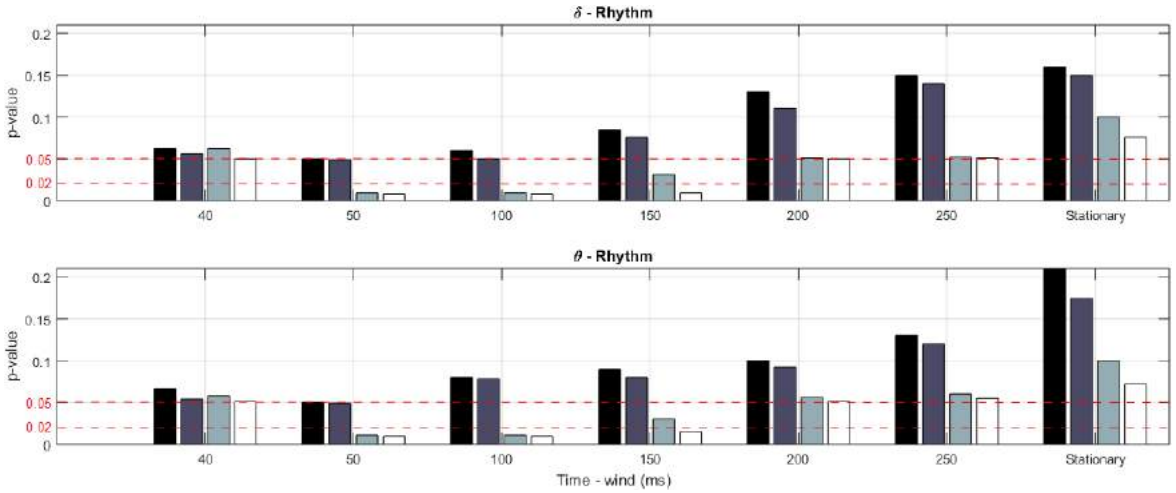

(a) Auditory stimulation

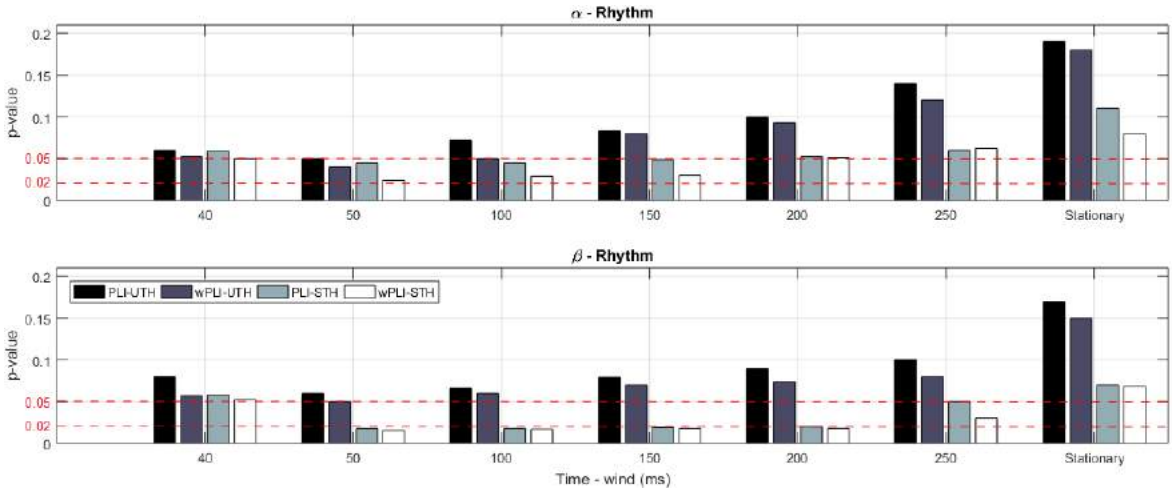

(b) Visual stimulation

Figure 4.2: Obtained results of confidence p for the supervised thresholding rule performed by the compared FC metrics in the cases of stationary (i.e., by adjusting to $\tau{=}T$) and non-stationary computation for different values of τ. Notation *Stat* stands for stationary FC metrics. Red lines present two different confidence levels, fulfilling $p{\leq}0.05$ and $p{\leq}0.02$.

$\tau_i{\in}[0.21,\ 0.29\,0.42\,0.54\,0.63]$ for auditive stimulus and $\tau_i{\in}[0.21\,0.33\,0.5\,0.68]$ for visual stimulus. It is worth noting that the first change point directly relates to the end of the presented stimuli during the experimental design of the used Oddball Paradigm.

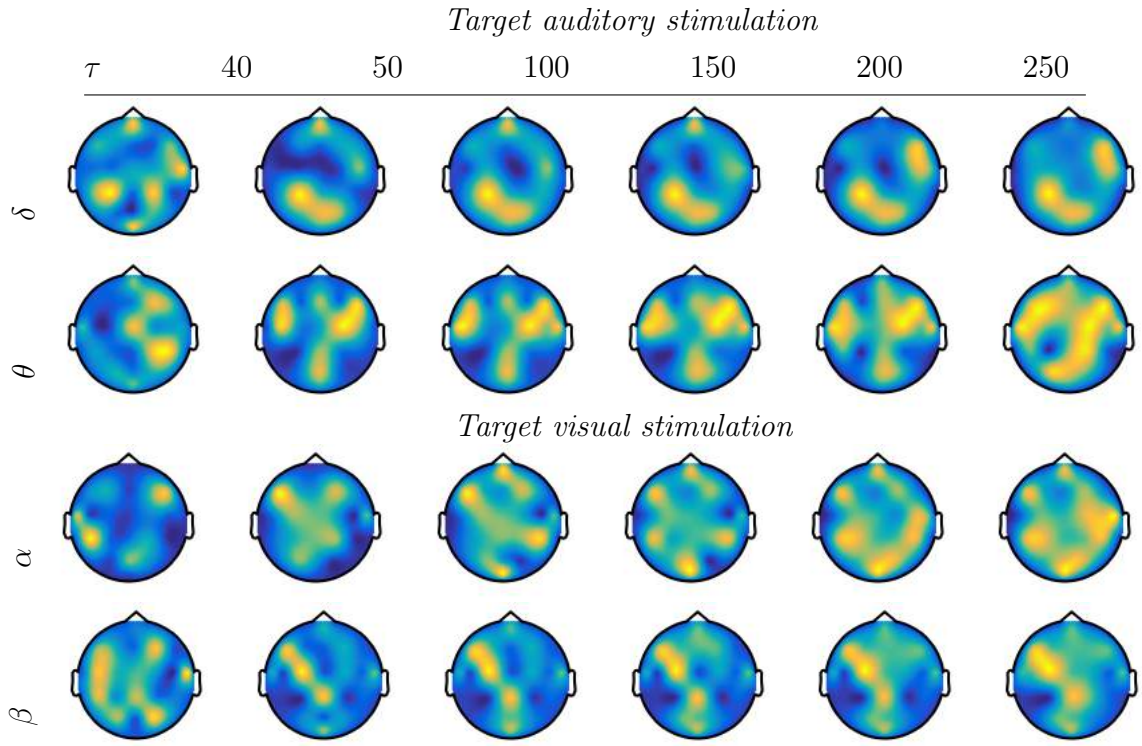

Figure 4.3: Topographic maps of significant nodes estimated by the piecewise *pSTh* rule of target stimulus, and extracted for a different non-overlapped interval τ.

To assess the influence of either piecewise segmentation strategy, 4.1 shows the reached values of confidence p, as well as the resulting number of connections, which are needed to fulfill different cut-off values q. Although both segmentation strategies satisfy the baseline confidence $p \leq 0.05$ just for $q = 0.6, 0.7$, the use of the variable time window results in a less quantity of connections.

Topoplot Brain Mapping of Group-level Connectivity Analysis: The goal is to identify spatial distributions of the brain activity related to the FC values following the developed group-level connectivity approach. 4.5 displays the topoplots that are computed for either piecewise segmentation strategy (fixed window is indicated by (τ) and variable window by (τ_i)). Both responses are displayed, target and non-target, showing a very low activity in the latter case. This assessed activity of non-target responses with no relevant brain areas is expected and illustrates the veracity of performing group analysis.

As observed from the target responses, the *pSTh* thresholding dispenses an increased

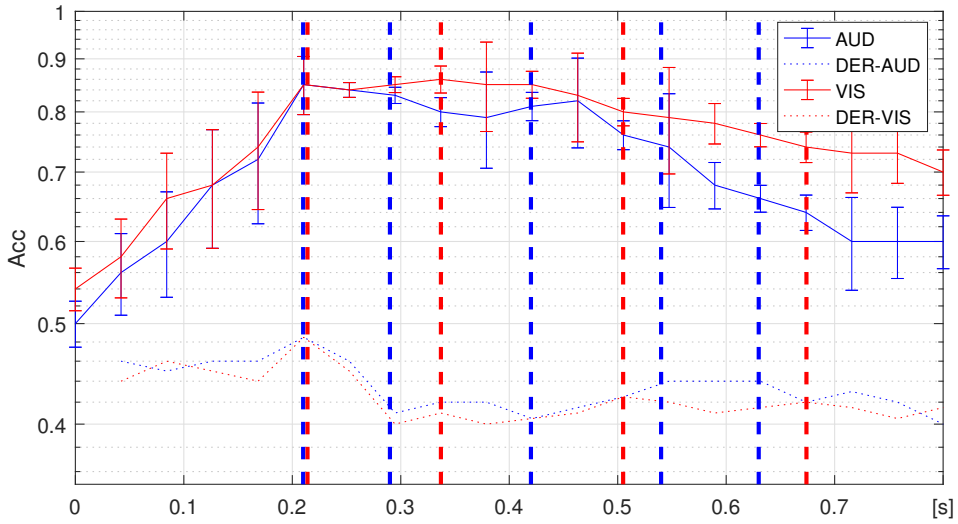

Figure 4.4: Temporal progression of classifier performance in discriminating between responses as well as its corresponding derivative (marked in dashed-dotted lines), achieved by auditive (solid blue line) and visual (solid red line) stimuli. The dashed demarcations stand at the identified change points within each non-overlapping time-window is delimited.

connectivity between the frontal and temporal/parietal electrodes of auditory target detection. This finding is reported in [Han et al., 2017]. Likewise, if θ and δ waves, $pSTh$ exposes an enhanced connectivity between the medial frontal cortex and other cortical regions (including the parietal) during attention and surprise/novelty processing; this conclusion is suggested also in [Gulbinaite et al., 2014]. In the case of visual tasks, parieto-central, parieto-temporal links and occipito-temporal and occipito-parietal links are observed with enhanced relevance as discussed in [Thee et al., 2018], associating all these links with object detection and visual processing.

As regards the piecewise interpretation of target responses, all the above-referenced findings become more distinctly seen when applying the variable-window. However, the unsupervised rule behaves worse regardless of the used time window, being most evident in the topoplots of β (visual) and δ (auditory) waves. Hence, we will further perform the brain graph analysis just for the supervised thresholding rule.

q	0.5		0.6		0.7		0.8	
Audit.	δ	θ	δ	θ	δ	θ	δ	θ
PLI	0.12(198)	0.13(156)	0.05(94)	0.06(78)	0.05(36)	0.05(33)	0.06-15	0.06(13)
wPLI	0.09(192)	0.12(155)	0.05(94)	0.05(76)	0.05(34)	0.05(31)	0.06(15)	0.06(13)
Visual	α	β	α	β	α	β	α	β
PLI	0.11(224)	0.12(186)	0.05(112)	0.06(110)	0.05(42)	0.06(42)	0.06(18)	0.06(16)
wPLI	0.10(222)	0.11(184)	0.05(110)	0.05(110)	0.05(42)	0.05(40)	0.06(15)	0.06(14)
Audit.	δ	θ	δ	θ	δ	θ	δ	θ
PLI	0.09(178)	0.076(148)	0.056(86)	0.58(76)	0.05(32)	0.05(30)	0.06-14	0.06(14)
wPLI	0.08(172)	0.7(144)	0.05(82)	0.05(74)	0.05(32)	0.05(31)	0.06(14)	0.06(14)
Visual	α	β	α	β	α	β	α	β
PLI	0.09(200)	0.08(172)	0.05(110)	0.06(100)	0.05(40)	0.06(42)	0.06(18)	0.06(16)
wPLI	0.08(198)	0.07(168)	0.05(104)	0.05(92)	0.05(40)	0.05(38)	0.058(14)	0.06(14)

Table 1. Influence of either piecewise segmentation on the unsupervised thresholding rule. The number of connections and q values that provide the baseline confidence value ($p \leq 0.05$) are shaded (fixed window is indicated by (τ) and variable window by (τ_i)).

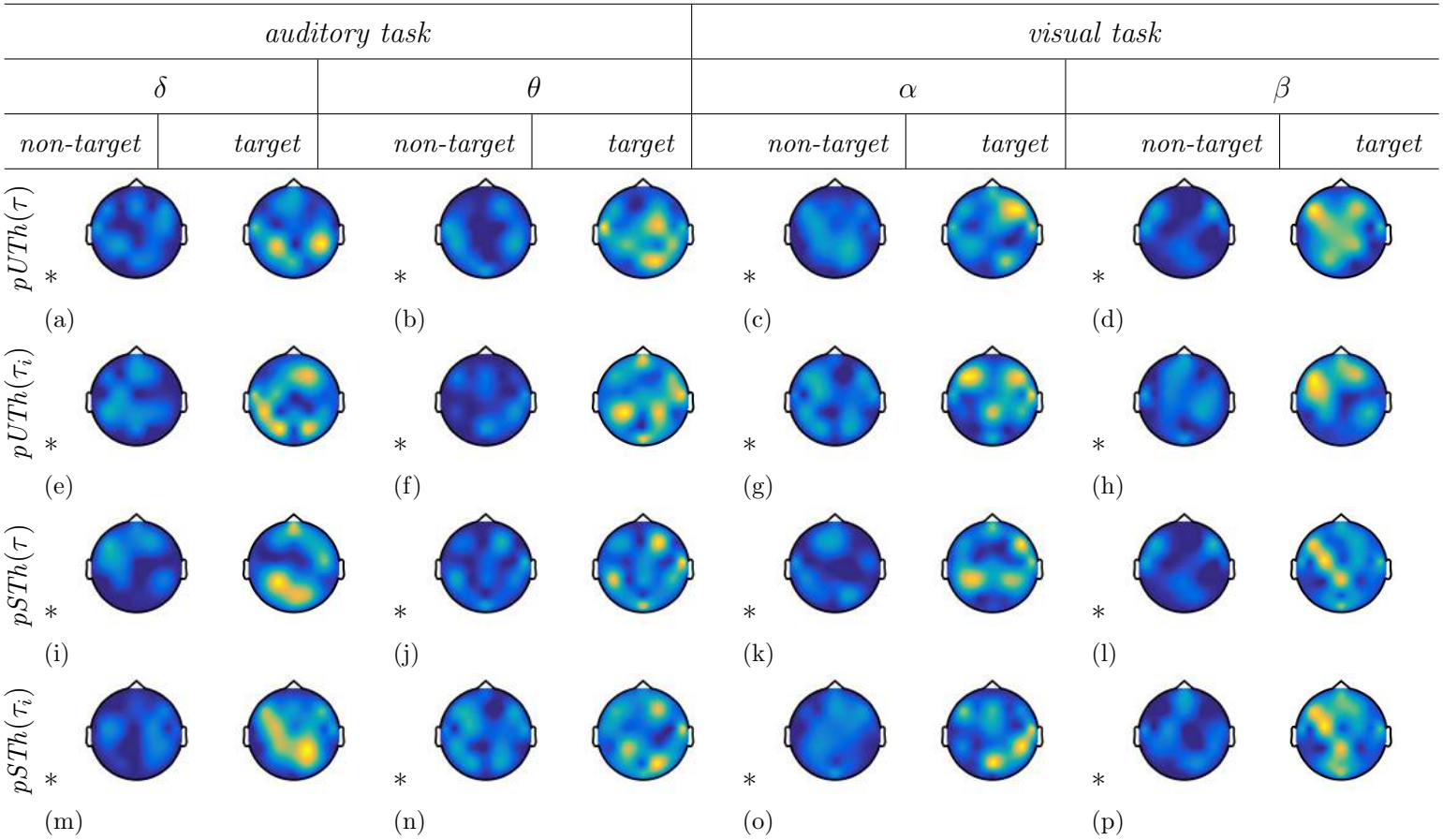

Figure 4.5: Brain graphs estimated by the piecewise thresholding using either rule ($pUTh$ and $pSTh$). Fixed window is indicated by (τ) and variable window by (τ_i).

4.3.3 Performed Piecewise Brain Graph Analysis

For both supervised oddball tasks, 4.6 presents the estimated node strength, $\gamma(c)$, that evolves along the time, resulting in slow variations of relevant nodes and changing synchronously with each evoked potential time-course (see the top row of each plot). Note that the network hub increases when the evoked target amplitude rises also. Likewise, the more complex the stimulus, the higher the averaged node strength, meaning that there should be more nodes to interpret complex oddball target responses.

Another aspect of spatial interpretability is the time-evolving trajectories described by $\gamma(c)$, showing that there is enough difference between the non-target (gray color) and target (black color) stimuli. Also, the use of a changeable window increases this separation and thus enhancing the discrimination between stimuli.

The bottom row of each plot in 4.6 displays how the relevant connectivity vector unfolds from one time-window to another, revealing that the contribution assessed for the link-node set gradually varies. Nonetheless, the neighboring paths are the most likely to change. Besides, since the amount of variable windows is less than the fixed ones, the number of representative connections decreases significantly, being more visible in the case of visual stimuli.

As a result, the obtained stochastically evolving network gives rise to asymptotic distribution, enabling a dynamical approach for the modeling of scale-free networks. Hence, the link evolution may supply additional information, mostly, about the smallest paths between any pair of nodes. Besides of confidently computing all links, therefore, an adequate tracking of evolving connectivity distribution across the time plays a role in ERP interpretation.

On the other hand, we investigate the consistency of performing group-level connectivity graphs by subtracting one (i.e., 16) and two subjects (15) from the whole training set (17). To this end, we determine whether the supervised thresholding rule fulfills the confidence level adjusted to $p = 0.05$, permuting several times each tested subject scenario. It is worth noting that the piecewise strategy is the only validated since the stationary version does not fulfill the required confidence, even managing the whole subject set.

As expected, the subtraction of training subjects decreases the piecewise group-level estimator consistency. Also, either piecewise window performs differently so that the fixed-segmentation graph gets a little worse value of confidence. As seen in 4.2, either segmentation strategy matches the needed value of $p = 0.05$ in all tested scenarios, except

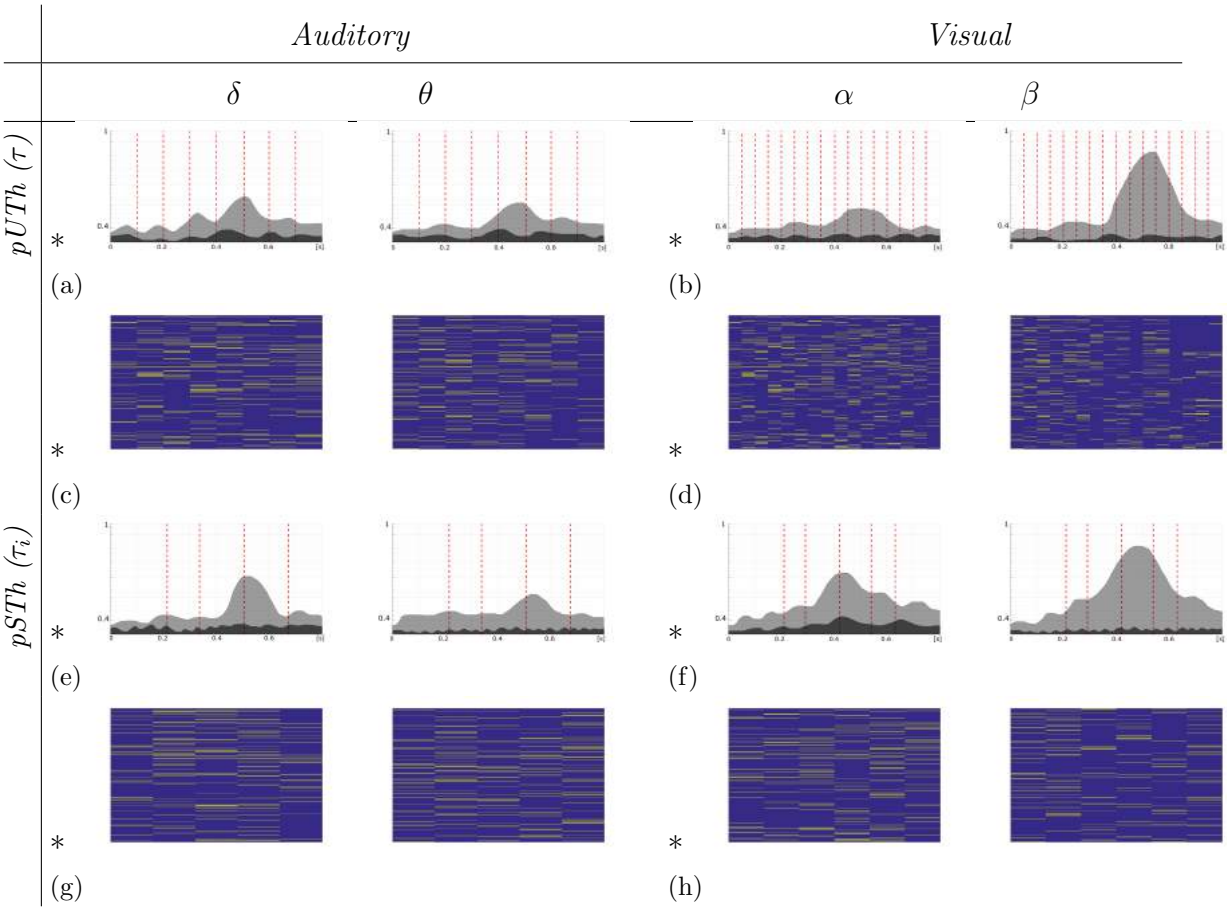

Figure 4.6: Brain graph evolution. Top row – Evolving node strength along the time, for which vertical red line indicates the stimulus onset time. Bottom row – Relevant connectivity unfolding on time.

the fixed window when withdrawing two subjects and extracting the β wave of visual paradigms. On average, the multi-subject analysis benefits more from adjusting the segmentation interval, getting lower values of p.

In addition, 4.2 also represents the estimated values of node density (indicated in parenthesis), revealing that the size of relevance connectivity vectors influences directly on the performed accuracy. So, having the whole training subject set, either piecewise window performs low values of D, facilitating high link consistency at the same time. As the amount of removed subjects increments, however, the node density also grows, but the confidence of connectivity estimation decreases. Besides, the variable piecewise segmentation requires some links less than the fixed window does.

	p-value						*D*					
	τ			τ_i			τ			τ_i		
	15	*16*	*17*	*15*	*16*	*17*	*15*	*16*	*17*	*15*	*16*	*17*
δ Auditory	5.0(44)	4.1(41)	0.8(38)	4.8(38)	2.3(36)	0.5(36)	6.3	6.0	6.0	6.1	5.8	5.1
θ Auditory	5.0(42)	3.9(42)	1.0(38)	3.5(40)	0.9(39)	0.9(38)	6.7	6.5	6.3	5.9	5.8	6.1
α Visual	5.0(38)	4.3(36)	2.4(36)	4.6(37)	3.1(36)	1.7(34)	7.1	6.3	6.3	6.0	5.5	5.4
β Visual	6.8(48)	5.0(44)	1.6(42)	4.7(44)	4.9(44)	0.8(40)	7.0	6.3	6.3	6.3	6.1	6.1
Average	5.4(43)	4.3(41)	1.4(39)	4.4(40)	2.8(39)	0.9(37)	6.8	6.3	6.2	6.0	5.8	5.6

Table 2. Confidence and node density (in parenthesis) of developed group-level analysis using piecewise segmentation. Evaluation is performed by subtracting one and two subjects from the whole training set (17).

Lastly, we analyze the group-level analysis in terms of performing graph connectivity. As a baseline connectogram, 4.7 shows the circular graphical representations of link networks regarding functional neural connectivity, achieved by the whole subject set. As seen, the low waves (δ, α) of either task have a connectivity structure with lesser complexity. Besides, both piecewise segmentation strategies result in a similar graph representation, being very close to the baseline connectogram. Nonetheless, by excluding one subject, some of the links may either appear (painted with a solid green line) or be lost (red line). This effect, which becomes more evident when extracting two subjects, deteriorates the estimated connectivity topology. Also, this on/off switching event mostly influences close links. However, the provided connections depend on the used piecewise window.

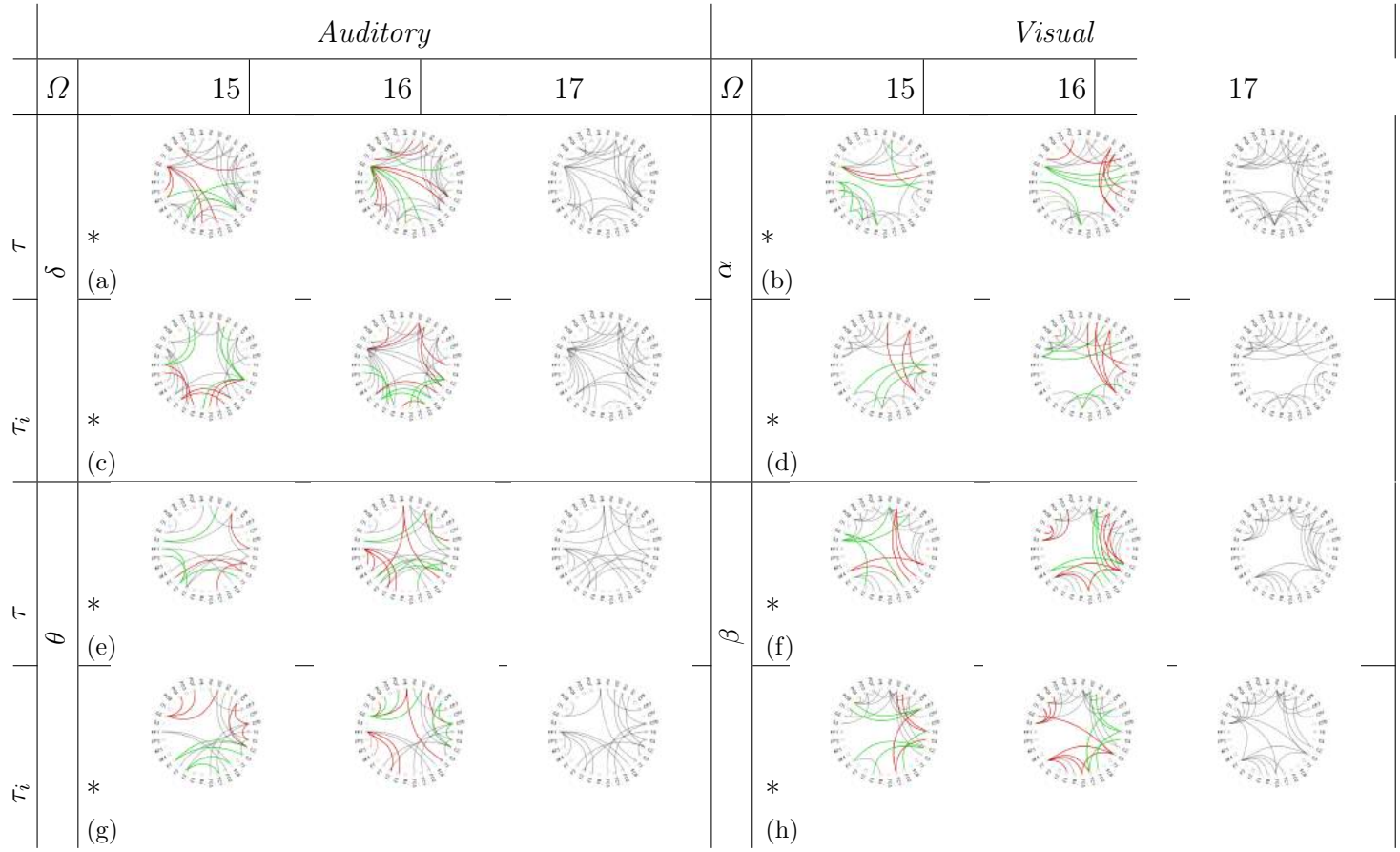

Figure 4.7: Graph connectivity of supervised group-level analysis performed by subtracting one and two subjects from the whole training set. Green line notes a newly appearing link, and red line - a disappearing path. Fixed window is indicated by (τ) and variable window by (τ_i).

4.4 Discussion and Concluding remarks

Validation of real-world EEG data shows that the use of piecewise segmentation, together with the supervised thresholding, results in a set of relevant brain areas, which are estimated with more confidence, enabling a meaningful explanation of oddball paradigm stimuli. Nonetheless, for implementation of the proposed supervised piecewise group-level analysis, the following aspects are to be regarded:

Pairwise estimation subject-level connectivity: We validate the proposed approach through the *weighted Phase Lock Index*, proving that this functional connectivity measure grows meaningfully after the stimulus onset. We obtain that the lower the wave, the higher the number of connections to agree the required confidence level, being even bigger in the case of visual tasks. Of note, the use of *wPLI*, together with stationary unsupervised thresholding, does not reach the fixed level of confidence $p \leq 0.05$.Overall, the used FC metric provides an adequate performance of multi-subject connectivity analysis, however, wPLI-based measures are ad hoc modifications to statistical methods, giving rise to questions related to formal interpretation. Although, there is no consensus about one standard method that would outperform the other connectivity approaches, it would of benefit to validate the proposed piecewise multi-subject analysis using another metric, like effective connectivity [Hassan and Wendling, 2018].

Piecewise computation of multi-subject connectivity graphs: To deal with the non-stationarity, we extract the connectivity assessments from a set of quasi-stationary time segments of EEG data. Further, through a developed thresholding algorithm, we evaluate the statistical differences in the measured functional connectivity within a set of non-overlapping time segments. The piecewise thresholding rule is validated across the whole subject set in two classification scenarios: unsupervised and supervised (between the labels of target and non-target sets). Although both learning scenarios outperform the conventional thresholding rule significantly when no segmentation is carried out, the inclusion of label sets into the rule positively provides better confidence.

Furthermore, we estimate the areas of relevance experimenting two strategies of piecewise segmentation of EEG recordings: an equally lasting time window, and a variable window with intervals placed at the change points of the time-varying classifier performance. Using the supervised thresholding rule, validation of real-world EEG data shows that the areas of relevance, estimated by the piecewise rule, allow explaining the more differentiating EEG channels in the case of validated oddball tasks. Moreover, the variable piecewise segmentation requires some links less than the fixed window

does, which are estimated with a few better confidence. As a result, the supervised variable-window strategy produces a group-level connectivity analysis, ruling a trade-off between computational cost and the required confidence of estimates ($p \leq 0.05$) even after withdrawing two subjects.

Still, two main issues of implementation are to be mentioned: Either tested piecewise strategy makes the EEG connectivity patterns shift gradually from one place to other neighboring electrodes, yielding a relevant connection set that depends on the used piecewise window. Therefore, the time window must be tuned carefully, and two improving approaches can be of interest: *i*) Measuring the statistical diversity among time segments. Though we apply the false discovery rate among time segments, having a low rate of false negatives, more rigorous tests are to be studied (like the Bonferroni correction), aiming to have a more robust comparison of physiological measurements. *ii*) Improving the changeable piecewise window that may include more robust approaches of adaptive segmentation for extracting connectivity patterns. In this regard, a considerable amount of work has been directed to assessing and characterizing dynamic FC, including segmenting the time-courses [Mahyari et al., 2016, Betzel and Bassett, 2017, Preti et al., 2017, Allen et al., 2018, Duc and Lee, 2019]

Brain graph topology: As said before, the node strength evolution varies slowly between neighboring electrodes along the evoked potential time-course, showing that an adequate tracking of evolving connectivity distribution across the time may help in ERP interpretation. Furthermore, to increase the distinction between classes, the piecewise thresholding can be further optimized by enlarging the difference between the node strength time-courses of stimuli.

As for future work, for validating the proposed non-stationary group-level analysis, we plan to experiment with the following key issues: more complex functional and effective measures of connectivity, thresholding rules with distances, including more priors about ERP dynamics and/or optimizing the distinction between multi-label classification tasks. A particular concern to study is the minimization of false-positive inferences by the developed in this work instantaneous interaction to determine whether field spread effects are too large to warrant analysis, as suggested in [Bastos and Schoffelen, 2016, Vinck et al., 2015].

Chapter 5

Clustering for analysis at group-level

5.1 Introduction

One of the most critical aspects of group analysis is selecting the subjects that will make up each partition since the selection directly influences the physiological interpretation [Padilla-Buritica et al., 2020]. This problem usually has been approached from different unsupervised learning strategies [Pereda et al., 2018]; however, some studies have shown that the grouping strategy requires additional details related to the information preprocessing, and the feature estimation [Bassett and Sporns, 2017] (in this case connectivity measurements).

In the case of EEG, the most used technique to group the subjects is according to the performance in classification [Velásquez-Martínez et al., 2019]. Another strategy is related to Independent component analysis -ICA [Huster et al., 2015]; we present an approach related directly to the properties of the networks, which have been estimated with graph theory from the functional connectivity measures.

The most frequent problems with the grouping of subjects are: type of clustering [Hinton, 2011], the number of groups, the validation of the clustering [Frömer et al., 2018] and specifically for the case of neuroscience, the homogeneity of the groups related to their respective physiological interpretability [Padilla-Buritica et al., 2016].

Therefore, we propose a methodology based on k-means clustering, with automatic adjustment of the value of the conformed groups, which considers the variability of the

subjects. This allowed us to build compact groups with better interpretation than other methodologies presented in state of the art. The tests of the proposed methodology were carried out on two Motor Imagery (MI) databases; It was verified that one should pay attention to the conformed groups since a good performance in the classification does not guarantee an appropriate physiological interpretation.

5.2 Materials and Methods

Ensemble-based Weighted Phase Locking Index (*wPLI*) :

$$\nu_2(c,c') = \frac{|\boldsymbol{E}\{\Im\{S(c,c';n,f)\} : \forall n \in N\}|}{\boldsymbol{E}\{|\Im\{S(c,c';n,f)\}| : \forall n \in N\}}, \quad \nu_2(,) \in [0,1] \tag{5.1}$$

where $S(c,c';n,f) \in \mathbb{C}$ is the cross-spectral density based on Morlet wavelets and $\Im\{\cdot\}$ stands for the imaginary part of a complex-valued function.

Besides, the following weighted network indexes are extracted from the either phase synchronization measures:
Strength is a local-scale property that accounts for the number of links connected to each node, computed as follows:

$$\varphi_1(c) = C\boldsymbol{E}\{\nu(c,c') : \forall c' \in C, c' \neq c\}. \tag{5.2}$$

Clustering Coefficient is a global-scale property that indicates the tendency of a network to form tightly connected neighborhoods, measuring the segregation brain's ability for specialized processing within densely interconnected regions, computed as follows:

$$\varphi_2(c) = \frac{1}{C^2}\boldsymbol{E}\{\frac{\pi_c}{\boldsymbol{E}\{\hat{\nu}(c,c')\boldsymbol{E}\{\hat{\nu}(c,c') - 1\}\}} : \forall c \in C, c' \neq c\} \tag{5.3}$$

where the binarized connection value $\hat{\nu}(c,c')=1$, if $\nu(c,c') > 0$, otherwise, $\hat{\nu}(c,c')=0$. $\pi_c \in \mathbb{N}$ is the number of triangles neighboring c-th node.

5.3 Experimental Setup

For evaluation purposes, we use the pipeline of the supervised piecewise network connectivity analysis shown in Figure 5.1, appraising two stages:

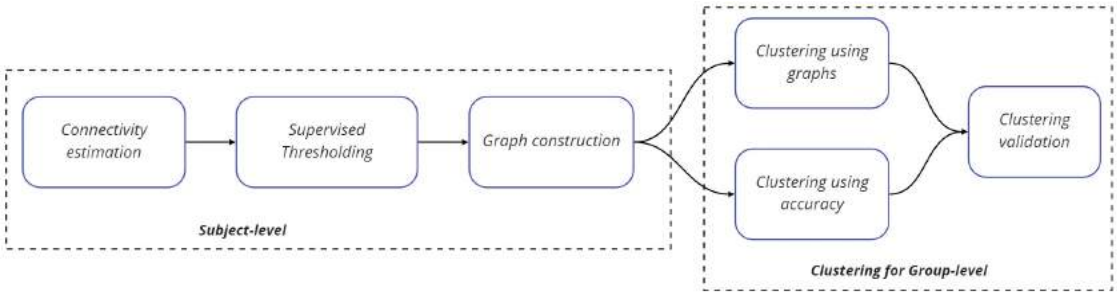

Figure 5.1: Pipeline of the clustering for Group contruction using the supervised piecewise network connectivity analysis.

MI Databases Description and Pre-processing

Gigadb - DBI: We explore the collection publicly available at[1] that holds EEG data obtained from fifty-two subjects (although only M=50 are available) using a 10-10 placement electrode system with C=64 channels. Each channel $\boldsymbol{x}(c)$ lasted T=7 s, and was sampled at F_s=512 Hz. At the beginning of the test, a fixation cross was displayed on a black screen during 2 s. Then, linked to either MI label λ=l or λ=l', a cue instruction appeared randomly on the screen within 3 texts. The cue asked each subject to imagine moving his fingers, starting to form the index finger and reaching the little finger, and touching each to his thumb. A blank screen was then displayed at the beginning of a break period, which ran randomly between 4.1 and 4.8 s. This procedure was repeated over 20 times to complete a single run and stopped at the end to complete a written cognitive quiz [Cho et al., 2017]. Every subject performed five or six runs. In addition, a single-trial resting-state recording, lasting 60 s, was collected from each subject.

Physionet - DBII: This database publicly available[2] holds M=105 volunteers who properly performed the left and right-hand MI tasks, collecting a total average of 46.62 ± 0.96 trials per subject. The 64-channel EEG signals were recorded using the 10-10 international system, and sampled at F_s=160 Hz, lasting 8.1 s. In addition, a single-trial resting-state recording, with a duration of 61 s, was collected from each subject.

[1] http://gigadb.org/dataset/100295
[2] https://physionet.org/content/eegmmidb/1.0.0/

Every raw EEG channel of either database was band-pass filtered in the frequency range $\boldsymbol{f} \in$[4-40] Hz, covering the sensorimotor rhythms considered (μ, β). Then, the band-passed EGG data are spatially filtered by a Laplacian filter centered on the selected electrode to improve the spatial resolution of EEG recordings, avoiding the influence of noise coming from neighboring channels and thus addressing the volume conduction problem[3]. Further, the electrophysiological indicator set, $\{\varphi_i\}$, based on phase synchronization is extracted using the *MNE package* in Python, while the graph predictors are estimated using the Brain Connectivity Toolbox [4].

5.3.1 Subject-level Graph Connectivity Extraction

Initially, a key parameter to fix is the window length to extract the functional connectivity measures considered. Table 5.1 presents the mean and standard deviation of accuracy, averaged across the subject set, and indicates that the length of τ=2 s can be considered a convenient trade-off between accuracy and the number of samples to be processed.

τ	0.5	1	1.5	2
DBI	85.6±9.0	85.7 ± 10.9	87.6±11.3	**87.2±11.6**
DBII	48.7± 8.6	54.2 ± 12.8	55.9±13.4	**56.4±13.6**

Table 1. Performed bi-class accuracy averaged by the subject sets of both considered databases.

The following parameter to adjust is the connection threshold q that is a widely used functional connectivity analysis technique to remove false connections and noise. With different values available, q=0.7 was selected since it presents the best $p-value$ value (p<0.05.) as a comprise value that preserves a sufficient amount of links.

Figure 5.2 displays the results of both graph metrics performed by DBI and DBII. The first column presents the subjects' values of strength computed along the time axis. Note that the subjects are placed along the vertical axis, from top to bottom of the plots, ranked in decreasing order of achieved accuracy. The time series obtained by α

[3]This filtering procedure was carried out using *Biosig Toolbox* that is free available at http://biosig.sourceforge.net

[4]brain-connectivity-toolbox.net

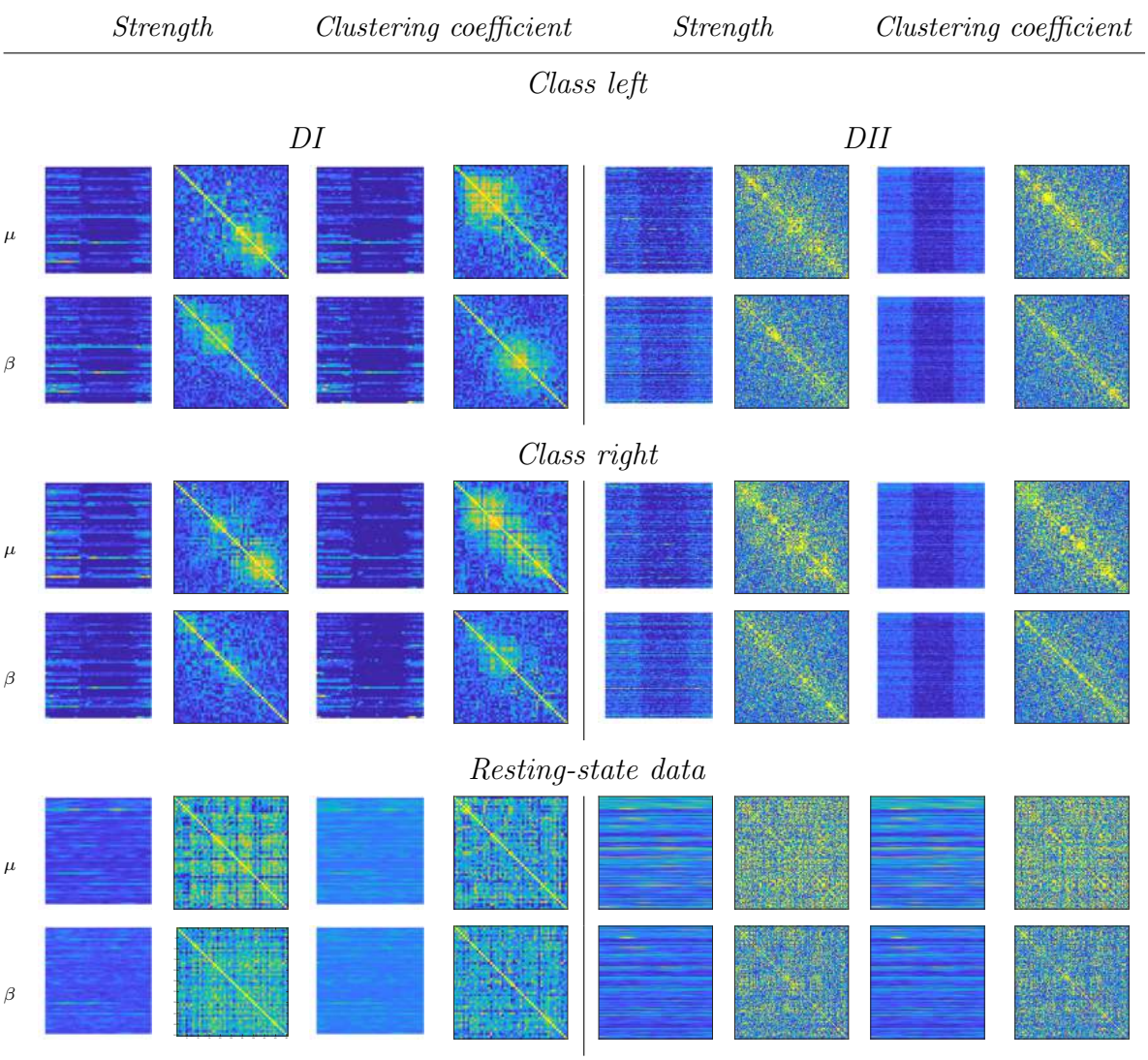

Figure 5.2: Estimation of time-varying graph metrics using Weighted Phase Locking Index (wPLI) performed within sensorimotor rhythms μ and β_{low}. The subjects (vertical axis) are displayed in decreasing order of accuracy.

and β_{low} are displayed in the first and second rows (for the left-labeled data), while the third and fourth rows display the time-varying values achieved by the right label. Regardless of the label, the arranged time-series evidence a dynamic behavior of either graph metric over time, discriminating the baseline wakefulness interval from the MI period. The break period is also visible in the graph metrics extracted from DBII (fifth

and seventh columns).

The covariance matrix estimated over the whole subject set is shown in the second column (strength) and fourth column (clustering coefficient), identifying some groups of similarities between subjects. This situation becomes evident in the subject set of DBII (see sixth and eighth columns). The last couple of rows present the results performed by both graph metrics using the resting-state EEG data and show higher similarity for DBI than for DBII with large variability since it holds twice the number of subjects.

To provide a better physiological interpretation, Figure 5.3 displays the topographic representation reconstructed within the intervals $\Delta T2$ and $\Delta T3$, which three representative individuals perform according to the inefficiency groups:

Subject #14 reaching the best accuracy (group i), subject #49 (group ii), and subject #9, achieving very low discriminability between MI tasks. In the case of the node strength measure, the spatial patterns of time-varying neural activity performed by each sensorimotor rhythm related to some extent (especially within intervals ΔT_1 and $\Delta T2$), producing variations after the cue applied, that, in the intervals ΔT_3, ΔT_4, and ΔT_5. However, the spatial patterns between each labeled MI response vary significantly regardless of the subject, using the full electrode arrangement (FCh). Besides, all three subjects present a topogram representation with very high node strength values at the occipital region within the intervals ΔT_1 and ΔT_2, which may be associated with brain responses to the visual stimuli elicited at the paradigm beginning during the presentation of cue instructions. Nonetheless, within the next MI intervals, the occipital intensity fades, and shifts to the sensorimotor cortex (enclosed within a red square), scattering distinctly in each subject. Note that the occipital lobe activity becomes once again concentrated for the subject # 49 in ΔT_5, suggesting an anticipated break of mental executions. On the other hand, the clustering coefficients' neural patterns are more scattered with higher intensity, but they resemble the findings of the node strength measure.

Further, we compute the wPLI values individually by averaging over the trial set within the entire EEG segment. Two brain network measures, including node strength and clustering coefficients, are implemented for comparison. Figure 5.3 displays the results of both graph metrics, highlighting the changes in connectivity patterns over the time domain (horizontal axis) evoked by either MI tasks (i.e., class) and by measured during

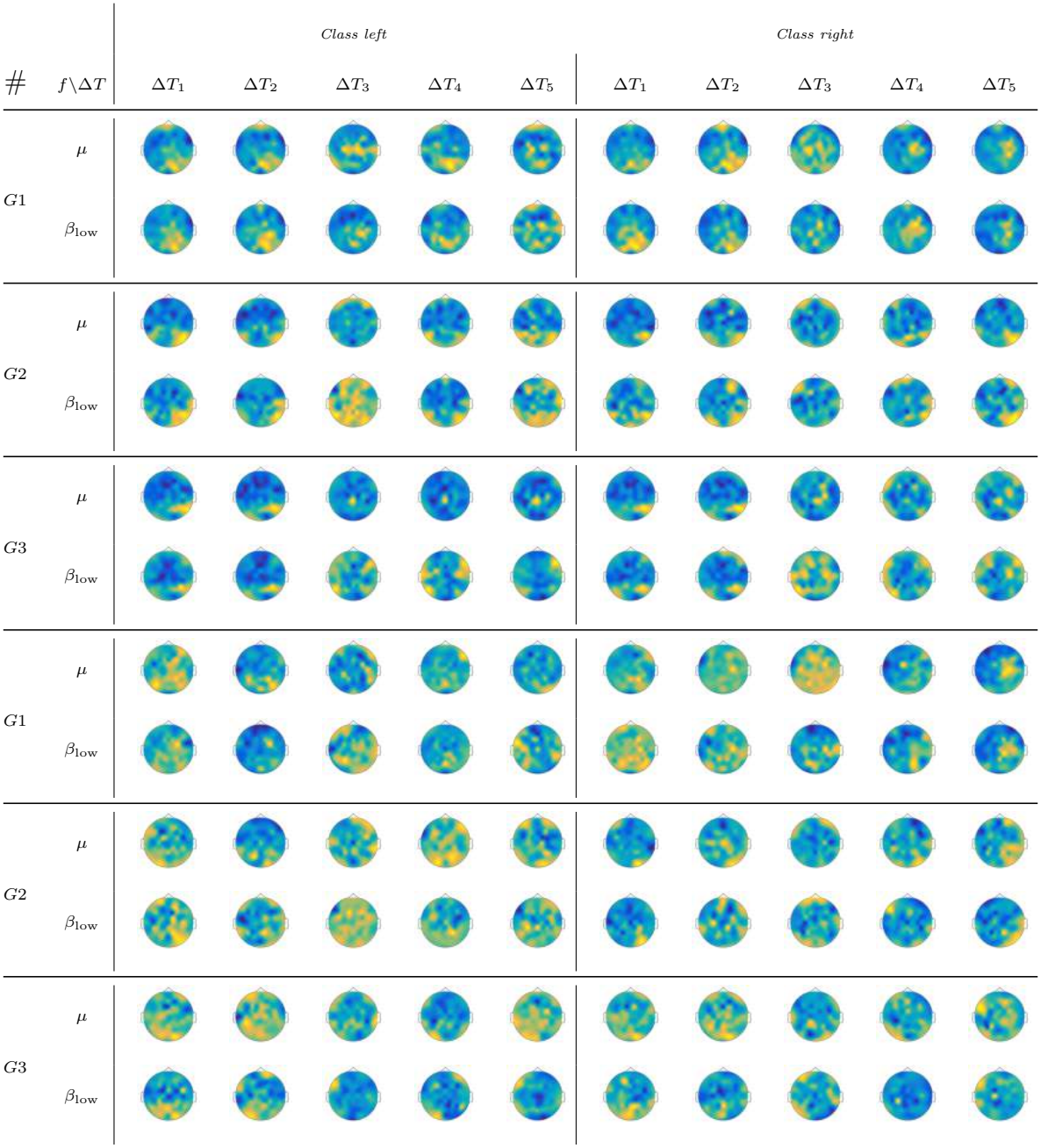

Figure 5.3: Time-varying topograms of three representative individuals performed by node strength and clustering coefficients, and extracted within the timing paradigm intervals.

resting state. Note that the subjects (vertical axis) arranged in decreasing order of accuracy. Both measures distinctly emphasize the neural patterns between the intervals before cue-onset and the segments of evoked MI responses. The differences are apparent in the topological network measures, depending on the examined sensorimotor rhythm. The covariance matrix is also displayed to illustrate the inter-subject variability that increases with the higher subband β_{low} and with individuals performing low values of accuracy, and also revealing some subtle differences between the labeled MI responses. In resting-state data, either brain network measure reflects functional connectivity with similar inter-subject variability and low intrasubject changes. This relatively low variability in the network structure is expected and can explained because of the absence of spontaneous brain activity to be measured.

Note that the occipital lobe activity becomes once again concentrated for the subject # 49 in ΔT_5, suggesting an anticipated break of mental executions. On the other hand, the clustering coefficients' neural patterns are more scattered with higher intensity, but they resemble the findings of the node strength measure. It is important to note that the subjects selected for the database DBII have activity distributed over the entire head, making it difficult to discriminate between different stimuli in the imagery engine tasks.

5.3.2 Clustering of intra/inter-subject variability

To consider the influence of BCI Inefficiency, we cluster the diversity in intra/inter-subject variability to obtain subject partitions with related variability levels of brain neural responses. For comparison purposes, we examine three strategies to infer the distinctiveness between a fixed number of subject partitions:
i) Baseline consideration a group with SMR and accuracy [Hammer et al., 2012].
ii) Group based on graph measurements and clustering coefficiency.

***i*) Grouping based on accuracy response and neural indicators.** We perform clustering of groups with a similar variability behavior under the assumption that the more accurate the subject in distinguishing between MI tasks, the more efficient the individual brain network, as evidenced in [Blankertz et al., 2010]. To estimate the number of partitions, as suggested in [Velasquez-Martinez et al., 2020], we feed the k-means algorithm with the accuracy sets accounting for the performance variability

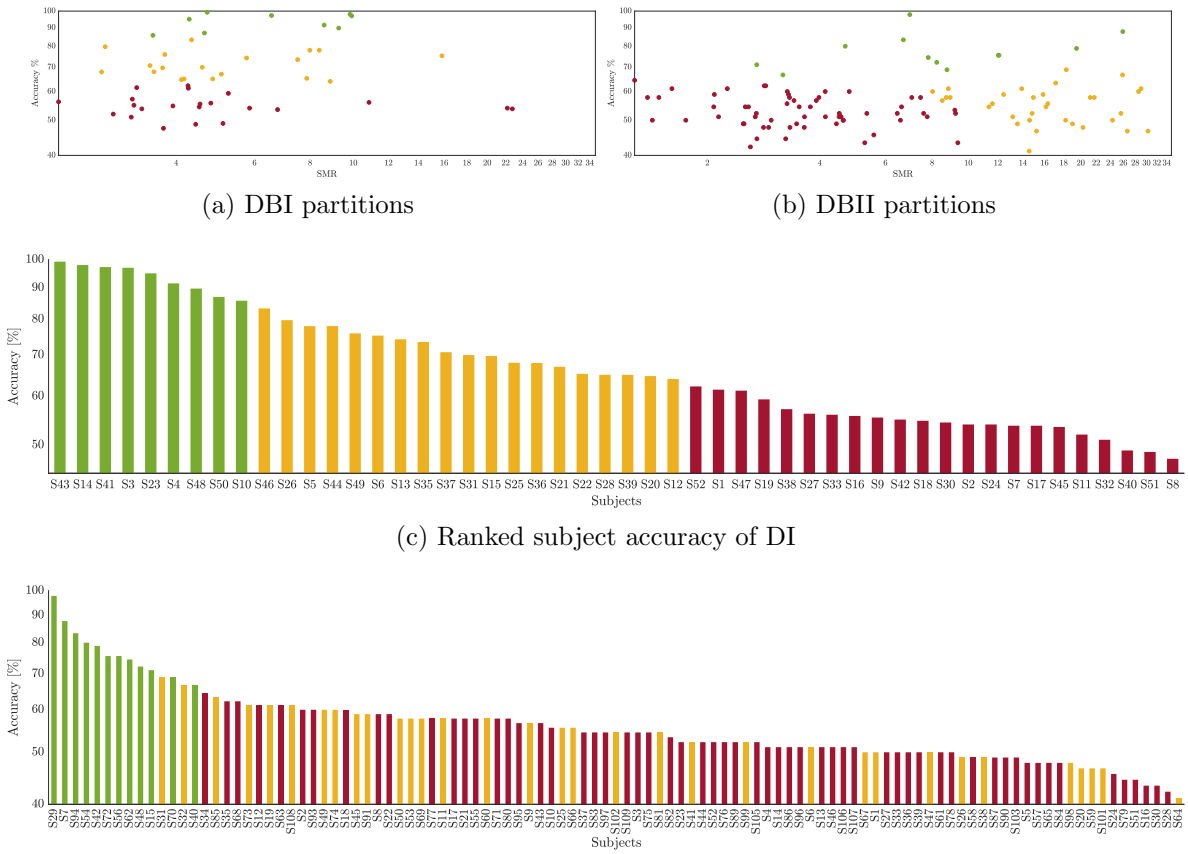

(a) DBI partitions

(b) DBII partitions

(c) Ranked subject accuracy of DI

(d) Ranked subject accuracy of DII

Figure 5.4: Subject clustering using correlates between accuracy and power-based indicators extracted from sensorimotor rhythms.

because of different evaluated extraction window lengths and the indicator values of neural desynchronization at rest over the sensorimotor area. Setting the cluster inertia by the Silhouette score, optining the number of partitions to be three.

For both datasets, the top row in Figures (5.4a-5.4b) presents the resulting clustering drawn in color bars: Group I holds the subjects performing the best (green color), Group II with the middle-performance (yellow color), Group III with the worst-performing individuals (red color). Although either database provides partitions with a low overlapping ratio, the DBI groups also follow the accuracy rank appropriately. As a result, the subjects are not intertwined, as seen in the middle row. In the case of DBII, for which some individuals from Groups II and III intermingle, coinciding within

a common accuracy range, as shown in the bottom row.

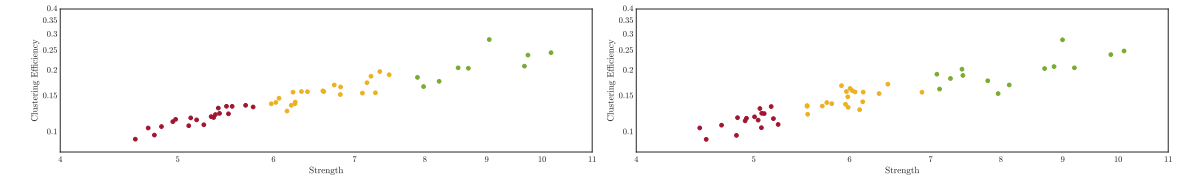

(a) DBI partitions clustering all channels

(b) DBI partitions clustering center channels

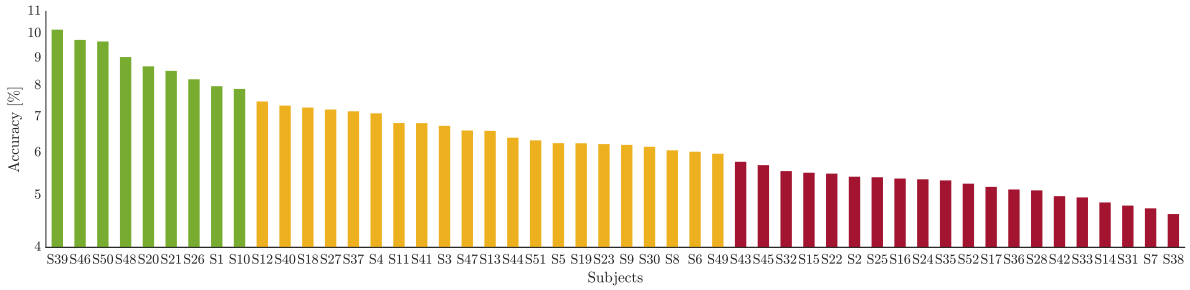

(c) DI

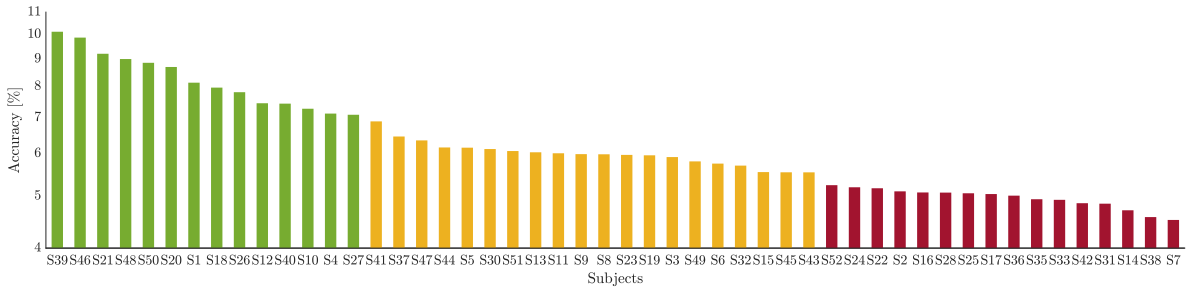

(d) DII

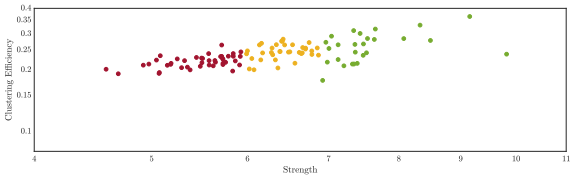

(e) DBII partitions clustering all channels

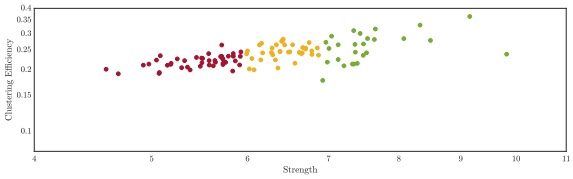

(f) DBII partitions clustering center channels

Figure 5.5: Clustering through graph measures.

***ii*) Subject clustering by Graphs.** After calculating the wPLI connectivity and performing the Clustering Coefficiency and Strength graph measurements, we perform

groupings and identify the internal behavior between MI tasks. For both data sets, in the top row in Figures(5.5a - 5.5b, 5.5e - 5.5f), present the resulting grouping in colored bars for DBI, where Group I contains the subjects that show better performance compared to the graph measures (Green color), Group II includes the average version (yellow), Group III with individuals with low performance (Red color). Taking into account that the analysis in ref fig: cl2a, we do the grouping taking into account all the connections. For ref fig: cl2b we only take into account the connections of the motor region, which allows me to identify the change in Group I and II that evidenced in Figures(5.5c - 5.5d), where there is an increase in subjects from Group I compared to Group II in DBI.

For DBII in Figures (5.5e - 5.5f), a grouping with all the connections or only those of the motor region presented with similar dynamics, which explains us with stability by having fewer connections for graph measurements. However, we can identify that it shows partitions without overlap between the three groups in both databases, which follows the range of precision in a pleasing way.
When observing the behavior in rest state when analyzing the power of the channels C_3 and C_4, we observe the difference in the activity that occurs, for which a distance using a kernel between the subjects of both bases of data, where the first 50 subjects belong to DBI and the following subjects to DBII, the lower triangular is part of the C_3 channel and the upper triangular C_4, observed that each database for these two channels their characteristics are close. However, between the databases, they are not so close in their information.
When reviewing the activity related to the connectivities of this group seen in Figure 5.6 it can found that the connections of the areas (frontoparietal, central, parietal-occipital, temporal), associated with tasks such as (information processing, analysis, memory, concentration, sensorimotor zone) which was also found in [Sun et al., 2019].

From the above, it is evident that when analyzing the two databases, for each grouping mentioned above, similar areas are presented such as the parietal, motor, and frontoparietal, this is generated by the results of connectivity when looking at integration as segregation, information that reveals the behavior of brain regions in the presence of tasks in motor imagination as seen in Figure 5.6.

Figure 5.6: Functional Connectivity using the mask in the motor imagery window for the selected subjects from each of the groups by accuracy.

Lastly, it is crucial to bear in mind that the grouping carried out exclusively by the success in classification allows separating the subjects according to their performance. Still, it does not guarantee an appropriate physiological interpretation since the zones with the most significant activation found in the (areas somatosensory) of the head.

Now, when the information obtained through the second grouping strategy is analyzed, which takes into account the measures of the group, e.g. (Strenght vs. Clustering coefficiency), it can be noted that the separability between the connections of the groups is clear according to Figure 5.5, later, brain activity is reviewed and can see in Figure 5.6, which highlights the connections of the areas (frontoparietal, central, parietal-occipital, temporal), associated with tasks such as (sensorimotor zone, memory, concentration, information processing) which also found in the works made by cite rodrigues2019 citesun2019
It can be noted according to cite sareen2020 that the best physiological interpretability for the task analyzed in this exercise related to motor imagination including the state of rest, this presents activation in the sensory and motor areas (coincidence with analysis of the graphs), Therefore, it is a strategy to consider at the time of group analysis while preserving physiological interpretability.
In summary, the need to make a grouping that highlights physiological interpretability is evident and a good strategy is to take advantage of connectivities and graph analysis. In the results obtained in Table5.2 it is evident that despite the quality of the clustering carried out, the high variability of the subjects, the heterogeneity of the connectivities, as well as the chosen threshold, notably affect the activity that will be finally analyzed. From the above, it is evident that when analyzing the two databases, for each grouping mentioned above, similar areas are presented such as the parietal, motor and fronto-parietal, this is generated by the results of connectivity when looking at integration as segregation, information that reveals the behavior of brain regions in the presence of tasks in motor imagination as seen in Figure 5.6 and at the link level in 5.7.

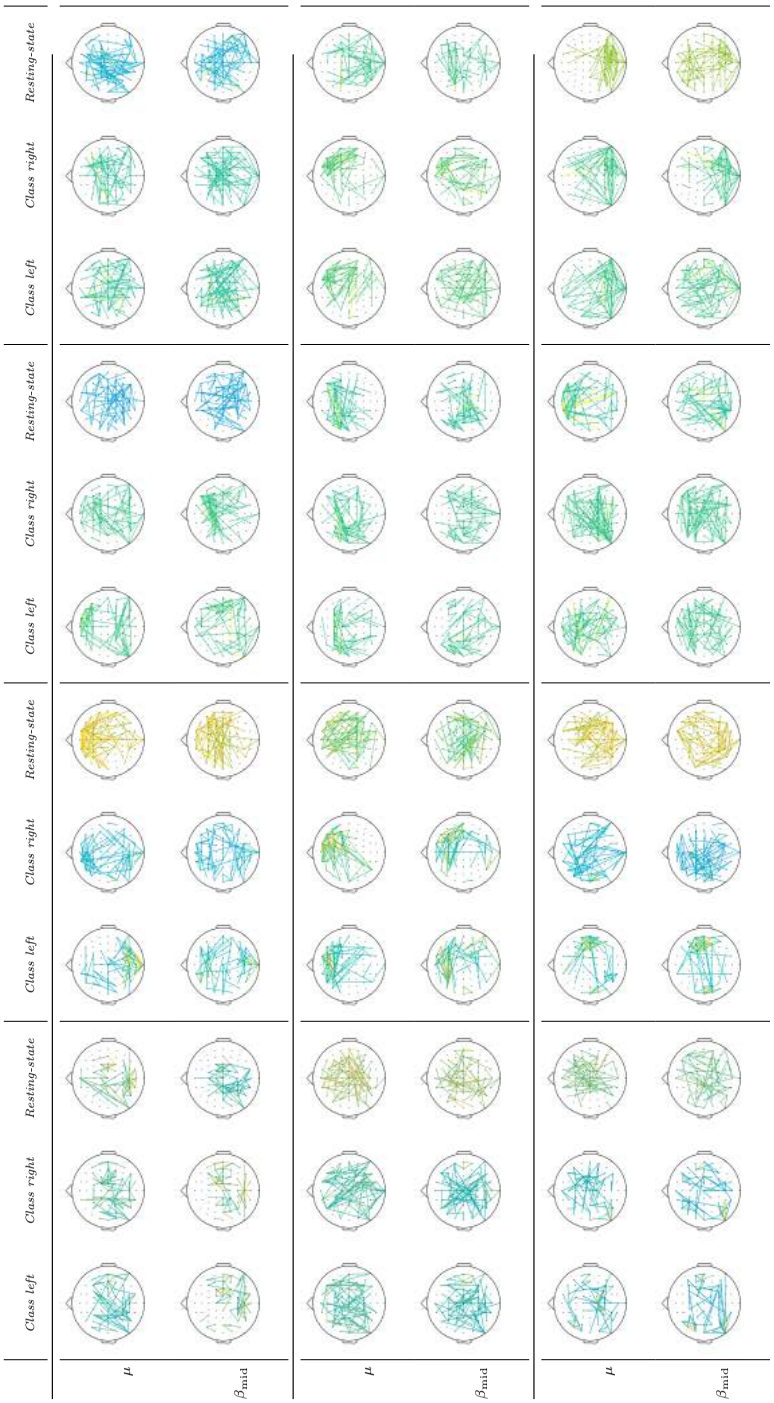

Figure 5.7: Brain connectivity network functional three representative individuals performed by node strength, and extracted within the interval ΔT.

According to Figure 5.7, where connectivity and correlation behaviors between subjects are analyzed, it can be noted that the DI database is more compact, homogeneous, similar between subjects, stable, has fewer subjects and is better the response of the subjects before the stimulus, in both databases, a similar behavior of the subjects can be seen in the Resting State, despite this, the correlation of the DII is lower. The results presented in resting coincide with the results reported in [Vecchio et al., 2016], [Zhang et al., 2015], [Iyer et al., 2015], where it is noted that there is no localized-concentrated brain activity. There is no pre-established activity, or a prior/a-priori disposition of the connections in both databases. It should be noted that using the same thresholding, same process conditions, there is less variability in the DI database than in DII, preserving more compact areas of activity for DI, related to the principles of neuronal integration and segregation according to appointment [Sporns, 2007][Sporns, 2018].
Finally, using the graph measurements, already seen in Figure 5.7 that the activity in the motor imagination window for each task, gives us a sense as is the response in the connections that stand out, for which a [Harper et al., 2017] test carried out to identify which connections show stable behavior in each of the groups, taking into account two types of selection, i) the connections that activated in all the subjects called AND, ii) the Connections that are activated if they want once in the OR subjects, after doing this, we look with the two measures of the Force graph and the clustering coefficient, to identify the activated regions of interest. From the above, analyzed how the dynamics are in Figure 5.8, where we show for DBI (first four columns) and DBII (the last four), the behavior of the groups in each graph measurement allowing us to identify how it is the dynamics of the connections, as we see the differences between the databases, implying that they present spatial differences. When observing at the group level, the activity reflected after estimating the strength measure in the DBI database found that the action is low in the groups with good performance G1 compared to the subjects with lower performance.

Figure 5.8: Application of the test between the classes to identify the connections that are relevant in the groups selected by the clustering of graphs, in the bands μ and β_{low}.

Therefore, its dynamics are related to connections with more information in the central-parietal zone, while when looking at the G3, one can see dynamics distributed over the entire surface. But when looking at the Clustering Coefficiency activity, we see that the G1 shows a higher clustering behavior in the μ band than the other groups. When analyzing the behavior of the second database, we see that for the activity analyzed in form (i), we see that the same connections are not activated for all subjects to make the test measurement later, so we look at the behavior in (ii), where more focused activity evidenced for both graph measurements after performing the test between the two classes. However, in groups G1 and G2, similar behavior is evidenced between the groups, although highlighted that in G1 there is a central-parietal activity, an area related to the motor imagination activity [Padilla-Buritica et al., 2020], while the other groups present not only the same place but also highlights a Frontal and occipital activity, related to the action of neural processes of thought and visual respectively.

Table 5.2: Different performance measures and average for each group

Database	DBI										DBII									
	Silhouette	Acc			Mutual info	rand score	Homogeneity	Density			Silhouette	Acc			Mutual info	rand score	Homogeneity	Density		
		G1	G2	G3				G1	G2	G3		G1	G2	G3				G1	G2	G3
Acc-SMR(r)	0.74	0.93	0.71	0.55	0.72	0.68	0.65	0.7	0.65	0.6	0.68	0.59	0.55	0.53	0.71	0.71	0.69	0.69	0.64	0.62
Graphs(r)	**0.84**	**0.91**	**0.69**	**0.67**	**0.78**	**0.76**	**0.75**	**0.81**	**0.79**	**0.72**	**0.82**	**0.78**	**0.64**	**0.56**	**0.76**	**0.75**	**0.72**	**0.76**	**0.74**	**0.68**

Table 5.2 contains different measures to quantify the clustering performance; We can note that doing the clustering with graph measures provides a high performance compared to the classification accuracy. This result shows that it is possible to consider the graph measures as input information for the clustering strategy since intra- and inter-group measurements are appropriate.

5.4 Discussion and Concluding remarks

One of the most important aspects of doing the connectivity analysis at the group level is establishing the subjects that will make up each set of subjects to make a fair comparison that avoids information bias and, above all, that allows comparing dynamics with similar behaviors. One of the most straightforward solutions that have been suggested in state of the art is clustering. However, we must overcome the obstacles related to clustering, that is, the grouping method, the number of groups, the distance of similarity between groups, and finally, an aspect that is usually given less importance and is to verify the quality of the clustering, taking into account the variability between and within the groups.

In this chapter, we have compared the most used strategy in neuroscience to do clustering (which is based on classification performance) with the simplest clustering method known (k-means). It is essential to mention that k-means have been chosen to show the benefits of characterizing with properties of the networks (connectivity and graphs) and clarify that the distribution of the data for each group of subjects allows the use of an algorithm easy. In both databases, it showed that it is feasible to use connectivity accompanied by the graph properties as input to do supervised and unsupervised learning so that the interpretability of the results is preserved in both cases.

Chapter 6

Conclusions and Future Work

6.1 General Conclusions and Main Contributions

Develop a methodology to obtain relevant connections using a supervised framework for statistical differences between neural responses

In chapter 3, we have studied differences in the connectivity patterns at the channel level during an oddball task to analyze the behavior of phase networks in attention tasks; here, the phase synchronization estimation was carried out through the a phase-locking value, a statistical metric for functional connectivity. Also, a selection methodology was proposed to choose relevant connections by finding the set of interactions that most discriminate the conditions target and non-target, in the sense of statistical difference.

As a result, we found that a reduced group of connectivity patterns allow differentiating the conditions target and non-target in the oddball paradigm. Moreover, the connections reported as significant in this chapter are related to frontal, temporal, and occipital channels in low-frequency bands. These EEG channels are associated with the cognitive processes involved in the oddball paradigm (auditory response, information processing, and memory).

Design of a time-varying framework to select a set of quasi-stationary segments for dynamic functional connectivity analysis

In chapter 4, we have developed a piecewise multi-subject analysis that is applied over a set of time intervals within the stationary assumption holds to deal with the time variability of neural responses. We experimented with a variable time window, which is segmented at the change points of the time-varying classifier performance, for segmenting the whole stimulus-locked epoch into multiple temporal windows. Employing the weighted Phase Lock Index as a functional connectivity measure, we have presented the validation in real-world EEG data, proving the effectiveness of variable time segmentation for connectivity extraction when combined with a supervised thresholding approach. Consequently, we performed a piecewise group-level analysis of electroencephalographic data that deals with non-stationary functional connectivity networks, evaluating more carefully the contribution of a link node-set in discriminating between the labeled oddball responses.

Develop a methodology to obtain relevant connections using a supervised framework for statistical differences between neural responses

Design of a time-varying framework to select a set of quasi-stationary segments for dynamic functional connectivity analysis

Design of a methodology based on graph network measurements to group subjects

In chapter 5, we propose a methodology based on unsupervised learning, with automatic adjustment of the value of the conformed groups, which considers the variability of the subjects. This allowed us to build compact groups with better interpretation than other methodologies presented in state of the art. The most important part of this chapter corresponds to the connectivity analysis at the group level, using graph measures related to integration and segregation principles, which allow preserving the physiological interpretability of the estimated results. The tests of the proposed methodology were

carried out on two Motor Imagery (MI) databases; It was verified that one should pay attention to the conformed groups since a good performance in the classification does not guarantee an appropriate physiological interpretation.

6.2 Future Work

Besides the method-specific analyses proposed above as future work, more general topics should also be considered:

EEG Mapping into source space

The low resolution of the EEG recordings, related to the number of electrodes (a couple of hundreds at best) located over the entire head surface, represents a problem where several thousands of brain activity generators are measured with the limited number of channels and do not faithfully represent the information in the brain source space. Therefore, the neurophysiological interpretation based of the EEG representation is complicated and no accurate. The connectivity measurements over EEG may be compromised by the volume conduction effects leading to possible fake connections or to lose important information. Accordingly, as a future work an EEG source imaging stage can be included to implement the proposed methodology over the estimated brain source signals and facilitate the interpretation of the results.

Graph theory approaches and effective connectivity

Graph theory is a field of mathematics in which the topological properties of networks are studied to model a system, in graph theoretical terms networks are collections of nodes (vertices) and edges(links) between pairs of nodes. In functional brain connectivity networks, brain regions are associated with nodes and connections between those brain regions with edges, and it can be represented with adjacency matrix of size, node x node. To perform network analysis, measures over the connectivity matrices are used to describe global properties of the entire network or individual aspects of the connections or nodes. These measures may supply valuable information in brain connectivity analysis. In addition to the above, it may be interesting to

include a temporal model of the variability of the connectivities so that the adjacency matrices encode more information between the relationships of the areas analyzed with connectivity.

Change point detection

It is necessary to try other strategies to segment the EEG signals into quasi-stationary pieces. One of the main problems in estimating connectivity and extracting features is the non-stationary nature of brain activity. Besides, this would allow the use of connectivity measures more simple, decreasing the computation time between multiple trials.There are methodologies based on statistical hypothesis tests for stationarity and Hidden Markov models, which point towards estimating segments where the second-order statistics remain stable over time.

Dynamic clustering for analysis at group-level

It is necessary to include other clustering schemes, including methods that adjust to the data distributions. This purpose is a connectivity analysis that takes into account the subject variability over time. It should consist of dynamic clustering to monitor the variability of the connectivities between subjects to take this methodology towards what is currently known as chronnectome. In this work, it has been shown that each database has its own set of parameters to tune in; therefore, it may be interesting to review the influence of a clustering that takes these factors into account.

Bibliography

[Acharya et al., 2015] Acharya, U. R., Sudarshan, V. K., Adeli, H., Santhosh, J., Koh, J. E., and Adeli, A. (2015). Computer-aided diagnosis of depression using eeg signals. *European neurology*, 73(5-6):329–336.

[Allen et al., 2018] Allen, E., Damaraju, E., Eichele, T., Wu, L., and Calhoun, V. D. (2018). EEG signatures of dynamic functional network connectivity states. *Brain topography*, 31(1):101–116.

[Allen et al., 2014] Allen, E. A., Damaraju, E., Plis, S. M., Erhardt, E. B., Eichele, T., and Calhoun, V. D. (2014). Tracking whole-brain connectivity dynamics in the resting state. *Cerebral cortex*, 24(3):663–676.

[Astolfi et al., 2007] Astolfi, L., De Vico Fallani, F., Cincotti, F., Mattia, D., Marciani, M., Bufalari, S., Salinari, S., Colosimo, A., Ding, L., Edgar, J., et al. (2007). Imaging functional brain connectivity patterns from high-resolution EEG and fMRI via graph theory. *Psychophysiology*, 44(6):880–893.

[Aviyente et al., 2017] Aviyente, S., Tootell, A., and Bernat, E. M. (2017). Time-frequency phase-synchrony approaches with ERPs. *International Journal of Psychophysiology*, 111:88–97.

[Babiloni et al., 2016] Babiloni, C., Lizio, R., Marzano, N., Capotosto, P., Soricelli, A., Triggiani, A. I., Cordone, S., Gesualdo, L., and Del Percio, C. (2016). Brain neural synchronization and functional coupling in alzheimer's disease as revealed by resting state EEG rhythms. *International Journal of Psychophysiology*, 103:88–102.

[Baillet et al., 2001] Baillet, S., Mosher, J. C., and Leahy, R. M. (2001). Electromagnetic brain mapping. *IEEE Signal processing magazine*, 18(6):14–30.

[Bakhshayesh et al., 2019] Bakhshayesh, H., Fitzgibbon, S. P., Janani, A. S., Grummett, T. S., and Pope, K. J. (2019). Detecting synchrony in EEG: A comparative study of functional connectivity measures. *Computers in Biology and Medicine*, 105:1–15.

[Bassett and Gazzaniga, 2011] Bassett, D. S. and Gazzaniga, M. S. (2011). Understanding complexity in the human brain. *Trends in cognitive sciences*, 15(5):200–209.

[Bassett and Sporns, 2017] Bassett, D. S. and Sporns, O. (2017). Network neuroscience. *Nature neuroscience*, 20(3):353.

[Bastos and Schoffelen, 2016] Bastos, A. M. and Schoffelen, J.-M. (2016). A tutorial review of functional connectivity analysis methods and their interpretational pitfalls. *Frontiers in systems neuroscience*, 9:175.

[Bathelt et al., 2013] Bathelt, J., O'reilly, H., Clayden, J. D., Cross, J. H., and de Haan, M. (2013). Functional brain network organisation of children between 2 and 5 years derived from reconstructed activity of cortical sources of high-density EEG recordings. *NeuroImage*, 82:595–604.

[Berger, 1934] Berger, H. (1934). Über das Elektrenkephalogramm des Menschen. *Deutsche Medizinische Wochenschrift*, 60(51):1947–1949.

[Betzel and Bassett, 2017] Betzel, R. F. and Bassett, D. S. (2017). Multi-scale brain networks. *Neuroimage*, 160:73–83.

[Betzel et al., 2012] Betzel, R. F., Erickson, M. A., Abell, M., O'Donnell, B. F., Hetrick, W. P., and Sporns, O. (2012). Synchronization dynamics and evidence for a repertoire of network states in resting EEG. *Frontiers in computational neuroscience*, 6:74.

[Bielczyk et al., 2018] Bielczyk, N. Z., Walocha, F., Ebel, P. W., Haak, K. V., Llera, A., Buitelaar, J. K., Glennon, J. C., and Beckmann, C. F. (2018). Thresholding functional connectomes by means of mixture modeling. *NeuroImage*, 171:402–414.

[Bijsterbosch et al., 2018] Bijsterbosch, J. D., Woolrich, M. W., Glasser, M. F., Robinson, E. C., Beckmann, C. F., Van Essen, D. C., Harrison, S. J., and Smith, S. M. (2018). The relationship between spatial configuration and functional connectivity of brain regions. *Elife*, 7:e32992.

[Blankertz et al., 2010] Blankertz, B., Sannelli, C., Halder, S., Hammer, E. M., Kübler, A., Müller, K.-R., Curio, G., and Dickhaus, T. (2010). Neurophysiological predictor of smr-based bci performance. *Neuroimage*, 51(4):1303–1309.

[Blinowska, 2011] Blinowska, K. J. (2011). Review of the methods of determination of directed connectivity from multichannel data. *Medical & biological engineering & computing*, 49(5):521–529.

[Blumenfeld, 2010] Blumenfeld, H. (2010). *Neuroanatomy through clinical cases*. Sinauer Associates Sunderland.

[Boccaletti et al., 2006] Boccaletti, S., Latora, V., Moreno, Y., Chavez, M., and Hwang, D.-U. (2006). Complex networks: Structure and dynamics. *Physics reports*, 424(4-5):175–308.

[Bowyer, 2016] Bowyer, S. M. (2016). Coherence a measure of the brain networks: past and present. *Neuropsychiatric Electrophysiology*, 2(1):1.

[Brázdil et al., 2007] Brázdil, M., Mikl, M., Mareček, R., Krupa, P., and Rektor, I. (2007). Effective connectivity in target stimulus processing: a dynamic causal modeling study of visual oddball task. *Neuroimage*, 35(2):827–835.

[Bridwell et al., 2018] Bridwell, D. A., Cavanagh, J. F., Collins, A. G., Nunez, M. D., Srinivasan, R., Stober, S., and Calhoun, V. D. (2018). Moving beyond ERP components: A selective review of approaches to integrate EEG and behavior. *Frontiers in human neuroscience*, 12:106.

[Buijink et al., 2015] Buijink, A. W., van der Stouwe, A. M., Broersma, M., Sharifi, S., Groot, P. F., Speelman, J. D., Maurits, N. M., and van Rootselaar, A.-F. (2015). Motor network disruption in essential tremor: a functional and effective connectivity study. *Brain*, 138(10):2934–2947.

[Carter, 2019] Carter, R. (2019). *The human brain book: An illustrated guide to its structure, function, and disorders*. Penguin.

[Chen et al., 2015] Chen, M., Han, J., Guo, L., Wang, J., and Patras, I. (2015). Identifying valence and arousal levels via connectivity between eeg channels. In *Affective Computing and Intelligent Interaction (ACII), 2015 International Conference on*, pages 63–69. IEEE.

[Chilla et al., 2015] Chilla, G. S., Tan, C. H., Xu, C., and Poh, C. L. (2015). Diffusion weighted magnetic resonance imaging and its recent trend—a survey. *Quantitative imaging in medicine and surgery*, 5(3):407.

[Cho et al., 2017] Cho, H., Ahn, M., Ahn, S., Kwon, M., and Jun, S. C. (2017). Eeg datasets for motor imagery brain–computer interface. *GigaScience*, 6(7):gix034.

[Cooper et al., 2016] Cooper, P. S., Darriba, Á., Karayanidis, F., and Barceló, F. (2016). Contextually sensitive power changes across multiple frequency bands underpin cognitive control. *NeuroImage*, 132:499–511.

[Crouch et al., 2018] Crouch, B., Sommerlade, L., Veselcic, P., Riedel, G., Schelter, B., and Platt, B. (2018). Detection of time-, frequency-and direction-resolved communication within brain networks. *Scientific reports*, 8(1):1–15.

[De Vico Fallani et al., 2014] De Vico Fallani, F., Richiardi, J., Chavez, M., and Achard, S. (2014). Graph analysis of functional brain networks: practical issues in translational neuroscience. *Philosophical Transactions of the Royal Society B: Biological Sciences*, 369(1653):20130521.

[Dimitriadis et al., 2017] Dimitriadis, S. I., Salis, C., Tarnanas, I., and Linden, D. E. (2017). Topological filtering of dynamic functional brain networks unfolds informative chronnectomics: a novel data-driven thresholding scheme based on orthogonal minimal spanning trees (omsts). *Frontiers in neuroinformatics*, 11:28.

[Ding et al., 2015] Ding, W., Ding, L., Li, F., Han, Y., and Mu, L. (2015). Neurodegeneration and cognition in parkinson's disease: a review. *Eur Rev Med Pharmacol Sci*, 19(12):2275–81.

[Dinh et al., 2019] Dinh, S. T., Nickel, M. M., Tiemann, L., May, E. S., Heitmann, H., Hohn, V. D., Edenharter, G., Utpadel-Fischler, D., Tölle, T. R., Sauseng, P., et al. (2019). Brain dysfunction in chronic pain patients assessed by resting-state electroencephalography. *Pain*, 160(12):2751.

[Dobson and Giovannoni, 2019] Dobson, R. and Giovannoni, G. (2019). Multiple sclerosis–a review. *European journal of neurology*, 26(1):27–40.

[Drysdale et al., 2017] Drysdale, A. T., Grosenick, L., Downar, J., Dunlop, K., Mansouri, F., Meng, Y., Fetcho, R. N., Zebley, B., Oathes, D. J., Etkin, A., et al.

(2017). Resting-state connectivity biomarkers define neurophysiological subtypes of depression. *Nature medicine*, 23(1):28.

[Duc and Lee, 2019] Duc, N. T. and Lee, B. (2019). Microstate functional connectivity in EEG cognitive tasks revealed by a multivariate gaussian hidden markov model with phase locking value. *Journal of neural engineering*, 16(2):026033.

[Ebrahim et al., 2014] Ebrahim, M., Khan, S., and Mohani, S. S. U. H. (2014). Peer-to-peer network simulators: an analytical review. *arXiv preprint arXiv:1405.0400*.

[Englot et al., 2016] Englot, D. J., Chang, E. F., and Vecht, C. J. (2016). Epilepsy and brain tumors. In *Handbook of clinical neurology*, volume 134, pages 267–285. Elsevier.

[Ergenoglu et al., 2004] Ergenoglu, T., Demiralp, T., Bayraktaroglu, Z., Ergen, M., Beydagi, H., and Uresin, Y. (2004). Alpha rhythm of the eeg modulates visual detection performance in humans. *Cognitive brain research*, 20(3):376–383.

[Finger, 2013] Finger, S. (2013). *Recovery from brain damage: Research and theory*. Springer Science & Business Media.

[Fornito et al., 2016] Fornito, A., Zalesky, A., and Bullmore, E. (2016). *Fundamentals of brain network analysis*. Academic Press.

[Fox, 2018] Fox, M. D. (2018). Mapping symptoms to brain networks with the human connectome. *New England Journal of Medicine*, 379(23):2237–2245.

[Friston, 2011] Friston, K. J. (2011). Functional and effective connectivity: a review. *Brain connectivity*, 1(1):13–36.

[Friston et al., 2003] Friston, K. J., Harrison, L., and Penny, W. (2003). Dynamic causal modelling. *Neuroimage*, 19(4):1273–1302.

[Frömer et al., 2018] Frömer, R., Maier, M., and Abdel Rahman, R. (2018). Group-level eeg-processing pipeline for flexible single trial-based analyses including linear mixed models. *Frontiers in Neuroscience*, 12:48.

[Garrison et al., 2015] Garrison, K. A., Scheinost, D., Finn, E. S., Shen, X., and Constable, R. T. (2015). The (in) stability of functional brain network measures across thresholds. *Neuroimage*, 118:651–661.

[Genovese et al., 2002] Genovese, C. R., Lazar, N. A., and Nichols, T. (2002). Thresholding of statistical maps in functional neuroimaging using the false discovery rate. *NeuroImage*, 15(4):870–878.

[Gola et al., 2013] Gola, M., Magnuski, M., Szumska, I., and Wróbel, A. (2013). Eeg beta band activity is related to attention and attentional deficits in the visual performance of elderly subjects. *International Journal of Psychophysiology*, 89(3):334–341.

[Gray and Goss, 1974] Gray, H. and Goss, C. M. (1974). Anatomy of the human body. *American Journal of Physical Medicine & Rehabilitation*, 53(6):293.

[Greenblatt et al., 2012] Greenblatt, R. E., Pflieger, M., and Ossadtchi, A. (2012). Connectivity measures applied to human brain electrophysiological data. *Journal of neuroscience methods*, 207(1):1–16.

[Gruber et al., 2018] Gruber, M., Hsieh, L.-T., Staresina, B. P., Elger, C. E., Fell, J., Axmacher, N., and Ranganath, C. (2018). Theta phase synchronization between the human hippocampus and prefrontal cortex increases during encoding of unexpected information: A case study. *Journal of Cognitive Neuroscience*.

[Gulbinaite et al., 2014] Gulbinaite, R., van Rijn, H., and Cohen, M. X. (2014). Fronto-parietal network oscillations reveal relationship between working memory capacity and cognitive control. *Frontiers in human neuroscience*, 8:761.

[Güntekin and Başar, 2010] Güntekin, B. and Başar, E. (2010). A new interpretation of P300 responses upon analysis of coherences. *Cognitive neurodynamics*, 4(2):107–118.

[Güntekin et al., 2008] Güntekin, B., Saatçi, E., and Yener, G. (2008). Decrease of evoked delta, theta and alpha coherences in alzheimer patients during a visual oddball paradigm. *Brain research*, 1235:109–116.

[Hamedi et al., 2016] Hamedi, M., Salleh, S.-H., and Noor, A. M. (2016). Electroencephalographic motor imagery brain connectivity analysis for bci: a review. *Neural computation*, 28(6):999–1041.

[Hammer et al., 2012] Hammer, E. M., Halder, S., Blankertz, B., Sannelli, C., Dickhaus, T., Kleih, S., Müller, K.-R., and Kübler, A. (2012). Psychological predictors of smr-bci performance. *Biological psychology*, 89(1):80–86.

[Han et al., 2017] Han, Y., Wang, K., Jia, J., and Wu, W. (2017). Changes of EEG spectra and functional connectivity during an object-location memory task in alzheimer's disease. *Frontiers in behavioral neuroscience*, 11:107.

[Hansen et al., 2015] Hansen, E. C., Battaglia, D., Spiegler, A., Deco, G., and Jirsa, V. K. (2015). Functional connectivity dynamics: modeling the switching behavior of the resting state. *Neuroimage*, 105:525–535.

[Hari and Puce, 2017] Hari, R. and Puce, A. (2017). *MEG-EEG Primer*. Oxford University Press.

[Harper et al., 2017] Harper, J., Malone, S. M., and Iacono, W. G. (2017). Theta-and delta-band EEG network dynamics during a novelty oddball task. *Psychophysiology*, 54(11):1590–1605.

[Hassan et al.,] Hassan, M., Gudnasonb, J., Terrien, J., Karlssonb, B., and Marque, C. Improved detection of nonlinearity in nonstationary signals by piecewise stationary segmentation.

[Hassan and Wendling, 2018] Hassan, M. and Wendling, F. (2018). Electroencephalography source connectivity: toward high time/space resolution brain networks. *arXiv preprint arXiv:1801.02549*.

[Hawrylycz et al., 2012] Hawrylycz, M. J., Lein, E. S., Guillozet-Bongaarts, A. L., Shen, E. H., Ng, L., Miller, J. A., Van De Lagemaat, L. N., Smith, K. A., Ebbert, A., Riley, Z. L., et al. (2012). An anatomically comprehensive atlas of the adult human brain transcriptome. *Nature*, 489(7416):391–399.

[Hendelman, 2015] Hendelman, W. (2015). *Atlas of functional neuroanatomy*. CRC press.

[Herculano, 2009] Herculano, Houzel, S. (2009). The human brain in numbers: a linearly scaled-up primate brain. *Frontiers in Human Neuroscience*, 3(November):1–11.

[Hinton, 2011] Hinton, G. E. (2011). Machine learning for neuroscience. *Neural systems & circuits*, 1(1):1–2.

[Hu and Zhang, 2019] Hu, L. and Zhang, Z. (2019). *EEG Signal Processing and Feature Extraction*. Springer.

[Hurtado-Rincon et al., 2014] Hurtado-Rincon, J., Rojas-Jaramillo, S., Ricardo-Cespedes, Y., Alvarez-Meza, A. M., and Castellanos-Dominguez, G. (2014). Motor imagery classification using feature relevance analysis: An emotiv-based bci system. In *Image, Signal Processing and Artificial Vision (STSIVA), 2014 XIX Symposium on*, pages 1–5. IEEE.

[Hurtado-Rincón et al., 2018a] Hurtado-Rincón, J. V., Restrepo, F., Padilla, J. I., Torres, H. F., and Castellanos-Dominguez, G. (2018a). Functional connectivity analysis using the oddball auditory paradigm for attention tasks. In *International Conference on Brain Informatics*, pages 99–108. Springer.

[Hurtado-Rincón et al., 2018b] Hurtado-Rincón, J. V., Restrepo, F., Padilla, J. I., Torres, H. F., and Castellanos-Dominguez, G. (2018b). Functional connectivity analysis using the oddball auditory paradigm for attention tasks. In *International Conference on Brain Informatics*, pages 99–108. Springer.

[Hussain et al., 2017] Hussain, L., Aziz, W., Saeed, S., Shah, S. A., Nadeem, M. S. A., Awan, I. A., Abbas, A., Majid, A., and Kazmi, S. Z. H. (2017). Complexity analysis of eeg motor movement with eye open and close subjects using multiscale permutation entropy (mpe) technique. *Biomedical Research*, 28(16):7104–7111.

[Huster et al., 2015] Huster, R., Plis, S. M., and Calhoun, V. D. (2015). Group-level component analyses of EEG: validation and evaluation. *Frontiers in neuroscience*, 9:254.

[Huster and Raud, 2018] Huster, R. J. and Raud, L. (2018). A tutorial review on multi-subject decomposition of EEG. *Brain topography*, 31(1):3–16.

[Hutchison et al., 2013] Hutchison, R. M., Womelsdorf, T., Allen, E. A., Bandettini, P. A., Calhoun, V. D., Corbetta, M., Della Penna, S., Duyn, J. H., Glover, G. H., Gonzalez-Castillo, J., et al. (2013). Dynamic functional connectivity: promise, issues, and interpretations. *Neuroimage*, 80:360–378.

[Ilmoniemi and Sarvas, 2017] Ilmoniemi, R. J. and Sarvas, J. (2017). *Brain Signals,Physics and Mathematics of MEG and EEG*. Oxford University Press.

[Iyer et al., 2015] Iyer, P. M., Egan, C., Pinto-Grau, M., Burke, T., Elamin, M., Nasseroleslami, B., Pender, N., Lalor, E. C., and Hardiman, O. (2015). Functional connectivity changes in resting-state eeg as potential biomarker for amyotrophic lateral sclerosis. *PloS one*, 10(6):e0128682.

[Kaplan et al., 2005] Kaplan, A. Y., Fingelkurts, A. A., Fingelkurts, A. A., Borisov, S. V., and Darkhovsky, B. S. (2005). Nonstationary nature of the brain activity as revealed by EEG/MEG: methodological, practical and conceptual challenges. *Signal processing*, 85(11):2190–2212.

[Kiat et al., 2018] Kiat, J. E., Long, D., and Belli, R. F. (2018). Attentional responses on an auditory oddball predict false memory susceptibility. *Cognitive, Affective, & Behavioral Neuroscience*, 18(5):1000–1014.

[Kiiski et al., 2020] Kiiski, H., Rueda-Delgado, L. M., Bennett, M., Knight, R., Rai, L., Roddy, D., Grogan, K., Bramham, J., Kelly, C., and Whelan, R. (2020). Functional EEG connectivity is a neuromarker for adult attention deficit hyperactivity disorder symptoms. *Clinical Neurophysiology*, 131(1):330–342.

[Kumar et al., 2015] Kumar, A., Singh, A., et al. (2015). A review on alzheimer's disease pathophysiology and its management: an update. *Pharmacological reports*, 67(2):195–203.

[Lang et al., 2012] Lang, E. W., Tomé, A. M., Keck, I. R., Górriz-Sáez, J., and Puntonet, C. G. (2012). Brain connectivity analysis: a short survey. *Computational intelligence and neuroscience*, 2012.

[Lee et al., 2014] Lee, G.-T., Lee, C., Kim, K. H., and Jung, K.-Y. (2014). Regional and inter-regional theta oscillation during episodic novelty processing. *Brain and cognition*, 90:70–75.

[Li et al., 2016a] Li, F., Chen, B., Li, H., Zhang, T., Wang, F., Jiang, Y., Li, P., Ma, T., Zhang, R., Tian, Y., et al. (2016a). The time-varying networks in P300: a task-evoked EEG study. *IEEE Transactions on Neural Systems and Rehabilitation Engineering*, 24(7):725–733.

[Li et al., 2020] Li, F., Tao, Q., Peng, W., Zhang, T., Si, Y., Zhang, Y., Yi, C., Biswal, B., Yao, D., and Xu, P. (2020). Inter-subject P300 variability relates to the efficiency of brain networks reconfigured from resting-to task-state: Evidence from a simultaneous event-related EEG-fMRI study. *NeuroImage*, 205:116285.

[Li et al., 2018] Li, F., Yi, C., Jiang, Y., Liao, Y., Si, Y., Dai, J., Yao, D., Zhang, Y., and Xu, P. (2018). Different contexts in the oddball paradigm induce distinct brain networks in generating the P300. *Frontiers in human neuroscience*, 12:520.

[Li et al., 2016b] Li, J., Wang, Y., Zhang, L., Cichocki, A., and Jung, T.-P. (2016b). Decoding EEG in cognitive tasks with time-frequency and connectivity masks. *IEEE Transactions on Cognitive and Developmental Systems*, 8(4):298–308.

[Lithari et al., 2010] Lithari, C., Klados, M., and Bamidis, P. (2010). Graph analysis on functional connectivity networks during an emotional paradigm. In *XII Mediterranean Conference on Medical and Biological Engineering and Computing 2010*, pages 115–118. Springer.

[Liu et al., 2017] Liu, Q., Farahibozorg, S., Porcaro, C., Wenderoth, N., and Mantini, D. (2017). Detecting large-scale networks in the human brain using high-density electroencephalography. *Human Brain Mapping*, 4643(June):4631–4643.

[Liu et al., 2019] Liu, X., Li, T., Tang, C., Xu, T., Chen, P., Bezerianos, A., and Wang, H. (2019). Emotion recognition and dynamic functional connectivity analysis based on EEG. *IEEE Access*, 7:143293–143302.

[Liuzzi et al., 2019] Liuzzi, L., Quinn, A. J., O'Neill, G. C., Woolrich, M. W., Brookes, M., Hillebrand, A., and Tewarie, P. (2019). How sensitive are conventional MEG functional connectivity metrics with sliding windows to detect genuine fluctuations in dynamic functional connectivity? *Frontiers in neuroscience*, 13:797.

[Lui et al., 2011] Lui, J. H., Hansen, D. V., and Kriegstein, A. R. (2011). Development and evolution of the human neocortex. *Cell*, 146(1):18–36.

[Lynn and Bassett, 2019] Lynn, C. W. and Bassett, D. S. (2019). The physics of brain network structure, function and control. *Nature Reviews Physics*, 1(5):318–332.

[Mahyari et al., 2016] Mahyari, A. G., Zoltowski, D. M., Bernat, E. M., and Aviyente, S. (2016). A tensor decomposition-based approach for detecting dynamic network states from EEG. *IEEE Transactions on Biomedical Engineering*, 64(1):225–237.

[Mai and Paxinos, 2011] Mai, J. K. and Paxinos, G. (2011). *The human nervous system*. Academic press.

[Malmivuo et al., 1995] Malmivuo, J., Plonsey, R., et al. (1995). *Principles and applications of bioelectric and biomagnetic field*.

[Marino et al., 2016] Marino, M., Liu, Q., Brem, S., Wenderoth, N., and Mantini, D. (2016). Automated detection and labeling of high-density EEG electrodes from structural MR images. *Journal of Neural Engineering*, 13(5):1–11.

[Morup et al., 2007] Morup, M., Hansen, L. K., and Arnfred, S. M. (2007). ERPWAVELAB: A toolbox for multi-channel analysis of time–frequency transformed event related potentials. *Journal of neuroscience methods*, 161(2):361–368.

[Mouchlianitis et al., 2016] Mouchlianitis, E., McCutcheon, R., and Howes, O. D. (2016). Brain-imaging studies of treatment-resistant schizophrenia: a systematic review. *The Lancet Psychiatry*, 3(5):451–463.

[Muraskin et al., 2018] Muraskin, J., Brown, T. R., Walz, J. M., Tu, T., Conroy, B., Goldman, R. I., and Sajda, P. (2018). A multimodal encoding model applied to imaging decision-related neural cascades in the human brain. *NeuroImage*, 180:211–222.

[Nili et al., 2020] Nili, H., Basti, A., Hauk, O., Marzetti, L., and Henson, R. (2020). Multivariate connectivity: a conceptual and mathematical review.

[Olejniczak, 2006] Olejniczak, P. (2006). Neurophysiologic basis of eeg. *Journal of clinical neurophysiology*, 23(3):186–189.

[Omidvarnia et al., 2013] Omidvarnia, A., Azemi, G., Colditz, P. B., and Boashash, B. (2013). A time–frequency based approach for generalized phase synchrony assessment in nonstationary multivariate signals.

[Padilla-Buritica et al., 2020] Padilla-Buritica, J. I., Ferrandez-Vicente, J. M., Castaño, G. A., and Acosta-Medina, C. D. (2020). Non-stationary group-level connectivity analysis for enhanced interpretability of oddball tasks. *Frontiers in Neuroscience*, 14.

[Padilla-Buritica et al., 2019] Padilla-Buritica, J. I., Hurtado, J. V., and Castellanos-Dominguez, G. (2019). Supervised piecewise network connectivity analysis for enhanced confidence of auditory oddball tasks. *Biomedical Signal Processing and Control*, 52:341–346.

[Padilla-Buritica et al., 2016] Padilla-Buritica, J. I., Martinez-Vargas, J. D., and Castellanos-Dominguez, G. (2016). Emotion discrimination using spatially compact regions of interest extracted from imaging eeg activity. *Frontiers in computational neuroscience*, 10:55.

[Padilla-Buriticá et al., 2017] Padilla-Buriticá, J. I., Martínez-Vargas, J. D., Suárez-Ruiz, A., Ferrández, J. M., and Castellanos-Dominguez, G. (2017). Spatial resolution of eeg source reconstruction in assessing brain connectivity analysis. In *International Work-Conference on the Interplay Between Natural and Artificial Computation*, pages 77–86. Springer.

[Padilla-Buriticá et al., 2018] Padilla-Buriticá, J. I., Torres, H. F., Pereda, E., Correa, A., and Castellanos-Domínguez, G. (2018). Influence of time-series extraction on binge drinking interpretability using functional connectivity analysis. In *International Conference on Brain Informatics*, pages 186–194. Springer.

[Penfield, 2015] Penfield, W. (2015). *Mystery of the mind: A critical study of consciousness and the human brain*. Princeton University Press.

[Pereda et al., 2018] Pereda, E., García-Torres, M., Melián-Batista, B., Mañas, S., Méndez, L., and González, J. J. (2018). The blessing of dimensionality: Feature selection outperforms functional connectivity-based feature transformation to classify ADHD subjects from EEG patterns of phase synchronisation. *PloS one*, 13(8):e0201660.

[Polich, 2007] Polich, J. (2007). Updating p300: an integrative theory of p3a and p3b. *Clinical neurophysiology*, 118(10):2128–2148.

[Preti et al., 2017] Preti, M. G., Bolton, T. A., and Van De Ville, D. (2017). The dynamic functional connectome: State-of-the-art and perspectives. *Neuroimage*, 160:41–54.

[Sakkalis, 2011] Sakkalis, V. (2011). Review of advanced techniques for the estimation of brain connectivity measured with EEG/MEG. *Computers in biology and medicine*, 41(12):1110–1117.

[Sanei and Chambers, 2013] Sanei, S. and Chambers, J. A. (2013). *EEG signal processing*. John Wiley & Sons.

[Schaadt et al., 2013] Schaadt, G., Pannekamp, A., and van der Meer, E. (2013). Auditory phoneme discrimination in illiterates: Mismatch negativity-a question of literacy? *Developmental psychology*, 49(11):2179.

[Schlüter and Bermeitinger, 2017] Schlüter, H. and Bermeitinger, C. (2017). Emotional oddball: A review on variants, results, and mechanisms. *Review of General Psychology*, 21(3):179–222.

[Schmidt et al., 2012] Schmidt, R. F., Dudel, J., Jaenig, W., and Zimmermann, M. (2012). *Fundamentals of neurophysiology*. Springer Science & Business Media.

[Schumacher et al., 2019] Schumacher, J., Peraza, L. R., Firbank, M., Thomas, A. J., Kaiser, M., Gallagher, P., O'Brien, J. T., Blamire, A. M., and Taylor, J.-P. (2019). Dynamic functional connectivity changes in dementia with lewy bodies and alzheimer's disease. *NeuroImage: Clinical*, 22:101812.

[Shim et al., 2014] Shim, M., Kim, D.-W., Lee, S.-H., and Im, C.-H. (2014). Disruptions in small-world cortical functional connectivity network during an auditory oddball paradigm task in patients with schizophrenia. *Schizophrenia research*, 156(2):197–203.

[Sporns, 2007] Sporns, O. (2007). Brain connectivity. *Scholarpedia*, 2(10):4695.

[Sporns, 2018] Sporns, O. (2018). Graph theory methods: applications in brain networks. *Dialogues in Clinical Neuroscience*, 20(2):111.

[Stevenson et al., 2014] Stevenson, C., Brookes, M., López, J. D., Troebinger, L., Mattout, J., Penny, W., Morris, P., Hillebrand, A., Henson, R., and Barnes, G. (2014). Does function fit structure? A ground truth for non-invasive neuroimaging. *NeuroImage*, 94:89–95.

[Sun et al., 2019] Sun, S., Li, X., Zhu, J., Wang, Y., La, R., Zhang, X., Wei, L., and Hu, B. (2019). Graph theory analysis of functional connectivity in major depression disorder with high-density resting state eeg data. *IEEE Transactions on Neural Systems and Rehabilitation Engineering*, 27(3):429–439.

[Terrien et al., 2013] Terrien, J., Germain, G., Marque, C., and Karlsson, B. (2013). Bivariate piecewise stationary segmentation; improved pre-treatment for synchronization measures used on non-stationary biological signals. *Medical engineering & physics*, 35(8):1188–1196.

[Thee et al., 2018] Thee, K. W., Nisar, H., and Soh, C. S. (2018). Graph theoretical analysis of functional brain networks in healthy subjects: Visual oddball paradigm. *IEEE Access*, 6:64708–64727.

[Thilaga et al., 2018] Thilaga, M., Ramasamy, V., Nadarajan, R., and Nandagopal, D. (2018). Shortest path based network analysis to characterize cognitive load states of human brain using EEG based functional brain networks. *Journal of integrative neuroscience*, 17(2):253–275.

[Thilaga et al., 2015] Thilaga, M., Vijayalakshmi, R., Nadarajan, R., Nandagopal, D., Cocks, B., Archana, C., and Dahal, N. (2015). A heuristic branch-and-bound based thresholding algorithm for unveiling cognitive activity from EEG data. *Neurocomputing*, 170:32–46.

[Toppi et al., 2012] Toppi, J., de Vico Fallani, F., Vecchiato, G., Maglione, A. G., Cincotti, F., Mattia, D., Salinari, S., Babiloni, F., and Astolfi, L. (2012). How the statistical validation of functional connectivity patterns can prevent erroneous definition of small-world properties of a brain connectivity network. *Computational and mathematical methods in medicine*, 2012.

[Toppi et al., 2014] Toppi, J., Mattia, D., Anzolin, A., Risetti, M., Petti, M., Cincotti, F., Babiloni, F., and Astolfi, L. (2014). Time varying effective connectivity for describing brain network changes induced by a memory rehabilitation treatment. In *Engineering in Medicine and Biology Society (EMBC), 2014 36th Annual International Conference of the IEEE*, pages 6786–6789. IEEE.

[Trans Cranial Technologies Ltd., 2012] Trans Cranial Technologies Ltd. (2012). 10 / 20 System Positioning Manual. Technical Report 1.

[van den Heuvel et al., 2017] van den Heuvel, M. P., de Lange, S. C., Zalesky, A., Seguin, C., Yeo, B. T., and Schmidt, R. (2017). Proportional thresholding in resting-state fMRI functional connectivity networks and consequences for patient-control connectome studies: Issues and recommendations. *Neuroimage*, 152:437–449.

[Van Essen et al., 2012] Van Essen, D. C., Ugurbil, K., Auerbach, E., Barch, D., Behrens, T., Bucholz, R., Chang, A., Chen, L., Corbetta, M., Curtiss, S. W., et al. (2012). The human connectome project: a data acquisition perspective. *Neuroimage*, 62(4):2222–2231.

[Van Mierlo et al., 2014] Van Mierlo, P., Papadopoulou, M., Carrette, E., Boon, P., Vandenberghe, S., Vonck, K., and Marinazzo, D. (2014). Functional brain connectivity from EEG in epilepsy: Seizure prediction and epileptogenic focus localization. *Progress in neurobiology*, 121:19–35.

[Van Wijk et al., 2010] Van Wijk, B. C., Stam, C. J., and Daffertshofer, A. (2010). Comparing brain networks of different size and connectivity density using graph theory. *PloS one*, 5(10):e13701.

[Vanderah and Gould, 2020] Vanderah, T. and Gould, D. J. (2020). *Nolte's The Human Brain E-Book: An Introduction to its Functional Anatomy*. Elsevier Health Sciences.

[Váša et al., 2018] Váša, F., Bullmore, E. T., and Patel, A. X. (2018). Probabilistic thresholding of functional connectomes: Application to schizophrenia. *Neuroimage*, 172:326–340.

[Vecchio et al., 2016] Vecchio, F., Miraglia, F., Quaranta, D., Granata, G., Romanello, R., Marra, C., Bramanti, P., and Rossini, P. M. (2016). Cortical connectivity and memory performance in cognitive decline: a study via graph theory from eeg data. *Neuroscience*, 316:143–150.

[Velasquez-Martinez et al., 2020] Velasquez-Martinez, L., Caicedo-Acosta, J., and Castellanos-Dominguez, G. (2020). Entropy-based estimation of event-related de/synchronization in motor imagery using vector-quantized patterns. *Entropy*, 22(6):703.

[Velasquez-Martinez et al., 2018] Velasquez-Martinez, L. F., Zapata-Castaño, F., Cárdenas-Peña, D., and Castellanos-Dominguez, G. (2018). Detecting EEG dynamic

changes using supervised temporal patterns. In *International Workshop on Artificial Intelligence and Pattern Recognition*, pages 351–358. Springer.

[Velásquez-Martínez et al., 2019] Velásquez-Martínez, L. F., Zapata-Castaño, F., Padilla-Buritica, J. I., Vicente, J. M. F., and Castellanos-Dominguez, G. (2019). Group differences in time-frequency relevant patterns for user-independent bci applications. In *International Work-Conference on the Interplay Between Natural and Artificial Computation*, pages 138–145. Springer.

[Venkataraman et al., 2011] Venkataraman, A., Rathi, Y., Kubicki, M., Westin, C.-F., and Golland, P. (2011). Joint modeling of anatomical and functional connectivity for population studies. *IEEE transactions on medical imaging*, 31(2):164–182.

[Vinck et al., 2015] Vinck, M., Huurdeman, L., Bosman, C. A., Fries, P., Battaglia, F. P., Pennartz, C. M., and Tiesinga, P. H. (2015). How to detect the granger-causal flow direction in the presence of additive noise? *Neuroimage*, 108:301–318.

[Vinck et al., 2011] Vinck, M., Oostenveld, R., Van Wingerden, M., Battaglia, F., and Pennartz, C. M. (2011). An improved index of phase-synchronization for electrophysiological data in the presence of volume-conduction, noise and sample-size bias. *Neuroimage*, 55(4):1548–1565.

[Volpe et al., 2007] Volpe, U., Mucci, A., Bucci, P., Merlotti, E., Galderisi, S., and Maj, M. (2007). The cortical generators of P3a and P3b: a LORETA study. *Brain research bulletin*, 73(4-6):220–230.

[Walz et al., 2013] Walz, J. M., Goldman, R. I., Carapezza, M., Muraskin, J., Brown, T. R., and Sajda, P. (2013). Simultaneous EEG-fMRI reveals temporal evolution of coupling between supramodal cortical attention networks and the brainstem. *Journal of Neuroscience*, 33(49):19212–19222.

[Wang et al., 2014] Wang, C., Xu, J., Lou, W., and Zhao, S. (2014). Dynamic information flow analysis in vascular dementia patients during the performance of a visual oddball task. *Neuroscience letters*, 580:108–113.

[Waxman, 2016] Waxman, S. G. (2016). *Clinical neuroanatomy*. McGraw-Hill Education.

[Wendling et al., 2009] Wendling, F., Ansari-Asl, K., Bartolomei, F., and Senhadji, L. (2009). From EEG signals to brain connectivity: a model-based evaluation of interdependence measures. *Journal of neuroscience methods*, 183(1):9–18.

[Zerouali et al., 2014] Zerouali, Y., Lina, J.-M., Sekerovic, Z., Godbout, J., Dube, J., Jolicoeur, P., and Carrier, J. (2014). A time-frequency analysis of the dynamics of cortical networks of sleep spindles from MEG-EEG recordings. *Frontiers in neuroscience*, 8:310.

[Zhang et al., 2018] Zhang, H., Watrous, A. J., Patel, A., and Jacobs, J. (2018). Theta and alpha oscillations are traveling waves in the human neocortex. *Neuron*, 98(6):1269–1281.

[Zhang et al., 2015] Zhang, R., Yao, D., Valdés-Sosa, P. A., Li, F., Li, P., Zhang, T., Ma, T., Li, Y., and Xu, P. (2015). Efficient resting-state eeg network facilitates motor imagery performance. *Journal of neural engineering*, 12(6):066024.